UNDERSTANDING HYDROLOGICAL PROCESSES AND WATER FLUXES LINKING WETLAND PONDS AND GROUNDWATER IN THE PRAIRIE POTHOLE REGION

A Thesis Submitted to the College of Graduate and Postdoctoral Studies

In Partial Fulfillment of the Requirements

For the Degree of Doctor of Philosophy

In the School of Environment and Sustainability

University of Saskatchewan

Saskatoon

EDWARD KOMLA PAPPAH BAM

PERMISSION TO USE

In presenting this thesis in partial fulfillment of the requirements for a Postgraduate degree from the University of Saskatchewan, I agree that the Libraries of this University may make it freely available for inspection. I further agree that permission for copying of this thesis in any manner, in whole or in part, for scholarly purposes may be granted by the professors who supervised my thesis work or, in their absence, by the Head of the Department or the Dean of the College in which my thesis work was done. It is understood that any copying or publication or use of this thesis or parts thereof for financial gain shall not be allowed without my written permission. It is also understood that due recognition shall be given to me and to the University of Saskatchewan and Global Institute for Water Security in any scholarly use which may be made of any material in my thesis.

DISCLAIMER

Reference in this thesis to any commercial products, process, or services by trade name, trademark, manufacturer, or otherwise, does not constitute or imply its endorsement, recommendation, or favoring by the University of Saskatchewan. The views and opinions of the author expressed herein do not state or reflect those of the University of Saskatchewan and shall not be used for advertising or product endorsement purposes.

Requests for permission to copy or to make other use of material in this thesis in whole or part should be addressed to:

Executive Director
School of Environment and Sustainability,
University of Saskatchewan
Room 323, Kirk Hall, 117 Science Place
Saskatoon, SK S7N 5C8, Canada

Or

Dean
College of Graduate and Postdoctoral Studies
University of Saskatchewan
116 Thorvaldsen Building, 110 Science Place
Saskatoon, SK S7N 5C9, Canada

ABSTRACT

Understanding surface water-groundwater interaction processes and quantification of hydrological fluxes remains a scientific challenge in hydrology. However, comprehensive understanding of groundwater interactions with the surface and more accurate estimates of hydrologic fluxes are essential for water resources and environmental management and policy. Numerous hydrological studies conducted in the glaciated Prairie Pothole region focused mainly on the importance of wetland ponds and their relationship with shallow groundwater in the till using physical, geophysical and water chemistry measurements, and numerical models. In this thesis, I combined field observations, isotopes of water and geochemical tracers (δ^2H, $\delta^{18}O$, lc-excess, ^3H and Cl^-, SO_4^{2-}), to develop a physical isotope model to quantify water fluxes, examine interactions between surface water and the relatively deeper intertill aquifers (< 50 m), and assess the pathways of water and solutes from the ponds, uplands and lowlands areas hummocky landscape. My field campaign spanned between 2013 and 2016 at the St Denis National Research Area in Saskatchewan, Canada, where additional soil, hydrometric and water isotope data were collected to complement the existing previously collected stable isotope, hydraulic and hydrometric data. The data show that water isotope compositions of ponds are reflective of seasons and residence time, and this property is useful for quantifying spatial surface water fluxes. Pond water infiltration rates estimated from the new model show that ephemeral ponds have the highest outflow rates, and pond-subsurface interactions can be determined without groundwater heads. The water isotopes and hydrometric measurements indicate that interaction between ponds and the intertill aquifer is limited to ponds upland, and water from ephemeral ponds are the dominant source of depression-focused recharge to the intertill aquifer. The stable isotopes and dissolved ions data showed that rapid downward advective movement of water occurs in the shallow weathered zone throughout the till and at all landscape positions and this water could serve as recharge water to the aquifer. The work represents a distinct contribution to the literature regarding our understanding of the hydrological processes linking wetland ponds and groundwater in the prairie pothole region.

ACKNOWLEDGEMENTS

This thesis would not be possible without the support and funding from the University of Saskatchewan Dean and Saskatchewan Innovation and Opportunity Scholarships, the Global Institute for Water Security, the Canadian Wildlife Service, my supervisor, advisory committee members and family. I would like to take this opportunity to express my sincere gratitude to my supervisor, Dr. Andrew M. Ireson for his patience and unreserved support in reviewing, commenting, and providing feedback throughout the course of this research. Secondarily, I would like to thank my advisory committee members, Emeritus Research Scientist Dr. Garth van der Kamp, Professors Jeffery J. McDonnell, Karl-Erich Lindenschmidt, M. Jim Hendry and Charles Maule, for guidance, and in reviewing the thesis. Thirdly, I would like to acknowledge the support from the National Hydrology Research Centre and the Canadian Wildlife Service, Saskatoon, Saskatchewan for site access and the legacy data. My sincere thanks go to my lovely wife Priscilla and children Rhema and Joel; my parents Joseph and Victoria Bam, and all my family here in Canada and Ghana for every sacrifice and encouragement over the years. I am thankful to my colleagues at Global Institute for Water Security who have encouraged, challenged, supported and motivated me. To Randy Schmidt, Heather Wilson, Emily Cavaliere, Erin Schmeling, Drs. Bob Clark, Melkamu Ali, and Dawn Kiem, thank you for your assistance during my fieldwork. Dr. Geoff Koehler and Mrs. Janzen Kim thank you for making time to analyze my water isotopes and reading through the final thesis.

DEDICATION

to God, the Judge of all,

TABLE OF CONTENTS

LIST OF TABLES

LIST OF FIGURES

LIST OF ABBREVIATIONS

A (m^2)	Area
BGL	Below ground level
δ_E (‰)	delta of evaporated water isotope composition
δ_j (‰)	delta of inflow water isotope composition
δ_p (‰)	delta of rainfall and snow isotope composition
δ_o (‰)	delta of water outflow isotope
$\delta^{18}O$	delta of Oxygen-18 isotope
$\delta^{2}H$	delta of hydrogen-2 isotope
ϵ (-)	Equilibrium isotopic separation between liquid and vapor
E (m/d)	Evaporation rate
GNIP	Global Network of Isotopes in Precipitation
H (-)	Relative humidity
J (m/d)	Inflow rate of overland runoff, rivers and groundwater
km	Kilometer
k (m)	Pond water depth
kPa	kilo Pascal
K (m/y)	Saturated hydraulic conductivity
lc-excess	Line condition excess
LELs	Local evaporation lines
MWLs	Meteoric water lines
m	Meter
masl	Meters above sea level
O (m/d)	Outflow rate of pond spillage and infiltration
p (-)	Basin profile parameter
‰	Per mil
%	Percentage
PPR	Prairie Pothole Region
P (m/d)	Precipitation rate over the pond
SKLMWL	Saskatoon Local Meteoric Water Line
SDNWA	St. Denis National Wildlife Area

s (m^2)	Scale parameter
VSMOW	Vienna snow mean ocean water
V (m^3)	Volume of surface water stored

CHAPTER 1: INTRODUCTION

1. 1. Background for the study

Water is crucial to the survival of any civilization in history. Surface water bodies and groundwater aqiufers provide water for drinking, crop production, electric power generation, oil and gas industry development, transportation and trade, and support ecosystem services such as plant and wildlife habitats (Murkin, 1998; Johnsgard, 2010; Warner and Ayotte, 2014). Understanding the interactions between groundwater and surface water is fundamental to the development of effective water-resource and environmental management, and policy because the two components are in continuous interaction with each other in the hydrologic system (Winter *et al.*, 1998). Sustainable water availability requires appropriate estimates of individual water balance components (that are precipitation, evaporation, transpiration, outflow, and inflows from surface and subsurface and storage) in the hydrologic system. A water balance accounts for the rates of water movement and the change in water storage at a particular time range and place for all or parts of the atmosphere, land surface, and subsurface (Healy *et al.*, 2007). Despite the importance of water balance in water sustainability, water balance calculations are saddled with large errors due to errors in the estimation of individual water balance input terms, and sometimes the equations used in the water balance estimation for a given catchment. By developing and applying appropriate water balance equations that are representative of the system, and reducing the errors associated with individual water balance input terms, the water balance estimate for a catchment can be significantly improved (Abtew and Assefa, 2013). In addition, the quantification of water movement in the subsurface requires a thorough qualitative understanding of water sources and hydrological processes in the unsaturated and saturated zones. However, understanding of unsaturated flow and solute transport, that contributes groundwater recharge, is still a challenging scientific issue in catchment hydrology (Manna *et al.*, 2017).

In the North American Prairie Pothole Region (PPR), water resources are becoming more vulnerable to changes imposed by land-use and climate change (Henderson and Sauchyn, 2008; Balas *et al.*, 2012; Wang *et al.*, 2013; Wright and Wimberly, 2013). Approximately 50% of wetlands in the PPR have been drained, mostly (> 80%) to make way for agricultural crop production (Euliss *et al.*, 2006). The PPR is characterized by dynamic inter-annual climate cycles of extreme dry and wet conditions leading to droughts often followed by floods (Winter and Rosenberry, 1998; McGinn, 2010; Balas *et al.*, 2012). In addition to changing climate conditions and land use, the geology, topography, and hydrology of the region are also complex. The underlying geology is made up of glacial deposits which form a thick sequence of clay-rich sediments (10-100s of a meter) interspersed with lacustrine sand and gravel deposits resulting in highly variable hydraulic conductivity (Keller *et al.*, 1985; Remenda *et al.*, 1996; Hayashi *et al.*, 1997). Within the surficial till (depths of 5-15 m below ground level), permeable units (sometimes referred to as transmission aquifers) occur in the weathered and fractured, and / or non-weathered and poorly fractured till (Keller *et al.*, 1985; Hayashi *et al.*, 1997; van der Kamp and Hayashi, 2009). Sand and gravel deposits in the till form isolated aquifer-aquitard systems that are diverse, from extensive sheets to long narrow channel deposits, and several small deposits of local extent (Hendry, 1983, 1988; Welsh and Kerkhoven, 2012; Nachshon *et al.*, 2013). The topography of the region characterized by extensive areas of low relief with hummocky terrain attributed to glaciation events resulting in thousands of depressions some of which results in wetlands called "potholes" or "sloughs" (Miller *et al.*, 1985; Hayashi *et al.*, 1997; van der Kamp and Hayashi, 2009; van der Kamp *et al.*, 2016). The complexity and highly variable nature of the climate, land-use, geology, and topography make it difficult to assess and quantify the contribution of wetland water to groundwater and surface water resources (Hayashi *et al.*, 2003; Fang *et al.*, 2007; Mekonnen *et al.*, 2014; Brannen *et al.*, 2015).

Wetlands in the PPR collect precipitation, wind-blown snow, and snowmelt runoff from upland areas serving as main sources of water to ponds. Pond water loss is by direct evaporation, infiltration leading to lateral transport of water to the pond riparian and upland zones, and, in certain cases, deep percolation (Woo and Rowsell, 1993; Su *et al.*, 2000; Fang *et al.*, 2007; Hayashi *et al.*, 2016). Water quantity in wetland ponds is essential for the survival and maintenance of ecosystem services. Sustainable management of wetlands and wetland water requires more

accurate estimates of inputs, losses, and storage, as much as possible (Mould *et al.*, 2010; Hayashi *et al.*, 2016). Wetland pond water budgets in semi-arid regions like the PPR are variable because the input fluxes such as evapotranspiration, precipitation, recharge or discharge, and storage volumes are highly variable with seasons (Conly *et al.*, 2004; Heagle *et al.*, 2007; Jolly *et al.*, 2008). The high variability in water budgets also leads to variability in dissolved ion content, which may be concentrated or diluted depending on the season and amount of rainfall runoff that enters the ponds. Precipitation runoff from upland areas (snowmelt or rainfall) could wash soluble salt ions into ponds and increasing pond water salinity in even known fresh water wetlands (Nachshon *et al.*, 2014). The phenomenon makes it difficult to effectively interpret pond's water chemistry as a result of only simple pond evaporation and dilution (Heagle *et al.*, 2007; Nachshon *et al.*, 2014). Thus, scientific efforts that depend on soluble salt ion concentrations to identify wetland pond types and hydrologic function in the PPR are limited (Stewart and Kantrud, 1971, 1972; Richardson *et al.*, 1994; Seelig and DeKeyser, 2006; Pennock *et al.*, 2014). The use of conservative chemical tracers also face an equal challenge from surface runoff dilution of pond water, and any attempt to use chemical tracers for chemical-water-mass-balance estimates of hydrologic fluxes may not be reliable in such an environment (Dogramaci *et al.*, 2015; Skrzypek *et al.*, 2015).

The use of stable isotopes of water as tracers in isotope-water-mass balance models to predict pond hydrologic behavior and estimate ratios of water inputs to losses is less tedious and more common (Gonfiantini, 1986; Gibson *et al.*, 2008b; Steinman *et al.*, 2010; Dogramaci *et al.*, 2015; Skrzypek *et al.*, 2015). The existing models, however, are incapable of directly estimating evaporation and infiltration fluxes from small water bodies as the ones found in the PPR. In seasonal drought-prone climates like the PPR, water balance and lake residence time are controlled by climate variables, and the surface area to volume ratios of the basin holding the water (Benson and Paillet, 1989; Steinman *et al.*, 2010; Hayashi *et al.*, 2016). And these factors are mostly missing in existing isotope-water-mass balance models largely because they are designed for large lakes and rivers which are not easily affected by such changes. A new isotope-water-mass balance model that incorporates climate parameters such as time varying rainfall, basin area, shape factors, and capable of estimating evaporation and infiltration across the PPR and similar climatic regions is, therefore, desirable. And improved evaporation and infiltration estimates will reduce errors in water budget calculations for surface water bodies.

A more accurate water balance estimation in a catchment requires an understanding of the relationship between the surface water and groundwater systems. Studies in wetland environments (Siegel, 1988; Devito *et al.*, 1996; Euliss *et al.*, 2004) show that groundwater flows can have significant controls on the hydrologic functions and behavior of wetlands and can invariably affect the water balance. In the PPR, the contribution of wetland ponds to the shallow subsurface groundwater, the environment, and biodiversity is known to be spatially and temporally diverse (van der Kamp and Hayashi, 1998; Hayashi *et al.*, 2003; van der Kamp *et al.*, 2003; Berthold and Hayashi, 2004; Euliss *et al.*, 2004; Johnson *et al.*, 2010; Nachshon *et al.*, 2014; Pennock *et al.*, 2014). However, the extent of the contribution of wetland ponds to the relatively deep intertill aquifers in the PPR is poorly understood (Hayashi *et al.*, 2003; van der Kamp and Hayashi, 2009). For example, depression-focused recharge from ponds and wetlands is documented as the main source of shallow groundwater recharge on Prairies (van der Kamp and Hayashi, 1998). Currently, however, there is no consensus on whether the relatively deep aquifers (< 50 m) are recharged with modern water or not, and published isotope data (Wallick, 1981; Bacon and Keller, 1998; Hendry and Wassenaar, 1999; Grasby *et al.*, 2000; Grasby and Betcher, 2002; Jasechko *et al.*, 2014) are ambiguous. Some researchers have suggested these aquifers are predominately old water (Wallick, 1981; Keller *et al.*, 1988; Fortin *et al.*, 1991; Hendry and Wassenaar, 1999; Grasby and Betcher, 2002), while others have suggested that aquifers contain recharged water from depressions, which is to say snow and snowmelt runoff collect in depressions and infiltrates after the soil thaws to produce groundwater recharge (Bacon and Keller, 1998; Jasechko *et al.*, 2014; Gleeson *et al.*, 2015). Previous studies (Meyboom, 1966; Zebarth *et al.*, 1989; Woo and Rowsell, 1993; Winter and Rosenberry, 1995; Hayashi *et al.*, 1998; van der Kamp *et al.*, 2003; Berthold and Hayashi, 2004; Parsons *et al.*, 2004), which report on groundwater recharge sources as from wetlands, were mostly small scale hydraulic and geophysical measurements, and in some few cases dissolved ions or numerical models were employed. These studies were also largely concentrated in the shallow (<20 m depth) subsurface and on more semi-permananet and permanent ponds. Data and information on water stable isotopes, groundwater recharge and water and solute pathways from small temporary/ephemeral and seasonal ponds, which are widespread on the landscape, uplands, and the relatively deep intertill aquifer (~ 40 m) are lacking. Understanding the source(s) of groundwater and the spatial variability in recharge from wetlands at local and intermediate scales in this region is critical for assessing the route and potential sources of contamination to underlying

aquifers. To bridge the existing gaps in knowledge, an integrated approach that combines hydraulic and tracer analysis (dissolved ions and isotopes) is needed to identify the source(s) and the extent to which wetland ponds interact with the intertill aquifer and vice versa. Also, for solute transport and pollution prevention purposes, it is important to understand flow paths of the water that leads to groundwater recharge (if any) with respect to the characteristics of the till unsaturated zone. This scientific understanding will help in the development of sustainable and effective water use systems for the many sectors of the economy.

In summary, it is recognized that knowledge gaps exist in understanding of hydrological processes and quantifying fluxes in the PPR landscape. These suggest a need for new studies to improve our understanding of the PPR intertill aquifer–wetland pond water interactions, water flow and solute transport mechanisms and also quantify water fluxes. This could be achieved by combining existing data with new field observations (hydrometric and hydrogeologic), chemical and isotopes analyses from the various units in the till. The data collected should provide new knowledge that would lead to the development of new models that will enhance our understanding of the system, quantify various hydrological fluxes, and also could be applied in similar seasonally frozen climates globally.

I have shown in this thesis that valuable knowledge can be generated from the combination of isotopes of water, dissolved ions, and physical measurements. The information has led to understanding wetland pond water-groundwater interactions, quantifying hydrologic fluxes, and determining the flow pathways of water and solute from the soli surface to intertill aquifers in a complex systems as the PPR. This work differs from other published works in many ways because: *i)* I employed long term field observations, hydrometric and isotope data, that spaned over two decades of on a variety of wetland ponds to understand the wetland pond hydrologic regime, The presentation of stable isotope data in conjunction with hydrological data from multiple ponds and groundwater for wetland systems is rare. The variety of ponds examined in terms of permanence and relation to groundwater makes this a very robust study; *ii)* I developed a new isotope -water-mass balance model that is formulated based on time-tested area-depth-volume relationships for wetland ponds to quantify wetland water fluxes. Previous isotope-water mass balance models cannot to quantify independently fluxes such as evaporation and infiltration neither do they include time-varying precipitation and such surface area-volume relationships; *iii)* the work makes a

unique contribution to the literature regarding our understanding of the hydrological processes linking wetland ponds and the regional intertill aquifer at the depths below 30 m., and *iv)* I provided an improved understanding of the pathways water and solute take from a variety of locations to the intertill aquifer. The combination of dissolved ions and isotope data from lowlands and ponds, and uplands, provided the opportunity to examine flow and transport processes governing groundwater recharge in the till, which is not common. The understanding gained, and data obtained in this thesis could be used to improve the predictive capabilities of existing operational hydrological models for water balance and contaminant transport modelling. Such models could translate into tools to explore and test management interventions and assess impacts of climate change conditions on water resources in the region.

1. 2. Research hypothesis

Hydrological processes and fluxes related to surface and groundwater in the prairies are complex and highly variable due to the nature of the landscape and difficult to measure directly. We hypothesize that with a combination of methodologies, including physical and chemical (involving stable isotopes) tracer observation from the field, and physically based water-isotope mass balance model, the processes can be better understood and the quantitative estimates determined with much improved certainty. Thus an integrated physical and chemical methods will allow for *i)* the determination of whether there is a connection between the inter-till aquifer, the shallow groundwater and/or surface water system, and on what timescale (continuous or ephemeral); *ii)* the partitioning of pond water losses between infiltration and evaporation and could help infer individual pond hydrologic behaviour; and *iii)* a better understanding of hydrological processes from the upland hillslope and low-land –open-water bodies could be gained.

1. 3. Research goal and objectives

The overall goal of this thesis is to integrate hydrometric field observations, chemical tracers (involving isotopes of water and dissolved ions) and a physically based isotope model to quantify surface water fluxes and improve understanding of hydrological processes in the PPR.

The main objectives to achieve this goal are:

1. To develop an isotope- water mass balance equation representative of wetland system and capable of quantifying the fluxes of evaporation, infiltration, and storage from a variety of wetland ponds (i.e., of different sizes and shapes) receiving time-varying rainfall inputs and undergoing volume and isotopic change;
2. To investigate and determine which category of wetland ponds play dominant role in the recharge of prairie aquifers and more specifically, the interactions between various wetland ponds, the shallow groundwater, aquitards and the relatively deep intertill aquifers; and
3. To provide a mechanistic understanding of water flow and solute transport from the various landscape positions (wetland, lowland, and upland) through the unsaturated zone to the subsurface aquitards and aquifers in the glacial till.

1. 4. Thesis outline

This Thesis is written in a manuscript dissertation style. Following the Introduction, the Chapters 2, 3, and 4 have been structured as three separate manuscripts each mapped to the objectives stated above. The Figure and Table numbers, referencing style, and the page numbers in the submitted manuscripts have been reformatted from the original versions for inclusion in this thesis and the manuscripts themselves may be revised based on reviewer comments if necessary. Chapter 5 provides a set of conclusions from this research and discusses the links between the findings of each manuscript to literature cited in the introduction within the broader context of the hydrology literature. It also discusses the limitations of this work and makes recommendations for future work.

The fieldwork for this research was conducted at St Denis National Wildlife Area, SDNWA. The site has 3.85 km^2 area and located 40 km (52.8 N, 106.8 W) east of the city of Saskatoon in the Province of Saskatchewan Canada between August 2013 and July 2016. The site is extensively instrumented and monitored for physical and chemical measurements for over five decades (van der Kamp and Hayashi, 2009; Hayashi *et al.*, 2016). Data collected from the site include the geographic information system (GIS) maps, climate records of temperature and relative humidity (1993 to 2014), pond bathymetry measurements (2000 and 2009), pond, shallow piezometer and intertill aquifer water levels (1993 to 2016) pond , shallow piezometer and intertill aquifer water chemistry, tritium and stable isotopes (1993 to 2016), soil cores (2014) and stable isotopes for

precipitation, shallow piezometer groundwater (1993 to 2014) and the intertill aquifer (2015). The data was made up of isotopes in Saskatoon precipitation data from 1990 to 2014, SDNWA pond, s water levels, chemistry, and stable isotopes data from 1993 to 2016, and SDNWA precipitation from 2013 to 2014. The isotope, climatic and hydrometric data were processed and interpreted in Chapters 2 and Chapter 3 to estimate water fluxes and provide understanding on groundwater surface interactions. In Chapter 4, some of the isotope data for precipitation, ponds, and groundwater discussed in Chapter 2 and 3 were combined with high-resolution pore water isotopes and chemistry data and used to interpret the mechanisms of water and solute transport in the till.

1. 5. Terms and definitions

Here the terms used throughout this thesis with reference to water bodies are defined. A *wetland* is defined as a surface hydrological unit in a depression where the soils are gleyed and normally saturated, and which may contain *pond(s)* of varying size and persistence (van der Kamp *et al.*, 2016). A *pond* is defined as the flooded portion of the wetland (Hayashi *et al.*, 2016). The area with saturated and nearly saturated soil around the pond occupied by hydrophilic vegetation (grass and trees) is called the *riparian area*. The rest of the drainage basin is the *upland* (van der Kamp and Hayashi, 2009; Nachshon *et al.*, 2013). A *recharge pond* is a pond that, on average, loses water to groundwater, and tends to be fresh. A *discharge pond* is a pond that, on average, receives water from groundwater, and tends to be saline (Nachshon *et al.*, 2013; van der Kamp *et al.*, 2016). A *semi-permanent pond* is one that rarely, if ever, dries out. *Permanent ponds* retain large volumes of water from previous years and are associated with large depressions with permanent deep water that verge on functioning as lakes. An *ephemeral pond* is dry by the end of summer and may dry out within days of the end of the snowmelt period. Where the term *ephemeral wetland pond* is used in this thesis, it has been used solely in reference to the residence time of water in the wetland/ pothole. In some cases, the soil and vegetation cover of the ponded area may not meet the fundamental definition of wetlands (Richardson *et al.*, 1994; van der Kamp *et al.*, 2016). *Ephemeral wetland pond* when used includes wetland ponds that are periodically covered by standing or slow moving water and typically have open water for only a few weeks after snowmelt or several days after heavy storm events (i.e., *temporary ponds*) and ponds that come during the spring either by stream flow that disappear before the summer or during the summer (i.e., *seasonal*

ponds) (Stewart and Kantrud, 1971). A *flow-through pond* is at an intermediate location along a groundwater flow path, and both receives and loses groundwater. A *terminal pond* is in a depression such that it does not spill surface water to the surrounding landscape. Note, a terminal pond can be a recharge pond or a discharge pond, and a terminal pond may or may not receive surface water inputs. *Fill and spill* is the term used to describe the process by which ponds may exchange surface water (Spence and Woo, 2003; Shaw *et al.*, 2012a). Clay-rich *aquitards* are restricting layers of clay found between the shallow groundwater and the intertill aquifers that inhibit the flow of groundwater within the till (Hendry et al., 2004). *Shallow groundwater* is an unconfined groundwater system that is found a few meters below the ground surface in the weathered glacial till (Mcmonagle, 1987; Barr and County, 1996). The shallow groundwater is underlain by an *intertill aquifer*, and this is a confined gravel and sand aquifer system that lies between aquitards and the shallow groundwater, and here we are interested in the uppermost of such aquifer in the profile.

Chapter 2 is a detailed description of the development of a new water-isotope-mass balance model and the model performance in relation to the established models and methods in the literature. The new model was used to estimate evaporation, infiltration, and storage volume with outputs that represent the water balance over the summer months. The model takes into account the influence of time-varying precipitation on water levels (volume) and isotope compositions as well as pond basin bathymetry on the fluxes and corresponding isotope compositions of ponds. It is also demonstrated in this Chapter, the usefulness of stable isotope data from wetland ponds in identifying and characterizing the hydrology of wetland ponds in the face of changing climate and extreme wet years. Wetland pond water levels and chemistry vary seasonally and multi-yearly in seasonally frozen semi-arid climates. The variability makes it difficult to identify, classify or predict hydrologic function and behaviour of wetland ponds using dissolved ions (Heagle *et al.*, 2013; Goldhaber *et al.*, 2014; Nachshon *et al.*, 2014; Cressey *et al.*, 2016; Hayashi *et al.*, 2016). In much the same way, the use of conservative dissolved ions to estimate fluxes are also hampered because their sources and geochemical reactions are not easy to quantitatively estimate (Heagle *et al.*, 2007; Pennock *et al.*, 2014). The spatial and temporal variations in pond isotope and pond water level data allow for the use of an isotope-mass balanced equation to quantify and partition infiltration losses from evaporation. Stable isotope tracers which are an inherent part of the water

molecule itself and therefore serve as ideal tracers and have been used in quantitative models (e.g., (Skrzypek *et al.*, 2015) to estimate hydrologic fluxes. However, the assumptions upon which these models are based, are not entirely representative of the hydrological conditions that impact the vast variety of wetland ponds in the semi-arid glaciated plains of the PPR and wetlands globally.

Chapter 3 is focused on understanding the relationships between various wetland ponds, the shallow groundwater, aquitards and the intertill aquifer at SDNWA. It is shown in this Chapter that depression-focused recharge is a good conceptual model for this landscape, but ephemeral ponds, which are easy to overlook, play a dominant role in intertill aquifer recharge. The role and contribution of wetlands in supplying water to shallow groundwater systems in the Prairies are well documented (van der Kamp and Hayashi, 2009; Johnson *et al.*, 2010; Nachshon *et al.*, 2014; Pennock *et al.*, 2014) and Chapter 2 supports this. Here, this work is extended to evaluate the interactions between the various types of ponds, the shallow groundwater, aquitards, and intertill-aquifer. Wetland pond hydrologic functions are shown to be strongly influenced by subsurface groundwater (Devito *et al.*, 1996). Thus, understanding the relative connections between the underlying intermediate intertill aquifer, aquitards and the wetlands will be highly beneficial for management purposes in the region.
An integrated approach involving physical measurements, and water isotopes (^{18}O, ^{2}H, and ^{3}H) analysis was used to determine qualitatively, the sources and interactions between the wetland ponds, shallow groundwater, aquitard, and the intermediate intertill aquifer (<50m). Inter-comparison was made between individual ponds, shallow groundwater, aquitards and the intertill aquifer on a small scale. A similar comparison was made between water from the ponds, shallow groundwater, aquitards and intertill aquifers at the reach scale. This analysis was made with respect to the Saskatoon local meteoric water line, and precipitation (snow melt-runoff and rainfall) isotopes and hydraulic head measurements at the site. Tritium measurements of five-selected shallow groundwater, aquitards, and the aquifers were used to infer semi-quantitative ages and travel velocities of the subsurface groundwater units.

In Chapter 4, the objective is to provide an understanding of the groundwater recharge mechanism(s) through analysis of water flow and solute transport from a recharge wetland pond, lowland and upland areas to the intertill aquifers using water chemistry and stable isotopes of

water. It is shown here that the major processes responsible for the intertill aquifer replenishment is macropore flow through fractures in the shallow weathered till from both upland and lowland depressions. The flow process is curtailed in the deeper till by poorly fractured till resulting in slow matrix flow. In addition, the difficulty in obtaining useful inferences about the flow processes from observed dissolved ion profiles in this environment is highlighted following the complex combination of processes responsible for dissolved ion concentrations in the till.

In Chapter 2, it is shown that the relatively deep intertill aquifers (< 50 m) in the glacial till are recharged by ephemeral ponds. However, the contribution from other landscape (i.e., the uplands and lowlands areas) and the flow paths and flow rates from these are not known and often assumed to be negligible (Woo and Rowsell, 1993). Studies on groundwater recharge pathways which involves the water flow and solute transport from the ground surface to relatively deep intertill aquifer (0-50 m depth) are not common, and the few that exists (Remenda *et al.*, 1996; Stumpp and Hendry, 2012) are mostly limited to upper 25 m depths or are concentrated on the deeper fractured till (11 to 50 m depth) (Hendry *et al.*, 2015b). The understanding of groundwater recharge pathways is essential for preventing contamination to vulnerable aquifers and obtaining more reliable recharge flux estimates to avoid over-abstraction (Healy and Scanlon, 2010). And it is important for water resource and salt management, in the semi-arid/ arid regions and the North America Prairies where, salinity is a major problem for farmers, and evapotranspiration exceeds precipitation. To improve our understanding of groundwater recharge sources and mechanisms of recharge in relatively deeper the glaciated till, a multi-tracer approach using stable isotopes tracers (^{18}O, ^{2}H, and line condition (lc)-excess), dissolved ions, chloride (Cl^-) and sulphate (SO_4^{2-}) and soil properties was employed to investigate the flow of water and transport of solutes. High-resolution pore waters from 0-14 m at approximately 0.15 m interval was obtained from a recharge pond, upland and lowland areas (near a pond) at three locations, and this data was analyzed together with archived data from pond, piezometers and the intertill aquifers at 41 m depths. Spatial differences in soil properties, isotope tracers, and chemistry, were interpreted to infer water flow and solute transport.

CHAPTER 2: QUANTIFYING WETLAND WATER BALANCES

Status: Under review Journal of Hydrology, January, 2018

Citation: Bam, Edward K.P, Ireson, Andrew M., McDonnell, Jeffrey J. (2018), Quantifying wetland water balances. Journal of Hydrology Manuscript # HYDROL27156 under review

2. 1. Abstract

The water balance of wetland ponds is controlled by interactions with the subsurface and is highly sensitive to changes in precipitation and temperature, especially in semi-arid environments. Interactions with the subsurface vary both spatially, that is between ponds in different parts of the landscape, and temporally, that is as a function of climate variability and change. We demonstrate how physical and isotopic observations can be combined to partition the separate losses of water of evaporation and infiltration from a pond. An isotope-mass-balance model was developed and applied to quantify fluxes for four wetland ponds in the Canadian Prairies, during the unfrozen spring-summer-fall period. Pond infiltration rates ranged between 0.99 and 9.2 mm/d, while open water evaporation rates ranged between 0.88 and 2.8 mm/d. Infiltration rates were highest in the ephemeral ponds, that is ponds that dry out within days or weeks of the spring melt period, and in these ponds, infiltration exceeded evaporation. In permanent ponds, that is ponds that do not dry out, evaporation exceeded infiltration. Evaporation rates were largest for permanent ponds that were not sheltered by topography or riparian vegetation. The approach here can be used to identify how particular ponds interact with the subsurface, independent of any groundwater observations, and to quantify the spatial variability in hydrological fluxes across landscapes.

2. 2. Introduction

Wetlands provide important ecosystem services, including flood mitigation, groundwater recharge, sediment and pollutant trapping, and fish and wildlife habitat. Wetland Ponds (defined as open water areas within wetlands) serve as important sources of food and breeding grounds for migratory birds and other living organisms (Bortolotti *et al.*, 2013). In the Great Plains of North America, there are millions of wetland ponds in the so-called Prairie pothole region (Hayashi and Van Der Kamp, 2000; Steinman *et al.*, 2010; Hayashi *et al.*, 2016). The eco-hydrological functionalities of wetlands in this semi-arid climate depends on the seasonal water cycles (Labaugh *et al.*, 1996, 1997; Winter, 2000; Jolly *et al.*, 2008; van der Kamp *et al.*, 2008; van der Kamp and Hayashi, 2009; LaBaugh *et al.*, 2016). Accurate estimation of water budget components and the accompanying physical and chemical changes in the wetland pond, groundwater and riparian zone are essential for calibration and validation of hydrological and biogeochemical models.

Wetlands form in topographic depressions, and within the wetland there is often a pond, which may be types 1 and 2, i.e., ephemeral/temporary ponds (free surface water after lasting only few days to weeks but dries up in the summer after snowmelt or storm events in early spring) or type 3 i.e., seasonal ponds (ponds are characterized by shallow marsh vegetation, which generally occurs in the deepest part of the pond and usually dry by midsummer). Also the wetland ponds may be semi-permanent (type 4) i.e., ponds that maintain surface water throughout the growing season, i.e., from May to September or lacks of persistence most of the years. They are dominated by marsh vegetation at the central zone of the wetland, as well as coarse emergent plants or submerged aquatics, including cattails, bulrushes and pondweeds. Permanent wetland ponds (type 5) are ponds that always hold large volume of open water for most years in central zone. They are generally devoid of vegetation but submerged plants may be present in the deepest zone, while emergent plants (such as cattails, red swampfire and spiral ditchgrass) are found along the edges (Stewart and Kantrud, 1971). The water balance of wetland ponds are controlled by meteorological forcing, subject to strong seasonal and inter-annual variability, and by spatially and temporally variable surface and subsurface processes (Jolly *et al.*, 2008; van der Kamp and Hayashi, 2009; Hayashi *et al.*, 2016). In seasonal drought-prone climates like the Prairies, water balance and lake residence time are controlled by climate variables and lake parameters of area, volume and shape (Benson and Paillet, 1989; Steinman *et al.*, 2010; Hayashi *et al.*, 2016). Ponds are fed by direct

precipitation, snowmelt- and rainfall-runoff, and in some cases channelized inflows. Ponds lose water by evaporation, infiltration and if the storage exceeds some threshold, spill which forms either overland flow or channelized outflow. Water that infiltrates may become transpiration from the riparian zone or recharge to the underlying groundwater system. The direction of groundwater-surface water interactions varies spatially as a function of landscape position ("recharge ponds" tend to lose water to groundwater, while "discharge ponds" tend to gain water from groundwater) and temporally as a function of seasonal and inter-annual meteorological forcing (Leibowitz and Vining, 2003; Brannen *et al.*, 2015; Leibowitz *et al.*, 2016).

Whilst the main water balance controls are well known, at least conceptually, the chemistry of ponds is less well understood especially in terms of seasonal and inter-annual variability (Labaugh *et al.*, 1997; Pennock *et al.*, 2014). These temporal chemical dynamics are often difficult to explain as simply resulting from dilution by precipitation and subsequent enrichment by evaporation (Heagle *et al.*, 2013; Goldhaber *et al.*, 2014). Ponds typically receive solutes from surface runoff, but solute additions from groundwater exfiltration can also occur in some ponds (Leibowitz and Vining, 2003; Nachshon *et al.*, 2014; Goldhaber *et al.*, 2016; Leibowitz *et al.*, 2016). The subsequent geochemical and biochemical interactions within the pond and underlying wetland soils may add or remove solutes from the wetland (Heagle *et al.*, 2007; Pennock *et al.*, 2014; LaBaugh *et al.*, 2016). The long-term fluctuations in chemistry of wetland ponds are also caused by multi-year, wet-dry variations of meteorological forcing (Goldhaber *et al.*, 2014, 2016; Cressey *et al.*, 2016; LaBaugh *et al.*, 2016) and typically, ponds that lose water to the groundwater system tend to have lower salinity than ponds that gain water from the groundwater system. Nachshon *et al.*, (2014) showed that extreme wet conditions can cause groundwater discharge and surface runoff of salts from the upland area into freshwater ponds resulting in fresh water ponds becoming salinized. The significant variations in soluble ion concentrations, as a result, extreme wet conditions mean that it is possible to misinterpret short-term datasets of pond water chemistry. The impact of the seasonal variability also could hamper our ability in using water chemistry, salinity and electrical conductivity measurements (for example, Pennock *et al.*, 2014) to describe wetland ponds hydrology. Furthermore, the implication is that the seasonal variability associated with changing precipitation amount combined with complex biogeochemical processes that occur

within a wetland pond, will make it difficult to use chemical ions/solutes as effective tracers when estimating hydrological fluxes in such terrain (Dogramaci *et al.*, 2015; Skrzypek *et al.*, 2015).

Studies involving the qualitative and quantitative analysis of stable isotopes of surface water bodies have been reported in the Prairie Pothole region of North America (Fritz *et al.*, 1987; Gibson *et al.*, 1993, 1998, 2002, 2005; Gammons *et al.*, 2006; Pham *et al.*, 2009; Steinman *et al.*, 2010; Wassenaar *et al.*, 2011; Gibson and Reid, 2014), Europe (Jones *et al.*, 2016), Latin America, Asia and Africa (Gat and Levy, 1978; Dincer *et al.*, 1979; Zuber, 1983; Gonfiantini, 1986; Kebede *et al.*, 2009). These studies show that seasonal isotopic variability within surface water bodies is significant and contains useful information about the hydrological processes, but only a few studies have used stable isotopes thus far to describe the variability in the functioning of different wetland ponds particularly in the North American Prairies and seasonally cold semi-arid regions. It is our goal to interpret the differences in stable isotope compositions of various types of wetland ponds and hence to describe their differing hydrologic regimes.

Globally, quantitative models (Gonfiantini, 1986; Gibson *et al.*, 1996, 2002, 2008b, 2016; Steinman *et al.*, 2010; Skrzypek *et al.*, 2013, 2015) formulated based on the isotope-evaporation equation of Craig, and Gordon (1965) and large lake water-budget equation of Gonfiantini (1986) have been developed and used to describe surface water response to meteorological forcing and estimate evaporation to water input ratios in data scarce regions. The models consider the initial and final isotope compositions of the water body, relative humidity and temperature and atmospheric water vapour isotope compositions to compute the fraction of water loss to evaporation or evaporation- inflow ratios. The effect of isotopic inputs from isotopically distinct water (e.g. rainfall) on computed fractions or evaporation-inflow ratio is considered negligible, largely because the lake and river volumes are assumed to be too large to be affected by such additions (Skrzypek *et al.*, 2015). The models also assumed that the water bodies do not leak (lose water by infiltration), and have a constant surface area, and hence ignore how surface area reduces as the water level declines. Laboratory studies on isotope enrichment in leaking containers, however, have shown that the key parameter controlling the degree of isotope enrichment is the remaining fraction of water in the container (Rozanski and Chmura, 2008)). Thus the neglecting the impact of infiltration on water bodies in estimating evaporation fluxes from isotope-mass-balance models will be ridden with large errors. Overall, these assumptions are problematic for

areas where rainfall over small lakes and ponds are significant, ponds leaks, and/or water level declines or increases and could thereby significantly altering the isotopic composition of the surface water body. The key next step is, therefore, to develop a new physically-based isotope-water balance model that incorporates time-varying rainfall amount and isotope compositions, and basin area and shape factors.

In this paper, we combined field measurements of water levels, atmospheric measurements, and water isotopes to understand, and model the isotope and water mass balance of various Prairie wetlands. This work was performed at the well-studied St Denis National Wildlife Area (van der Kamp and Hayashi, 2009; Bortolotti *et al.*, 2013; Nachshon *et al.*, 2014; Pennock *et al.*, 2014; Hayashi *et al.*, 2016). Our objectives are to i) explore the use of stable isotope composition records of wetland ponds to characterize them; ii) to develop a new physically based isotope-water balance model that accounts for additions of precipitation (resulting in volume and isotope composition changes) and different pond geometries through the summer ice-free season; iii) test the model sensitivities to changing pond geometries and climate parameters; and iv) to compare our model results with independent estimates of evaporation, infiltration, and storage from the existing models where feasible.

2. 3. Study Site and Field Methods

2. 3. 1. The study site

Fieldwork was conducted between May and October of 2014 to 2016 at the 385-ha St. Denis National Wildlife Area, SDNWA, (52.8 N, 106.8 W) in the Canadian Prairies, shown in Figure 2. 1a. The study area and the wetland ponds locations at the SDNWA are shown in Figure 2. 1b with the wetlands studied identified in numbers. This site is 40 km east of Saskatoon, Saskatchewan, Canada. The SDNWA was established in 1968 as a long-term study site for the ecological monitoring of the prairie wetland complex (Hogan and Conly, 2002). There are close to one-hundred ponds of varying size and hydrological seasonality at the SDNWA (Woo and Rowsell, 1993; van der Kamp and Hayashi, 2009). The climate is semi-arid with significant inter-annual variability in precipitation and temperature during the summer (April to September) and winter (October to March) months. The mean annual non-adjusted (for wind-caused under-reported winter snowfall) precipitation at Saskatoon is 360 mm, with about 280 mm occurring as rainfall in

April to October (Parsons *et al.*, 2004; Nachshon *et al.*, 2014). The monthly mean temperature varies between -20°C in the period December to February to 19°C in the period July to August (Wittrock and Beaulieu, 2015). Just like other prairie sites, the annual lake evaporation exceeds the total annual precipitation (Parsons *et al.*, 2004).

The arithmetic mean for a twenty-four year monthly integrated record of isotopes in precipitation for Saskatoon is -17.0‰ and -131.0‰ for $\delta^{18}O$ and $\delta^{2}H$, respectively. The amount-weighted mean values of $\delta^{18}O$ and $\delta^{2}H$ for the period June 1990 to November 2014 are -14.4‰ and -112.5‰, respectively (Unpublished data Kholer personal communication). The summary of the values of monthly amount precipitation, temperature, $\delta^{18}O$, $\delta^{2}H$ and the local Saskatoon meteoric water line for the period 1990 to 2014 is given in Figure 2.2.

The study was conducted at pond 50, 109, 117 and 120. The wetlands were selected based on previous wetland pond classification of Stewart and Kantrud (1971): Ephemeral pond (117); Semi-permanent pond (120); and Permanent pond (109 and 50). Ponds 117, 120 and 109 can be described as "recharge ponds", since they have hydraulic head values that are elevated above the potentiometric surface of the underlying confined aquifer system as shown in Figure 3.5 in Chapter 3. Pond 50 has a hydraulic head that is more-or-less in the same head stage with the underlying groundwater system and is therefore neither a recharge pond nor a discharge pond (see Chapter 3, Figure 3.5). The hydro-meteorological tower near pond 109 on the site collects half-hourly measurements of air temperature, relative humidity, and precipitation at 2 m and 10 m heights for the 2014 season.

Figure 2.1. a) Location of the Prairie Pothole Region in the midcontinent of North America (van der Kamp and Hayashi, 2009) **showing SDNWA.**

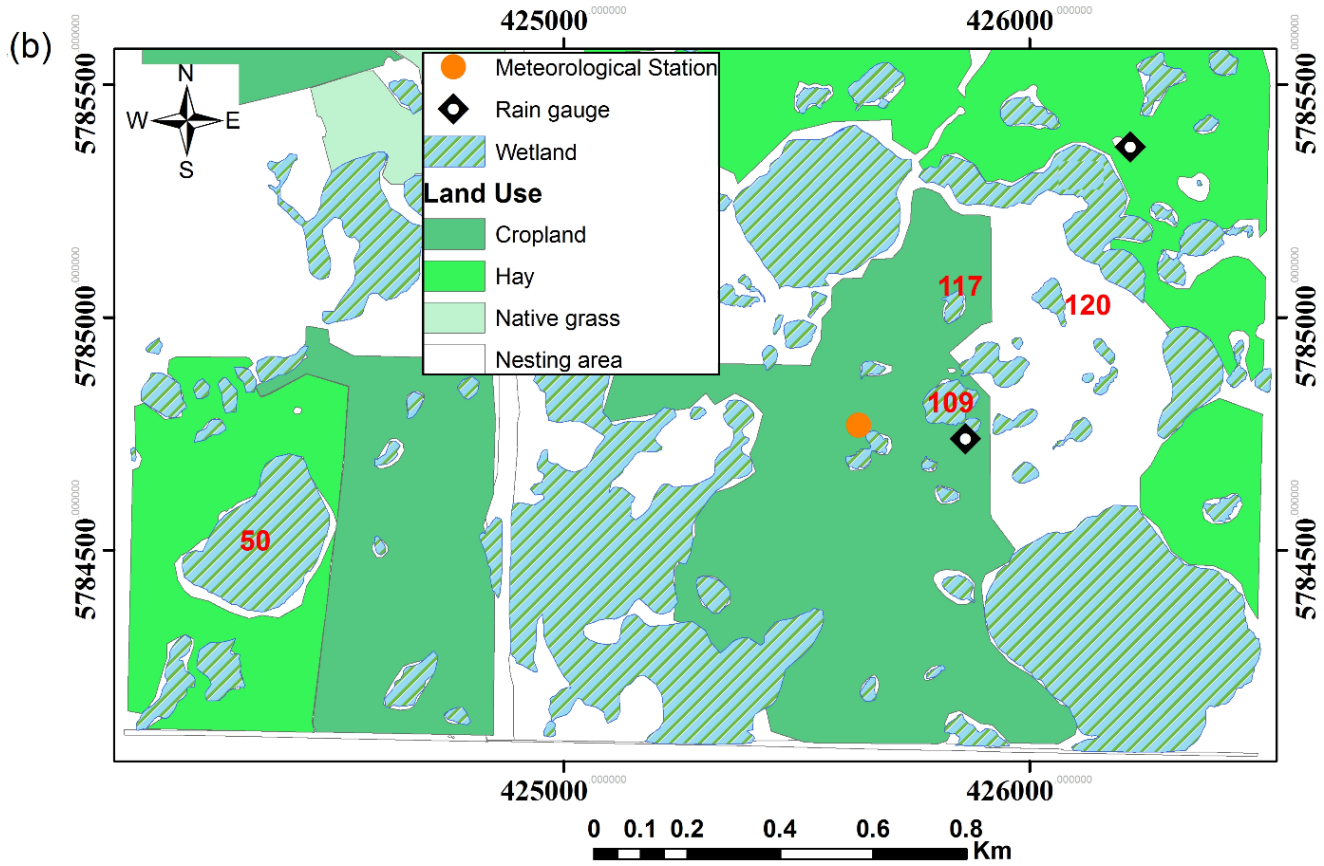

Figure 2.1. b). The St. Denis National Wildlife Area, Saskatchewan showing wetland in numbers used in this study and other wetlands and land use in the area.

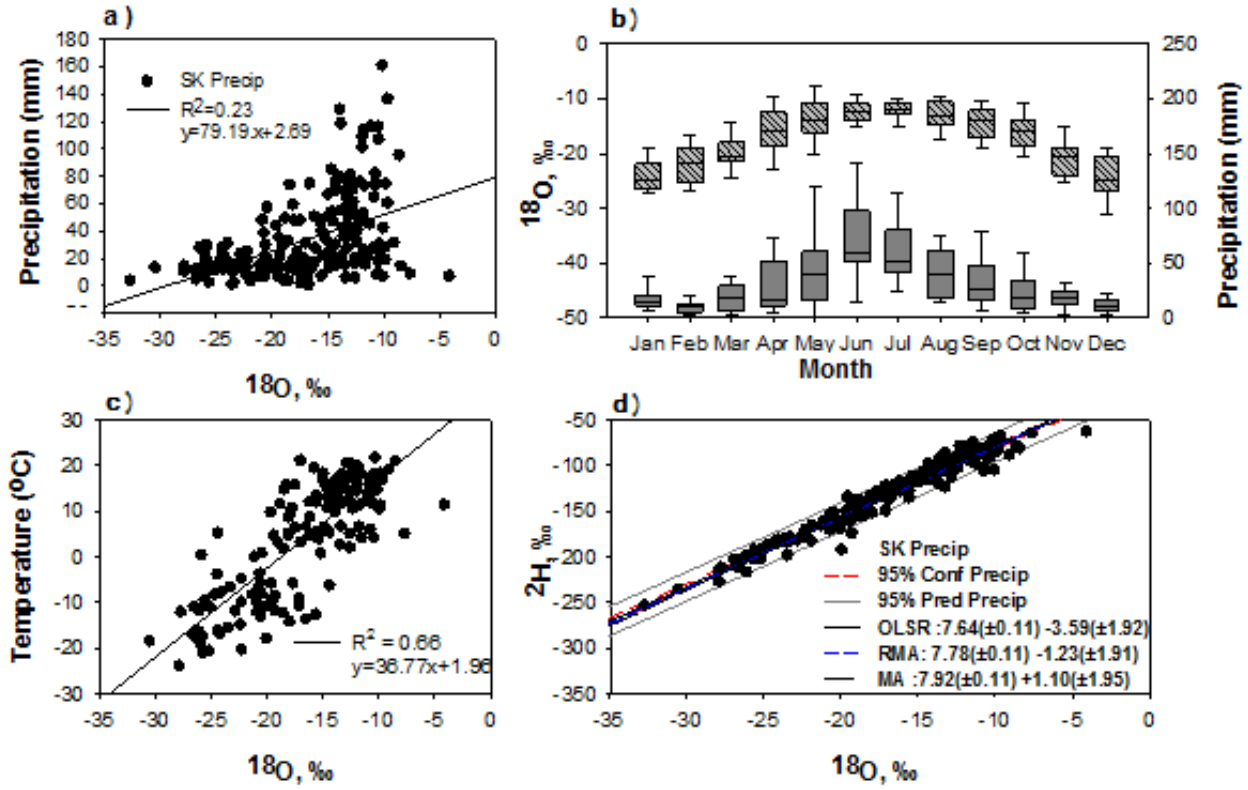

Figure 2.2. Monthly integrated $\delta^{18}O$ variations with temperature and non-adjusted precipitation amount in Saskatoon precipitation June 1990 to December 2014. Included are equations for the local meteoric water line predicted for various statistical methods.

2. 3. 2. Hydrological measurements

The water level in the pond was measured at reference poles installed within the wetlands (Conly *et al.*, 2004) and then converted to the depth of water (in meters) at the deepest location in the wetland. The area, A (m^2), and volume, V(m^3), of surface water stored in the wetland was estimated using the equations described in Hayashi and Van Der Kamp, (2000) and Hayashi et al., (2016) as a function of water depth, k (m):

$$A = sk^{2/p} \quad (2.\ 1)$$

$$V = \frac{sk^{(1+2/p)}}{1+2/p} \quad (2.\ 2)$$

where s (m^2) is a scale parameter (equal to the pond surface area when the depth is 1 m), and p is parameter the defines the shape of the idealized pond cross section, where $p = 1$ is an inverted

cone, $p = 2$ is a parabola, and larger values represent a bathtub-shaped basin with a flat bottom and steep sides (Hayashi and van der Kamp 2000). The constants s and p were determined using bathymetry survey data of ponds 50, 109, 120 (Hayashi and Van Der Kamp, 2000; Heagle *et al.*, 2013) and pond 117 (personal comm. van der Kamp, 2009). Meteorological data for SDNWA was collected from the Global Water Institute climate tower installed at the site.

2. 3. 3. Water sampling and isotope analysis

Wetland pond water samples were collected bi-weekly (and sometimes monthly) during the ice-free season (April–October) of 2014. Pond water samples were collected about 2 m from the bank at depths well below the pond water surface into the narrow mouth 50 ml Polypropylene (PP) bottles and sealed. Wetland pond temperature at various locations suggests that the pond water was well mixed. Rainfall samples were collected in between rain events at the location of the rain gauge indicated in Figure 2.1b for comparison with Saskatoon records and amounts recorded during the period was used in 2014 model calculations. All water samples were transported to the Stable Isotope Laboratory at the National Hydrology Research Centre, Saskatoon. The samples were left for debris to settle before stable isotope analysis. The samples were then analyzed for ^{2}H and ^{18}O were using a Los Gatos Research DLT-100 liquid isotope water analyzer system coupled with a CTC LC-PAL liquid auto sampler (Los Gatos Inc., California) at the National Hydrology Research Centre, Saskatoon (Lis *et al.*, 2008) and values are reported in the usual δ notation in units of ‰, vs. Vienna Standard Mean Ocean Water (VSMOW). Analytical precision is approximately ± 0.2‰ for $\delta^{18}O$, and ± 1.0‰ for $\delta^{2}H$, respectively.

2. 3. 4. Archived data

Wetland pond water depths, water temperature, and isotope data, obtained from for the period of 1991–2016 and maintained by the National Hydrology Research Centre, Saskatoon was used. Pond area, volume, and, shape factors obtained from the survey data of van der Kamp (2009, personal communication) and other relevant data found in published works (Hayashi and Van Der Kamp, 2000; Heagle, 2008; Heagle *et al.*, 2013; Hayashi *et al.*, 2016) were also employed. The archived data on precipitation records, relative humidity, and atmospheric temperature measurements of Saskatoon available from Saskatchewan Research Council climate records (http://climate.weather.gc.ca/climateData/dailydata_e.html?).

2. 4. Wetland water and isotope mass balance model

2. 4. 1. Model Development

The water balance equation for a wetland pond is given as:

$$dV = A(P + J - O - E)dt \quad (2.3)$$

where A (m^2) is the area of open water of the wetland, dV (m^3/d) is the change in volume of water in wetland over the time period dt (d), P (m/d) is direct precipitation into the wetland, J (m/d) is the lumped surface and subsurface inflow per unit area, O (m/d) is the lumped surface and subsurface outflow per unit area, and E (m/d) is the direct evaporation rate from the wetland surface.

The change in isotope mass in the wetland is expressed as

$$\frac{d(V\delta)}{dt} = \delta\frac{dV}{dt} + V\frac{d\delta}{dt} = A\left(J\delta_j + P\delta_p - O\delta_o - E\delta_E\right) \quad (2.4)$$

where δ (‰) is the isotope composition and subscripts relate to the water balance equation components defined above, and δ with no subscript refers to pond water.

Equations 2.3 and 2.4 can be generally applied to any surface water body. In general, inflow terms (runoff and groundwater discharge), J, may carry isotopically distinct waters and hence modify the isotopic composition of the water body, while outflow (spillage, infiltration and transpiration) terms, O, remove water and isotope mass, but do not modify the isotopic composition of the water body. In small, well mixed, relatively shallow and seasonally dynamic ponds such as found in the North American Prairies during the ice free-spring to fall period, some simplifying assumptions about these terms can be made. Specifically, the assumption that $J = 0$, and that outflow is due only to sum of infiltration and transpiration, I, into the subsurface which is to say $O = I$, and the justification for these assumptions is stated as follows. The main input of water to the ponds, other than direct precipitation, comes from snowmelt and snowmelt runoff. For the period after the snow and ice melt, that the analysis of this paper is restricted to, we ignore the runoff processes and use initial conditions based on the water levels and isotopic compositions caused by the runoff. Heavy rainfall events can also cause surface runoff to occur, though these are historically fairly rare (Coles et al., 2017). In our dataset there was one year (i.e., 2014) when this did happen, and in that case, the model was initialized after the runoff event. Some ponds receive a significant amount of water

from groundwater - i.e. discharge ponds (Nachshon *et al.*, 2013). To simulate discharge ponds with this model it would be necessary to estimate the isotopic composition of the groundwater, which is a significant challenge worthy of further research, but not addressed here. In this study we are not dealing with any discharge ponds and therefore we do not include groundwater inflow. In terms of pond outflows, it is not necessary to assume that infiltration and transpiration is the only outflow, but we do so here because we know that the ponds selected did not spill during the study period. A significant amount of the infiltration below the pond goes to support riparian zone transpiration (Nachshon et al., 2013), with the remainder going to groundwater recharge (Millar, 1971; Parsons *et al.*, 2004) and also see Chapter 3. However, water loss to both riparian zone plant transpiration and groundwater recharge from the pond do not induce isotope fractionation in the pond water (Gibson and Edwards, 2002; Yepez et al., 2003; Rothfuss et al., 2010; Jasechko et al., 2013), and so the process has not been represented explicitly in this model. Thus, the infiltration reported is responsible for lateral seepage to transpiring marginal vegetation, soil evaporation and groundwater recharge. To constrain each individual flux from the infiltration component, into transpiration and groundwater/soil water recharge, a coupled solute balance method similar to isotope balance could be applied (e.g., Dincer *et al.*, 1979). The solute balance method could, however, be complicated due effects of dilution, mineral precipitation and/or absorption by soil (Heagle *et al.*, 2007; Goldhaber *et al.*, 2014). Hence, no attempt have been made to distinguish how this flux, infiltration, is partitioned between groundwater recharge and transpiration fluxes in this paper, though this is an important problem which has to be looked at in future.

Substituting $J = 0$, $O = I$ and $\delta_o = \delta$ reduces Equations 2. 3 and 2. 4 to Equations 2.5 and 2 6 respectively.

$$dV = A(P - I - E)dt \tag{2.5}$$

$$\delta\frac{dV}{dt} + V\frac{d\delta}{dt} = A\left(P\delta_p - I\delta - E\delta_E\right) \tag{2.6}$$

Replacing dV/dt in Equation 2. 6 with equation 2. 5 yields:

$$V\frac{d\delta}{dt} + \delta[A(P - I - E)] = A\left(P\delta_p - I\delta - E\delta_E\right) \tag{2.7}$$

which reduces to

$$\frac{d\delta}{dt} = \frac{A}{V}\left[P(\delta_p - \delta) - E(\delta_E - \delta)\right] \tag{2.8}$$

While the terms A, V, P, δ and δ_p can be measured directly in the field (or laboratory), E and δ_E cannot. The isotopic composition of moisture evaporating from the lake surface, δ_E, is estimated by a linear resistance model of Craig and Gordon (1965) as defined (Gammons *et al.*, 2006; Horita *et al.*, 2008):

$$\delta_E = \frac{1}{1 - H + \frac{\Delta\epsilon}{1000}}\left(\frac{\delta - \epsilon}{\alpha} - H\delta_a - \frac{\Delta\epsilon}{1000}\right) \quad (2.9)$$

Where ϵ (-) and $\Delta\epsilon$ are the equilibrium and kinetic isotopic separation between liquid and vapor, respectively, α (-) is the fractionation factor and H (-) is the relative humidity. The Craig and Gordon (1965) model was developed to describe the isotopic fractionation associated with evaporation. The model assumes the atmosphere above a given liquid surface to be three discrete layers: (i) a saturated sublayer with 100% relative humidity that attains isotopic equilibrium at the liquid- air interface; (ii) a laminar layer less than 100% relative humidity above layer 1 where vertical transport of water molecule due to the molecular diffusion across the humidity gradient resulting in isotopic fractionation; and (iii) a turbulent atmosphere where turbulent transport dominates with no isotopic fractionation. The equilibrium isotopic separation between liquid and vapor, $\epsilon\,(-)$, is calculated as (Gammons *et al.*, 2006)

$$\epsilon = 1000 * (\alpha - 1) \quad (2.10)$$

where α is the fractionation factor which is a function of temperature, T (K). The equations of the liquid water-vapor fractionation factor (valid between 0 and 374 °C) obtained from laboratory experiments, are given for $\delta^{18}O$ and δD as follows (Horita and Wesolowski, 1994):

$$\ln \alpha_{18O} \times 10^3 = -7.685 + 6.7123\left(\frac{10^3}{T}\right) - 1.6664\left(\frac{10^6}{T^2}\right) + 0.35041\left(\frac{10^9}{T^3}\right) \quad (2.11)$$

$$\ln \alpha_D \times 10^3 = 1158.8\left(\frac{T^3}{10^9}\right) - 1620.1\left(\frac{T^2}{10^6}\right) + 794.84\left(\frac{T}{10^3}\right) - 161.04 + 2.9992\left(\frac{10^9}{T^3}\right) \quad (2.12)$$

The equivalent kinetic isotopic separation based on wind tunnel experiments is calculated from (Gonfiantini, 1986):

$$\Delta\epsilon = (1 - H)\theta n C_k \quad (2.13)$$

where $n = 0.5$ for rough surface, e.g., open water bodies and $n = 1$ for soil water, $\theta = (1 - H_o)(1 - H)$ is an advection term to account for the potential influence of humidity buildup,

H_o is the adjusted humidity of the downwind atmosphere following admixture of evaporating moisture over the surface, often set to $\theta = 1$ for small water bodies, and C_k is the kinetic fractionation constant, which is 28.6% and 25.0% for oxygen-18 and deuterium, respectively (Araguas-Araguas *et al.*, 2000). As a result, we have here

$$\Delta\epsilon_{18O} = 14.2(1 - H) \tag{2.14}$$

$$\Delta\epsilon_{D} = 12.5(1 - H) \tag{2.15}$$

If the relative humidity, *H*, is measured near the pond/lake, it must be normalized to reflect the relative humidity over the pond surface under saturated conditions. The saturated vapor pressure, e_s (kPa), can be estimated from (Allen *et al.*, 1998):

$$e_s = 0.6108e^{\left[\frac{17.27(T-273)}{T}\right]} \tag{2. 16}$$

where T (Kelvin) is the temperature measured near the pond. The normalized relative humidity, e_s is calculated from the ratio of e_s in air (e_{sa}) and e_s in water (e_{sw}) based on temperature measurements and multiplied by the relative humidity measured near at the site.

Substituting Equation 9 into Equation 8 yields

$$\frac{d\delta}{dt} = \frac{A}{V}\left[P(\delta_p - \delta) - \frac{E}{1 - H + [\frac{\Delta\epsilon}{1000}]}\left(\frac{\delta - \epsilon}{\alpha} - H\delta_a - \frac{\Delta\epsilon}{1000}\right) - E\delta)\right] \tag{2.17}$$

and factorizing and re-arranging, gives

$$\frac{d\delta}{dt} = \frac{A}{V}\left[P\left(\delta_p - \delta\right) + E(B - C\delta)\right] \tag{2.18}$$

where

$$B = \frac{H\delta_a + \frac{\Delta\epsilon}{1000} + \frac{\epsilon}{\alpha}}{1 - H + \left[\frac{\Delta\epsilon}{1000}\right]} \tag{2.19}$$

and

$$C = \frac{H - \left[\frac{\Delta\epsilon}{1000}\right] - \frac{\epsilon}{1000 * \alpha}}{1 - H + \left[\frac{\Delta\epsilon}{1000}\right]} \tag{2.20}$$

Integrating Equation 2. 18, the isotope composition of the pond water at time *t* is:

$$\delta(t) = \delta_i e^{-\frac{(AP+AEC)t}{V}} + \frac{EB + P\delta_p}{P + EC}\left(1 - e^{-\frac{(AP+AEC)t}{V}}\right) \tag{2.21}$$

δ_i refers to the initial isotopic composition of the pond.

Estimating the water balance using the wetland pond water level, we substituted Equations 2. 1 and 2. 2 into Equation 5 resulting in

$$d\left[\frac{sh^{1+2/p}}{(1+\frac{2}{p})(sh^{2/p}}\right] = (P - I - E)dt \tag{2.22}$$

Integrating with respect to h and factorizing the pond water level is given as

$$h(t) = h_i + \sqrt{\frac{P(t) - I(t) - E(t)}{2(\frac{2}{p}+1)}} \tag{2.23}$$

h_i refers to the initial water level of the pond.

Equations 2.23 and 2.21 solve the water balance and isotope mass balance, respectively. The water balance equation simulates the pond water level, given some specified total loss from the pond (E and I combined). Thus, given observations of pond levels, inverse modelling can be used to identify the total loss i.e., $E + I$, but not the partitioning between these variables. Similarly, the isotope mass model takes some specified E to simulate the pond isotope concentration. Given observations of the pond isotope compositions, inverse modelling can be used to identifyE, and henceI. Inverse modelling was achieved here by optimization, minimizing the RMSE of pond level (stage 1) or pond isotopic concentration (stage 2), by changing $E + I$ (stage 1) and E (stage 2). Optimization was performed in Python 2.7 using the Scipy function fmin, which uses a Nelder-Mead simplex algorithm (https://docs.scipy.org/doc/scipy/reference/generated/scipy.optimize.fmin.html).

This model can be used to i) estimate E and I from a specific pond from past observations of pond/climate variables, or to ii) project pond isotope concentrations into the future, given some prescribed partitioning of E and I, along with projections of the hydrometeorological variables. The model scripts are attached as supplementary material in the Appendix A. This script was written and run in Python 2.7.2 (Python Software Foundation, US, 2011), and reads input data from Microsoft Excel files.

2. 4. 2. Stable isotope composition of ambient atmospheric water vapour

The ambient atmospheric water vapour, δ_a, can be measured directly, estimated from precipitation values, or calculated from local evaporation lines of surface water within the catchment (Jacob and Sonntag, 1991; Clark and Fritz, 1997; Gammons *et al.*, 2006; Gibson and Reid, 2014; Skrzypek *et al.*, 2015). Here the ambient atmospheric water vapour (δ_a) were computed using the local evaporation lines (LEL, Table 2.1) obtained from the multiple measurements of the isotopic changes within each individual wetland pond (Bennett *et al.*, 2008; Gibson *et al.*, 2008a, 2016; Gibson and Reid, 2014; Skrzypek *et al.*, 2015). Because the isotopic compositions of pond water in the prairie environment is strongly influenced by seasonal climatic effects (i.e.. Figure 2.3 and Figure 2.4) resulting in highly seasonal evaporation rates, the ambient atmospheric water vapour is calculated assuming the atmosphere is in equilibrium with precipitation during the evaporation season (Gibson, 2002a; Gibson *et al.*, 2016). Thus, an effective precipitation-vapour separation ($\in$ effective, Gibson *et al.*, 2016)) is assumed where the evaporation line slope and the effective isotopic separation between amount-weighted precipitation (falling near the intersection of local evaporation line and meteoric water line) and evaporation-flux weighted moisture, is less than the equilibrium separation. The δ_a was estimated from local records of the spring-summer rainfall stable isotope composition (δ_p) as follows (Bennett *et al.*, 2008; Gibson and Reid, 2014; Skrzypek *et al.*, 2015; Gibson *et al.*, 2016):

$$\delta_a = (\delta_p - f * \epsilon)\text{rain}/(1 - f * \in * 1/1000) \tag{2.24}$$

where (δ_p) is the stable isotope composition of rain (δD and $\delta^{18}O$) and $\in$ is the equilibrium isotopic separation between liquid and vapor; which depends only on temperature as described in equations 2.10 to 2.12 (Horita and Wesolowski, 1994). Initially, equation 2.24 was solved using $f = 1.0$ and then the slope of LEL was calculated from equation 2.25:

$$\text{Slope}_{(\text{LEL})} = \frac{\left[\frac{H*\left(\frac{\delta D_{atm} - \delta D_{rain}}{1000}\right) + \frac{\varepsilon}{1000}*\left(1+\frac{\delta D_{rain}}{1000}\right)}{H - \frac{\varepsilon}{1000}}\right]D}{\left[\frac{H*\left(\frac{\delta^{18}O_{atm} - \delta^{18}O_{rain}}{1000}\right) + \frac{\varepsilon}{1000}*\left(1+\frac{\delta^{18}O_{rain}}{1000}\right)}{H - \frac{\varepsilon}{1000}}\right]O} \tag{2.25}$$

where H is air relative humidity (given as a fraction) ε is the total fractionation factor and equals the sum of the equilibrium isotope fractionation factor $\in$, as given above plus the kinetic isotope fractionation factor $\Delta\in$ (Gibson and Reid, 2010):

$$\varepsilon = \frac{\epsilon}{\alpha} + \Delta\epsilon \quad (2.26)$$

The calculation was then repeated a number of times using f between 1.0 and 0.1. The final δ_a values were selected from the f parameter that gave the lowest difference between the calculated slope of LEL (equation 2.25) and the observed slope of LEL obtained from field measurements (in this case f reached the boundary values between 0.6 and 1.0). The slope of LEL and the final δ_a values for the ponds (Table 2.1) were generally within the range of values reported from the global basis analysis of the International Atomic Energy Agency's Global Network for Isotopes in Precipitation database (Gibson *et al.*, 2008a).

2. 4. 3 Sensitivity analyses

Before the results of such calculations are presented, we first assess the effects of variation of the model parameters (pond bathymetry parameters s and p, and climate parameters P, H, T, and δ_a) on the modelled state variables δ and h and modelled fluxes E and I. Sensitivity simulations were conducted on a monthly time step for the 2014 model year. A univariate sensitivity analysis was performed using baseline pond parameters and average values of the climatic parameters obtained from the site. The effect of each individual parameter on the model was tested one at a time by increasing and decreasing the parameter by a constant percentage. The percentages were determined on the basis of the coefficient of variation of each parameter over the period simulated (4th June and 31st October 2014 simulation months). For the sensitivity analyses, $E + I$ was fixed at an arbitrary value that ensured a reasonable water balance, and the ratio $E/(E + I)$ was varied from 0.1 (infiltration dominates) to 0.9 (evaporation dominates).

Table 2.1. Summary of average climate, isotopic and basin bathymetry parameters of ponds tested using the Prairie wetland isotope-water mass balance model at St Denis National Wildlife Area, Saskatchewan.

		Precipitation			Atmospheric parameters				Shape parameters		
Pond	**Year**	**Amount** (mm)	$\delta^{18}O_p$ (‰)	$\delta^{2}H_p$ (‰)	**T** (˚C)	**H** (-)	$\delta^{18}O_a$ (‰)	$\delta^{2}H_a$ (‰)	**s** (m^2)	**p** (-)	**LEL** (-)
50	1994	173	-11.9	-96.4	15.4	0.68	-19.7	-155.6	29500	2.5	5.4
50	1998	84	-11.7	-96.9	16.9	0.63	-20.4	-161.7	29500	2.5	5.3
50	1999	150	-13.0	-107.2	16.4	0.61	-22.7	-171.95	29500	2.5	5.3
50	2014	67	-13.2	-107.2	14.8	0.70	-23.1	-179.7	29500	2.5	5.8
109	1994	157	-12.5	-103.0	15.4	0.68	-19.4	-154.8	3180	1.6	5.9
109	1997	118	-13.3	-102.3	16.8	0.66	-22.0	-166.8	3180	1.6	5.2
109	1998	108	-11.7	-96.9	16.9	0.63	-20.4	-161.7	3180	1.6	5.4
109	2014	108	-13.5	-103.7	11.2	0.68	-23.7	-179.9	3180	1.6	5.6
117	2014	88	-13.1	-104.6	11.9	0.70	-21.2	-166.0	2844	1.0	5.9
120	2014	165	-13.3	-103.3	11.2	0.70	-23.5	-179.5	2798	2.7	5.7

2. 4. 4. Model application to SDNWA

The model was applied to estimate E and I for four ponds in the SDNWA, one ephemeral (pond 117), one semi-permanent (pond 120), and two permanent (pond 50 and 109). The model driving data is given in Table 2.1. Since the model assumes there is no input to the pond, other than from direct rainfall, it must be initiated after snowmelt, or any major rainfall-runoff event has occurred. The initial conditions for the model are the water level and the isotopic composition of the pond water. The start and end date for each simulation (i.e. for each pond, each year) was chosen based on the periods where there was minimal surface runoff into the pond during the summer. The simulated years (1994, 1997, 1998, 1999 and 2014) were the years for which pond water levels,

isotope data, and climate data were available. The δ represent average isotope compositions of precipitation and ambient atmospheric moisture. s and p are the pond bathymetric parameters used in Equation 2.1 and 2.2.

2. 4. 5. Model comparison with the *Hydrocalculator* model

An existing model for estimating the evaporative loss of water from a surface water body using stable isotopes is available through the *Hydrocalculator* software (Skrzypek *et al.*, 2015). This is based on the Craig-Gordon model, and available in two formulations: i) the steady-state configuration, which aims to look at the long-term response of a water body under steady-conditions, where the inflow equals the outflow and there is no change in storage (hereafter the HCSS model); and ii) the non-steady-state configuration, which aims to look at the short-term response of a water body when there is a change in storage, but the only loss term is due to evaporation (hereafter the HCNS model). The major advantage of this model over our model is that much less observational data are required, and it is, therefore, useful to get estimates of evaporation from large water bodies in data sparse areas. However, for small prairie ponds, the Hydrocalculator model assumptions are not appropriate – the isotopic composition of the precipitation has a large impact on the pond isotope composition, the pond storage changes are highly significant, with ponds often emptying completely, and the water loses are due to infiltration as well as evaporation. None-the-less, we aimed to compare the evaporation estimates from these two models, HCSS and HCNS, with our estimates, to see how appropriate this simpler approach is for small dynamic prairie ponds.

2. 5. Results

2. 5. 1. Stable isotope characteristics of Prairie wetland ponds

Figure 2.3 shows the temporal variation in stable isotope compositions and pond depth as monitored in Prairie wetlands from 1993-2016 (spring-fall seasons). The water level is at its maximum after snowmelt, when the isotopic enrichment is minimum.

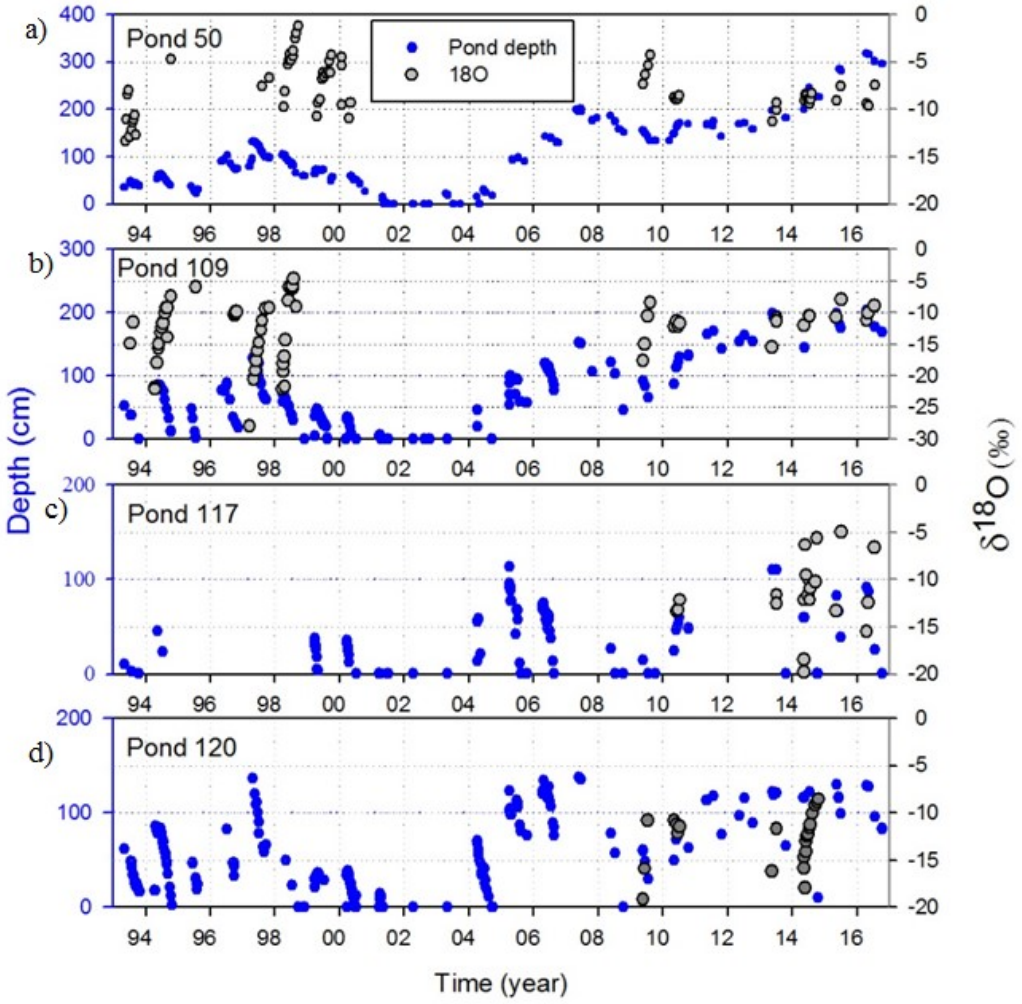

Figure 2.3. Yearly seasonal variations in pond depth and isotope compositions for wetland pond 50 (a), 109 (b), 117 (c), and 120 (d) from 1993 to 2016 at the St Denis Wildlife National Area.

Throughout the summer water levels drop via a combination of evapotranspiration and infiltration; isotopic enrichment develops progressively in response to evaporation. Figure 2.4 shows progressive enrichment in isotope values ($\delta^{18}O$ and $\delta^{2}H$) of the ponds between the years 2010 to 2016 from the month of May (spring) to September (fall). The stable isotope compositions of water found in the permanent ponds (50 and 109) were enriched even at the start of the season (spring) and the ephemeral pond water isotopes were more depleted.

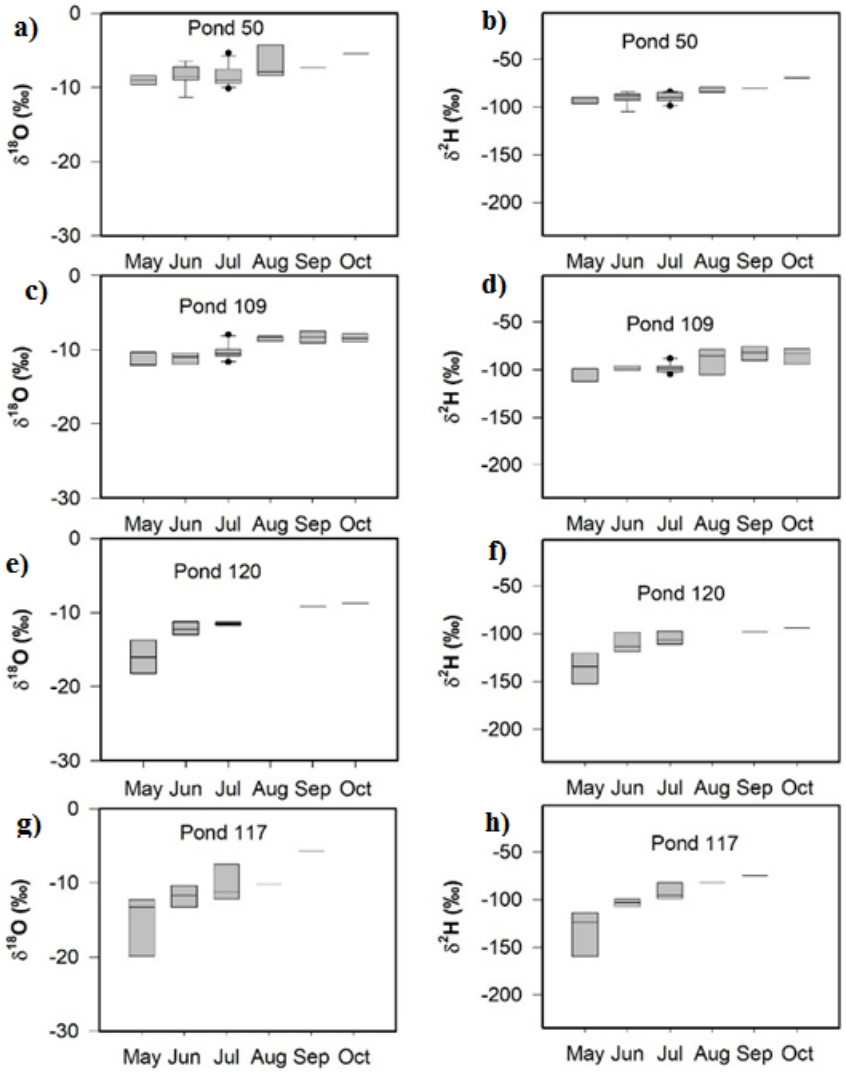

Figure 2.4. Monthly time series of pond isotope evolution within and between ponds for the period between May and October from 2010 to 2016.

Figure 2.5 shows a scatter plot of pond isotope values to examine the effect of evaporation on the wetland ponds for four wetland ponds 50, 109, 117 and 120 at the St Denis National Wildlife Area. The pond isotope values fall below the Saskatoon local meteoric water line defining local evaporation lines slopes between 5.2 and 6.4.

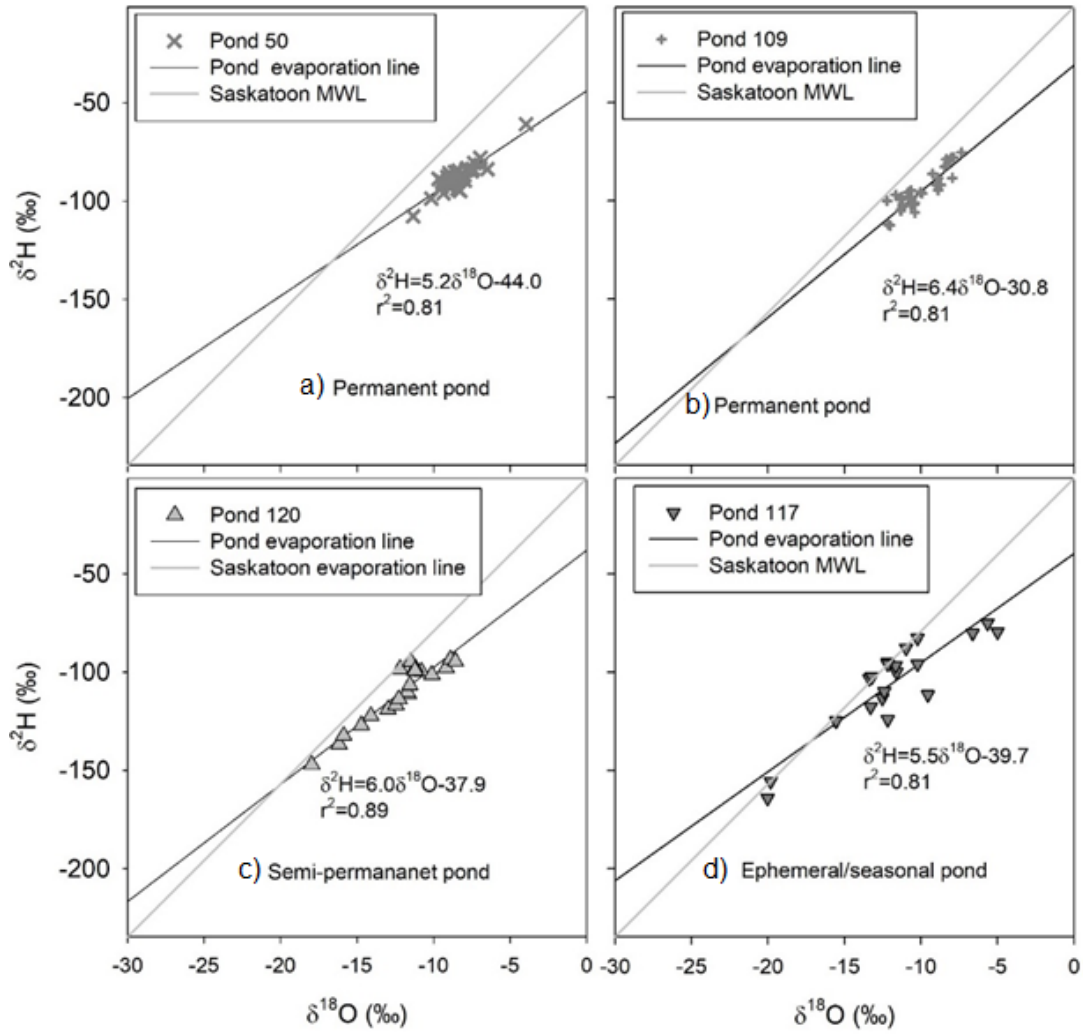

Figure 2.5. Scatter plot of δ^2H-$\delta^{18}O$ of ponds with Saskatoon Local Meteoric Water Line (SKLMWL) for May-October of 2010 to 2016 at St Denis Wildlife National Area.

2. 5. 2. Model sensitivity

Sensitivity tests were run to determine the effects of variations in the climatic variables, relative humidity, H, atmospheric vapor composition, δa, precipitation, P and temperature, T, and pond bathymetry parameters s and p, on the modelled pond isotope content, δ (t). Here the average estimated parameters used in the model for Pond 109 were varied between the maximum and minimum range found in the region. Figure 2.6. shows a contour plot of how the isotopic content of the pond changes as we impose changes in the relative proportion of evaporation to total pond losses (i.e. evaporation plus infiltration), and with perturbation to the parameter values. The

baseline condition (i.e. the center column in each of the subplots) shows how the pond isotope concentration is progressively enriched as the proportion of evaporation increases. The parametric perturbations are shown in the left and right columns in the same subplots, and the more sensitive a parameter is, the more these contours deviate from the baseline contour.

The model strongly affected by changes in relative humidity of the free vapour, H. With ± 15% in H moderate changes can be seen in the isotope compositions of the remaining pond water. The influence of kinetic fractionation process that occurs during evaporation of water vapour from surface water bodies are noted in equations 2.9, 2.13, 2.19 and 2.25. Also the influence of H on the local evaporation line, the ambient atmospheric water vapour composition, and the pond hydrologic balance (affecting evapotranspiration rates) is noted in equation 2.25 and Figure 2.6a. Lowering the relative humidity by 15% results in more enrichment of the isotopic composition of the remaining pond water and vice versa. The model results were also strongly sensitive to the atmospheric water vapour isotopic composition, δ_a, with lower δ_a values than baseline (-29%) causing more enrichment of the pond water (Figure 2.6b). Kinetic fractionation during non-equilibrium evaporation of water as the result of the enhanced diffusion of lighter water molecules ($^1H_2{}^{16}O$) relative to heavier water molecules $^1HD^{16}O$ and $^1H_2{}^{18}O$ from the boundary layer to open air is aided by the isotopic composition of air moisture (Gat, 2008). Precipitation, P, was moderately sensitive, causing differences in the pond isotope content as a simple function of dilution (or mixing). Temperature, T, was similarly sensitive to P. T influences evaporation rates, but again here this is controlled for, so the sensitivity being shown in Figure 2.6 is due to the direct control of T on the liquid-vapor equilibrium fractionation factor for evaporating water (Equations 2.11 and 2.12).

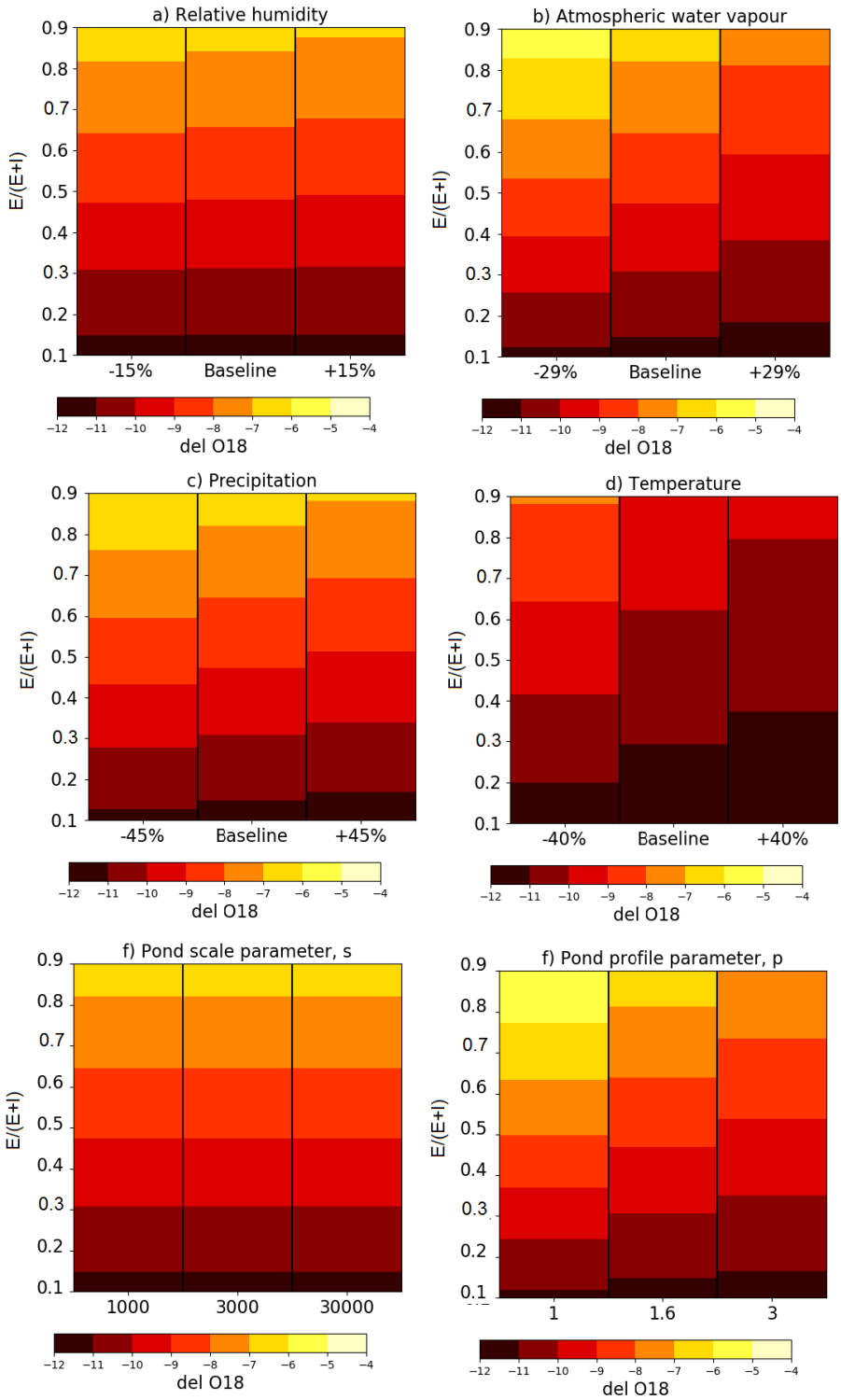

Figure 2.6. Contour plot showing the sensitivity of pond isotopic composition, $\delta^{18}O$, to climate and pond geometry parameters.

The pond scale parameter, s, determine the overall size of the pond surface area, as a function of pond depth, and is found to be insensitive. Conversely, the pond profile parameter, p, determines the form of the relationship between area and depth and is found to be highly sensitive.

2. 5. 3. Model application to SDNWA

The comparative results for model outputs and field observations are shown for the permanent ponds (50 and 109), the semi-permanent pond (120), and ephemeral pond (117) respectively in Figure 2.7. The root mean squared errors (RMSE) values for simulated model outputs and field observed data ranged between 0.00 and 0.29 m for pond water levels and 0.02 and 0.10 ‰ for isotope values in all ponds. The rest of the model performance results and field observations for the years 1997, 1998 and 1999 for pond 50 and 109 is presented in Appendix C.

Table 2 shows the water balance and the estimated partitioned fluxes of open-water evaporation and infiltration. Pond 109, a permanent recharge pond, has infiltration rates between 0.52.3 to 4.98 mm/d and evaporation rates of between 0.745 and 1.67 mm/d. The ratio of evaporation to total water loss, E/(E+I), ranges from 131% to 5140% (mean of 2930%) which shows that infiltration is the dominant loss, on average accounting for approximately two thirds of the total loss. Pond 50, also a permanent pond, but not a recharge pond, has infiltration rates of between 0.995 to 1.3 mm/d and evaporation rates between 0.971.1 to 2.83.4 mm/d. Evaporation accounts for 493% to 7480% (mean of 607%) of all water losses from pond 50, and evaporation is therefore the dominant loss, on average accounting for approximately two thirds of the total loss. Infiltration rates under the ephemeral Pond 117 and the semi-permanent pond 120 were 9.02 and to 5.81 mm/d, respectively, markedly higher than the permanent ponds in 2014 when isotope values and water levels in all ponds were measured. Evaporation rates in 2014 from ponds 117 and 120 were of a similar magnitude, at 1.00.88 and 0.71.2 mm/d, respectively. In the ponds 117 and 120, infiltration strongly dominate the water balance, accounting for 87 91% % and to 9083% of water loses, respec**tiv**ely.

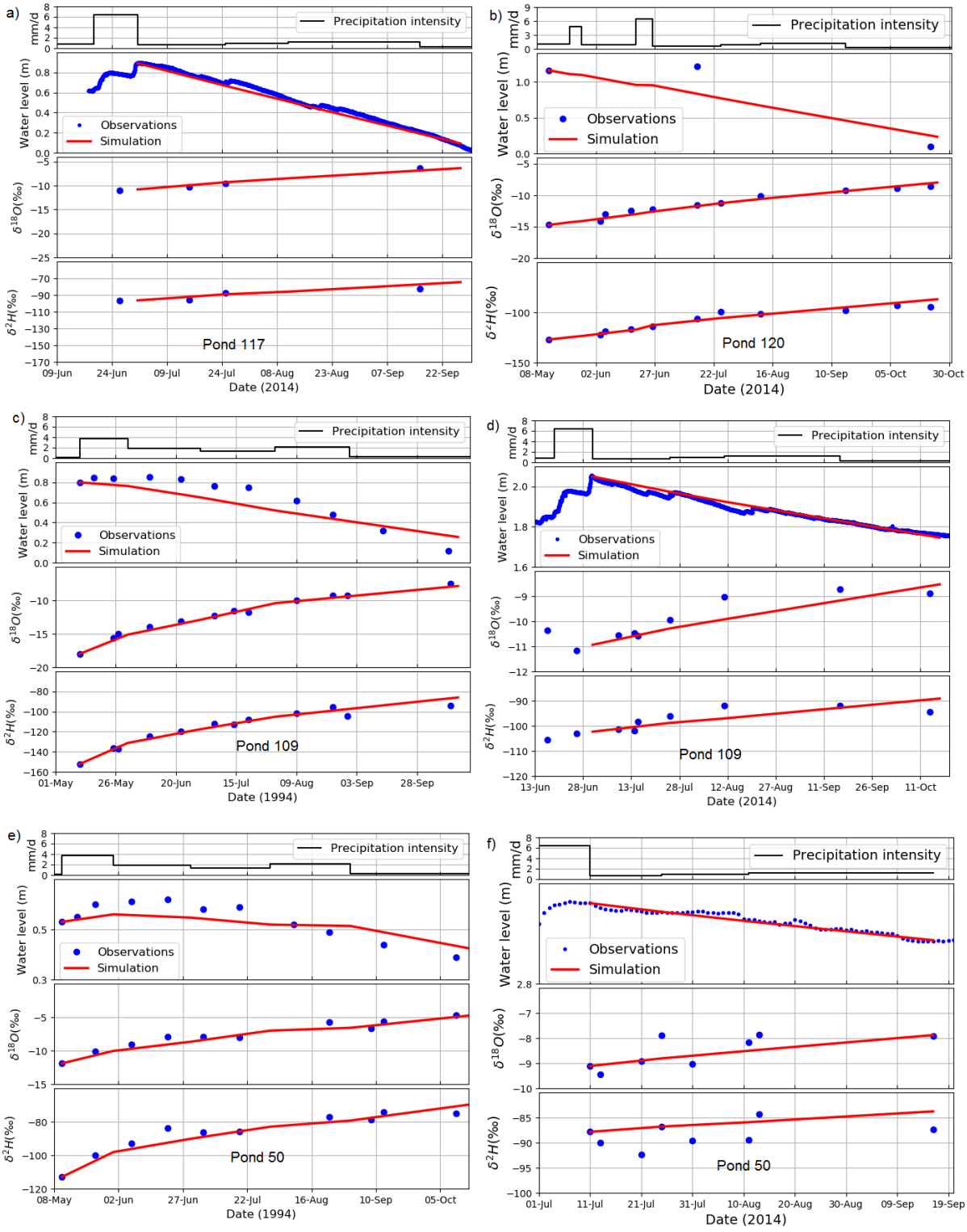

Figure 2.7. Model performance compared with field observations of water level, δ18O, and δ2H for the years 1994, , and 2014 for which all required field observations were available for pond 117, 120, 109, and 50.

Table 2.2. Simulation results for all ponds and all years. RMSE δ is the sum of the RMSE calculated for ^{18}O and ^{2}H.

Pond		**50**				**109**				**117**	**120**
Year		**1994**	**1998**	**1999**	**2014**	**1994**	**1997**	**1998**	**2014**	**2014**	**2014**
No. of days		173	84	150	67	157	118	108	108	88	165
Initial A m^2		17735	26365	22661	74762	2410	3701	1927	7756	2261	3124
Final A m^2		14039	20504	18746	71296	585	1594	702	6353	25	984
Initial h (m)		0.53	0.87	0.72	3.20	0.80	1.13	0.67	2.05	0.89	1.16
Final h (m)		0.4	0.64	0.57	3.02	0.26	0.57	0.30	1.75	0.09	0.23
ΔS (mm)		134	235	152	184	544	556	372	304	799	927
P	mm	254	95	222	66	328	105	70	108	85	218
	mm/d	1.47	1.13	1.48	0.99	2.09	0.89	0.65	1.00	0.97	1.32
E	mm	168	226	207	184	117	167	173	166	77	191
	mm/d	0.97	2.69	1.38	2.75	0.74	1.42	1.60	1.54	0.88	1.16
I	mm	220	103	167	66	755	494	269	247	807	955
	mm/d	1.27	1.23	1.11	0.99	4.81	4.19	2.49	2.28	9.17	5.79
$E/(E + I)$		**43%**	**69%**	**55%**	**74%**	**13%**	**25%**	**39%**	**40%**	**9%**	**16%**
RMSE δ (‰)		0.11	0.18	0.06	0.09	0.06	0.09	0.12	0.09	0.05	0.07
RMSE h (m)		0.03	0.01	0.05	0.01	0.12	0.04	0.00	0.02	0.02	0.24

2. 5. 4. Model comparison with the *Hydrocalculator* model

The HCSS model outputs the fraction of evaporation over inflow, and under the assumptions of steady-state conditions, inflow equals outflow, therefore this output is equivalent to $E/(E + I)$, which is the same as the metric used in our model. The HCNS model outputs the fraction of the total water in the water body (that is initial storage plus precipitation as defined in our model) that was evaporated, in other words, $E/(h_i + P)$. We calculated this same metric for our model, and then calculated the total seasonal evaporation estimate from each model, shown in Table 2.3.

Table 2.3. Comparison of the current model (New) with the steady-state (HCSS) and non-steady-state (HCNS) *Hydrocalculator* model (Skrzypek *et al.*, 2015).

Pond		**50**				**109**				**117**	**120**
Model	**Year**	**1994**	**1998**	**1999**	**2014**	**1994**	**1997**	**1998**	**2014**	**2014**	**2014**
HCSS	$E/(E+I)$	45%	40%	46%	10%	58%	59%	42%	26%	34%	40%
New	$E/(E+I)$	**43%**	**69%**	**55%**	**74%**	**13%**	**25%**	**39%**	**40%**	**9%**	**16%**
HCNS	$E/(h_i+P)$	35%	26%	30%	9%	32%	30%	13%	15%	34%	24%
New	$E/(hi+P)$	21%	23%	22%	6%	10%	14%	23%	8%	8%	12%
HCSS	E (mm)	104	20	141	32	146	19	39	33	40	106
HCNS	E (mm)	216	116	322	294	293	141	0	77	249	372
New	E (mm)	168	226	207	184	116	167	173	165	77	83

2. 6. Discussion

2. 6. 1. Stable isotope characteristics of Prairie wetland ponds

In the Canadian prairies, wetland ponds accumulate substantial deposits of snowfall and snowmelt runoff water during the winter and spring melt seasons and they tend to lose water to evaporation and infiltration during the summer period. The result is the regular seasonal variations in water levels as shown (Figure 2.3). The stable isotope compositions of ponds also change with time, following predictable seasonal pattern of depletion as water levels rise in the spring months and enrichment as water levels recede in the fall months (Figure 2.4). The isotope composition of water found in the permanent ponds are generally more enriched and less variable than the semi-permanent and ephemeral ponds. This is attributed to the presence of large volumes of evaporated and enriched water retained by the permanent ponds from previous years. Snowmelt water is depleted in isotopic composition and whenever this water mixes with residual evaporitic waters (i.e., from previous years) in the large semi-permanent or permanent ponds a more enriched isotope compositions are obtained even at the start of the spring season in the large permanent ponds. The large volumes of water stored in the permanent ponds suggest that a significantly large volumes of snowmelt water additions (of surface snowmelt runoff during the spring) may be required to significantly alter the isotope compositions of these types of ponds.

Semi-permanent and ephemeral ponds retain little or no evaporated water from previous season (i.e., fall) or years, as these may have dried up by the end of the summer or early fall. Snowmelt water which is depleted in its isotopic composition, therefore, serves as the initial water source for the ephemeral ponds and as such these ponds generally have depleted isotope compositions similar to that of snowmelt water in the spring (Figure 2.3). The observation suggests that the pond isotope composition of water found in ephemeral, semi-permanent and permanent ponds could be used to distinguish the hydrologic regimes of various wetland pond types in seasonally frozen semi-arid climates.

During the period of early May to late October (Figure 2.4), a consistent progressive enrichment have been observed in the water isotope compositions for all ponds and this due to seasonal changes in meteorological conditions leading to evaporation of the pond waters. The effect of open water evaporation on the ponds is reflected in the slopes values of the pond evaporation lines recorded for the individual ponds in Table 2.1 and Figure 2.5. The deviation of slopes of the evaporation lines of surface waters (in this case the ponds) from the local meteoric water line slope (i.e., lower than the slope meteoric water line) is indicative of kinetic fractionation induced by evaporation in an environment of relatively low humidity and isotope diffusion processes to attain isotopic equilibrium (Clark and Fritz, 1997; Gammons *et al.*, 2006; Gat, 2008).

The slopes of the local evaporation lines of the ponds reported here were similar suggesting open water evaporation may be the main cause of changes in pond isotope composition. Differences in the local evaporation slopes is reported from surface water found in different climates and also surface water receiving substantial groundwater discharge (Clark, 2015; Gibson *et al.*, 2016).

2. 6. 2. Model sensitivity

The isotope-mass-balance the model developed here suggests that the model is most sensitive to relative humidity and isotope composition of the atmospheric water vapour and therefore, will have significant impact on both the surface water hydrological flux estimates and pond isotope compositions. The effect of precipitation additions and temperature are similarly sensitive when the values of these parameters are estimated close to 50% of the original values. The model is also sensitive (moderately) to changing pond basin profile, p, but relatively insensitive to pond scale parameter, s (Figure 2.6). These observations are similar to those reported in earlier studies (Gibson *et al.*, 1993; Gibson, 2002b; Steinman *et al.*, 2010). Minimizing errors in measurement of

the sensitive parameters and assumptions about how these parameters vary with time will reduce uncertainty and improve model outputs.

The effect of relative humidity and atmospheric vapour, δa on the sensitivity of the isotope-mass balance model is driven by both kinetic and equilibrium isotope fractionation processes. Changes in surface water isotope compositions are driven by turbulent/diffusion mass transfer mechanisms and humidity (Craig and Gordon, 1965; Gonfiantini, 1986; Gibson, 2002b). Field observations and laboratory experiments (Craig *et al.*, 1963; Gat, 1995b; Kumar and Nachiappan, 1999) have shown that an isotopic build up will continue until the difference between the isotopic composition of the water body and that of its evaporate reaches an equilibrium condition even though this equilibrium is never reached. This means that the ambient atmospheric isotope composition has a strong impact on the estimated hydrological fluxes, and we need more accurate ways of evaluating this variable. The impact of precipitation amount and temperature on the isotope compositions of the remaining pond water is unsurprising. The equilibrium isotopic fractionation factor α between the liquid water and water vapour is controlled by the temperature (Horita and Wesolowski, 1994). This effect of temperature on the isotopic composition of lake water and isotope composition of precipitation in mid- and high latitude regions is well documented (Rozanski *et al.*, 1992; Gat, 1995a). The insensitivity of the pond scale parameter, s, which determines the overall size of the pond surface area as a function of pond depth is not surprising because the substitution of the expressions for A and V (Equations 2.1 and 2.2) into Equation 2.8, cancels out s. Conversely, the highly sensitive nature of the pond profile parameter, p, suggests the shape of the ponds (defining the relationship between area, depth, and volume) is important for estimating flux losses. It follows that the simplifying assumption that the pond area remains fixed as the depth changes are unsuitable for relatively small ponds considered in this study. The effect of changing area-depth ratio on evapotranspiration fluxes was reported in field studies (Millar, 1971; Hayashi *et al.*, 2016) conducted on prairie ponds.

2. 6. 3. Model application to SDNWA

The RMSE values for simulated model outputs and field observed data suggests that the performance of the model is good for simulating both isotope compositions and water levels. Errors are of a similar magnitude to the analytical precision for $\delta^{18}O$ and $\delta^{2}H$ measurements, which

is ± 0.2‰ and ± 1.0‰, respectively (Lis *et al.*, 2008), and the observational accuracy in determining maximum water depth from ponds, which is within 50 mm (Conly *et al.*, 2004).

The comparison of water balance components between different types of wetland pond show that infiltration rates are highest in the ephemeral/semi-permanent pond (117 and 120), lower in the permanent pond (pond 109) and lowest in the permanent pond (pond 50). The observation is consistent with our understanding of how these ponds function in the landscape with pond 109 identified as a recharge pond and pond 50 a discharge pond (Hayashi *et al.*, 1998; van der Kamp and Hayashi, 2009; Heagle *et al.*, 2013).

The relatively high evaporation rate from the larger pond (Pond 50) is attributed to the larger surface area, and the relatively high exposure of the pond to wind and radiation, compared with the more sheltered recharge pond. Vegetation cover can reduce the lateral advection of warm and dry air into, and cool and moist air out of the wetland. Another effect of vegetation is transpiration loses from the ponds by riparian zone plants and aquatic plants in the ponds, which induces lateral flow of water from the ponds into the subsurface and transpire water directly into the atmosphere, is well documented in the region (Millar, 1971; van der Kamp and Hayashi, 2009). In this study, such transpiration driven losses are lumped in with the infiltration term and cannot be distinguished from recharge to the shallow local groundwater systems.

2. 6. 4. Model comparison with field observations in the prairies

The infiltration rates vary widely from 0.9 to 9.2 mm/d and also between years and ponds. These infiltration rates are, however, comparable to the rates obtained from Darcy flux calculations, 0.83 to 1.38 mm/d (Woo and Rowsell, 1993) and head measurements 9.4 mm/d (Hayashi *et al.*, 1998). The variability has been attributed to the type of pond (i.e., dry or wet period and whether ephemeral/temporal, or semi-permanent, or permanent) and the antecedent moisture content of soil under the wetland pond before snow melt and meteorological conditions (Granger *et al.*, 1984; Hayashi *et al.*, 2016). Studies (Winter and Rosenberry, 1998; Parsons *et al.*, 2004; Waiser, 2006; Johnson *et al.*, 2010; Hayashi *et al.*, 2016) have shown that infiltration rates under wetland ponds that dry up during the summer (ephemeral/temporal ponds) are higher than wetland ponds that do not dry up (permanent ponds). Infiltration rates and proportions of the total water loss estimated using the new model compared very well with estimates obtained in previous hydrological studies at Pond 109 at the SDNWA. Using an artificial Bromide tracer, Parsons *et al.*, (2004) reported

daily infiltration rate of 1.7 mm/day in May and 4.5 mm/d in June-July, 1999 for the recharge Pond 109 which accounted for 47 % and 67 % of total pond water-loss in May and in June-July, respectively. The value gives an average infiltration of 3.9 mm/d, which compares well with our independent estimate of 3.4 mm/d.

The daily open-water evaporation rates for the recharge Pond 109 for the same period were 1.9 mm/d in May and 2.2 mm/d in June-July (Parsons *et al.*, 2004), with an average of 2.1 mm/d is higher compared to isotope balance estimate of 1.33 mm/d. Hayashi *et al.*, (1998a) reported open water evaporation rates in Pond 109 of ~3 mm/d, for a 2-week period in 1995, using Bowen ratio energy balance and evaporation pan measurements. Though this was a year when I did not have isotope observations, the magnitude is larger than our estimates but represents a shorter period when the evaporation rates would likely have been higher than the seasonal average. Other literature in the Prairies showed an estimated open-water evaporation rate of 3.9–5.1 mm/d in June–July for a lake in southern Saskatchewan (Morton, 1983) and 4.5 mm/d for a larger wetland with few trees in central North Dakota (Parkhurst *et al.*, 1998). The latter measurements were carried out on larger water bodies than the ones considered in this study, suggesting that care should be taken in generalizing these evaporation rates. These evaporation fluxes also suggest that using the existing model, these estimates may be grossly underestimated for evaporation especially in the case where the amount of inflows into the lakes are large and isotope compositions differ from the lake's original isotopic composition.

2. 6. 5. Model comparison with the *Hydrocalculator* model

It can be seen in Table 2.3 that the modelled estimates of E vary wildly between our model and the *Hydrocalculator* models, but this is not surprising, given that the three models have different assumptions and are designed to answer different questions. Here the model is assumed reliable, and the question is whether a simpler approach, i.e. the *Hydrocalculator* model, using less data, could give estimation of evaporation that is consistent with our model.

The HCNS model provides no insight into the partitioning of E and I, since I is assumed zero. It is still worth comparing the evaporation rates from this model, but the results are completely inconsistent with our modelled results (Table 2.3). There are no discernable patterns in differences in evaporation-inflow ratios between the different types of ponds, as with the new model but, the model overestimated the evaporation fraction for all ponds (Table 2.3). It is therefore, concluded

that the HCNS model is not suitable for prairie ponds. The HCSS model underestimated evaporation fraction in the more permanent pond (i.e., pond 50 and 109 in 2014) as compared with the new model. The ratio $E/(E + I)$ suggests that infiltration generally dominates water loss from these ponds in time. Compared with the new model, it is difficult to use the results of evaporation-inflow ratios obtained from the *hydrocalculator* models to differentiate between the different types of ponds using for the permanent ponds (ponds 109 and 50) and the ephemeral and semi-permanent ponds (ponds 117 and 120). The results suggest that the *hydrocalculator* model should not be applied to small ponds that lose water to infiltration, frequently dry up, and where isotopically distinct precipitation/inflows has a marked impact on the pond isotopic composition.

The results of the individual flux estimates from the various classes of wetland ponds suggest that the existing model predicted higher evaporation component in the smaller mostly the ephemeral and semi-permanent ponds but predicted almost the same percentage evaporation fractions for the larger permanent pond (Table 2.3). The result is not surprising because the previous models have been designed to simulate approximate component ratios for large lakes and rivers, where indeed precipitation additions have minimal effect and/or outflows balances inflows (Gilath and Gonfiantini, 1983; Gonfiantini, 1986; Gibson, 2002b; Skrzypek *et al.*, 2015). The results imply that while the precipitation additions, and size and shape considerations play critical roles in the estimation of water balance components of small lakes and ponds that may not be the case for large lakes and rivers.

2. 6. 6. Model limitations

The model developed in this paper is useful for modeling stable isotope evolution with time in surface water and the estimation of evaporation and infiltration fluxes. This model is not capable of distinguishing how the infiltration flux is partitioned between plant transpiration in the riparian zone and pond, and groundwater recharge, which is important for water resources management. Water budget for prairie potholes, particularly after the snowmelt period when emergent vegetation and vascular plants are established and begin to transpire is controlled by transpiration. Furthermore, all potholes seem to have either a willow ring or macrophytes (floating, emergent or submerged) which may be rapidly transpiring generally non-fractionated isotopic composition of input water to the atmosphere. Thus, the vapour loss by transpiration rather than evaporation will diminish the isotopic enrichment effect, which may also affect both the atmospheric water vapour

composition and seasonal evaporation rates. This effect can be catered for by direct monitoring and measurement of atmospheric water vapour isotope composition.

It is also limited in that it does not take into account progressive changes in pond salinity, and local atmospheric conditions (e.g., relative humidity, precipitation, temperature, solar radiation and wind speed) which affect evaporation and evapotranspiration rates (Gonfiantini, 1986; Horita *et al.*, 2008; Horita, 2009). The progressive enrichment in $\delta^{18}O$ and $\delta^{2}H$ compositions of surface water bodies during evaporation is influenced by physical changes (i.e., amount of water, surface area of pond and pond salinity) and the rate and extent of evaporation depends on the local meteorological conditions (Gat and Levy, 1978; Steinman *et al.*, 2010; Skrzypek *et al.*, 2015). It is expected that an increased sampling frequency and improved accuracy in measuring surface inflows (rainfall and surface runoff into the pond), temperature, relative humidity, and ambient atmospheric moisture isotope compositions will lead to more accurate water isotope and outflow flux estimations. Salinity effects can be worked into the model using the equations of Gonfiantini, (1986) when dealing with high saline wetlands. The model is able to capture the dynamic changes in pond water levels and isotope values, but the accuracy of predictions decrease significantly without accompanying isotope and runoff amount measurements (Figure 2.7a). This suggests that for periods of winter and summer surface runoffs and/or where groundwater discharge occurs, this model is not useful unless related amount inputs and isotope compositions are determined.

2. 7. Conclusions

Small wetland ponds are subject to significant seasonal fluctuations in water levels and isotopic composition, due to their relatively small residence times. I demonstrated that existing approaches in the literature to estimate evaporation volumes from surface water bodies using stable isotope compositions are inappropriate for such ponds. Also, a simple pond water isotope determination can give a useful indication of the permanence of the pond. A water and isotope mass balance model were developed to estimate the hydrological fluxes from such water bodies, and in particular to partition the water losses between evaporation and infiltration. This was applied to a number of wetland ponds in the Canadian prairies. The model provides credible estimates of evaporation and infiltration rates from the ponds, which were consistent with previous field-based estimates. I was also able to show with the model that there were variations in the infiltration rates between the

different types of ponds (i.e., infiltration rates are higher in ephemeral than permanent ponds). This is consistent with existing understanding of the groundwater-surface water interactions of these different ponds but was derived independently of any information about the groundwater system, demonstrating the utility of this method. This is a relatively data-intensive method, requiring roughly monthly measurements of pond levels, precipitation amounts, isotopic composition (^{18}O and ^{2}H) of ponds and precipitation, and basic meteorological variables, so it cannot replace the simpler approaches that have been developed for data sparse surface water bodies. The method can provide useful information about wetland pond water balances and isotopic content of pond water, which have important applications for water management, and biogeochemical and biological/ecological studies. The flux estimates could be useful for hydrological and hydrogeological modeling studies. Outstanding challenges that were not addressed by this study include how to partition infiltration from wetland ponds between riparian zone and pond transpiration and groundwater recharge, how to deal with rainfall runoff, snowmelt runoff, and groundwater discharge into the ponds, where the isotopic composition of such waters is not easy to observe.

2. 8. Transition statement

The Chapter affirms the spatial differences in both the isotope profiles and fluxes of various wetland ponds in the prairies. It is established that infiltration rates beneath ephemeral wetland ponds were higher than estimates beneath permanent large ponds. Open water evaporation rates from the ephemeral wetland ponds were lower than the large permanent ponds, with significant inter-annual variability. The flux estimates from the ponds will be useful data for hydrological models in the Prairies. The wide range of stable isotope compositions exhibited by the different ponds emphasized the need for careful consideration in stable isotope investigations. It is worth to explore the differences in the isotope compositions of the variety of ponds in the PPR region and their impact on significant on local groundwater, intermediate and/or regional aquifer recharge. This will be the focus of next Chapter to determine which ponds are the main source of groundwater recharge in the region.

2. 9. Acknowledgements

I thank Canadian Wildlife Service for site access; the Natural Sciences and Engineering Research Council, the Global Institute for Water Security (GIWS), and the University of Saskatchewan for funding support and, Dr. Bob Clark, Randy Schmidt, and Heather Wilson for field assistance. I also thank Environment Canada for the use of archived data and Geoff Koehler and for making unpublished water isotope data available. Emeritus Research Scientist Dr. Garth van der Kamp for providing me with archived isotope and water level data, as well his useful insights on the results, and comments on the manuscript.

2. 10. Author contributions

E.K.P.B. designed the study and field work, compiled each data set, did the geographic information system work, developed the equations, run the model and did the water balance calculations, and wrote the paper. A.M.I, supervised and funded the research, wrote the python script and did sensitivity analysis and model comparison, and J.J.M. discussed the results, commented on the manuscript and contributed to the text.

CHAPTER 3: EPHEMERAL WETLAND PONDS ARE A DOMINANT SOURCE OF DEPRESSION-FOCUSED GROUNDWATER RECHARGE

Status: Submitted November 2017 and Under Revision February 2018

Citation: Bam, Edward K.P, Ireson, Andrew M, van der Kamp, Garth, Hendry, M. Jim (2017), Ephemeral wetland ponds are a dominant source of depression focussed groundwater recharge Water Resources Research, Manuscript # 2017WR022182. Under revision

3. 1. Abstract

Depression-focused recharge is a concept that has been proposed to explain groundwater recharge processes in the Northern Prairie regions of North America. Topographic depressions in the generally flat landscape are ubiquitous, and in many of these depressions wetlands and ponds are formed. The ponds are diverse in their interaction with the subsurface, and with one another through the surface fill and spill processes. The concept of depression-focused recharge was tested to more broadly understand the interactions between the various groundwater units and surface water bodies using a combination of physical hydrometric measurements and water isotopes (δ^2H, $\delta\ ^{18}O$ and ^3H). The field site was the St Denis National Wildlife Area, Saskatchewan, where hundreds of diverse ponds are present, and the subsurface comprises a surficial groundwater (down to ~5 m depth) overlying a clay-rich aquitard, and an intertill aquifer at ~40 m depth. Hydraulic head data are used to identify recharge and discharge ponds (which lose or gain water to/from the deeper groundwater system). Tritium concentrations in the profile indicate that the water in the intertill aquifer is recharged with modern water (less than 70 years old). The stable isotopic composition of the intertill aquifer suggests that it was predominantly recharged by ephemeral wetland ponds. These ponds are numerous but short-lived, losing all their water in the spring/early summer to infiltration. Depression-focused recharge is a good conceptual model for this landscape, but ephemeral wetland ponds, which are easy to overlook, may play a dominant role in intertill aquifer recharge.

3. 2. Introduction

Wetlands influence water quality (Bullock and Acreman, 2003; Murkin, 1998), watershed storage and runoff (Shook *et al.*, 2013), evapotranspiration fluxes (Nilsson *et al.*, 2013) and groundwater recharge/discharge processes (van der Kamp & Hayashi, 1998). Interactions between wetlands (surface water) and groundwater can have important implications for water resources management, flood risk, hydrological and ecological functioning, and transport of contaminants (Nilsson *et al.*, 2013). In the glaciated Canadian Prairie landscape these interactions between wetland ponds, shallow groundwater, aquitards and intertill aquifer remain poorly defined (van der Kamp and Hayashi, 2009; Brannen *et al.*, 2015). The Canadian Prairies form part of the Prairie Pothole Region (PPR) found in mid-continent of North America. The region covers approximately 715,000 km^2 and extends from north-central Iowa in the USA to central Alberta in Canada as shown in. The landscape is dotted with hundreds of small depressions known as "potholes" or "sloughs", attributed to deglaciation at the end of the Pleistocene. In the prairies the uplands are productive for agriculture, the wetlands provide ecosystem services, such plant, and wildlife habitats, and groundwater serves as water supply for domestic and agricultural use (Yang *et al.*, 2008).

Wetlands in the PPR are vulnerable to changes imposed by land-use change and climate change (Wright and Wimberly, 2013). Approximately 50 % of all wetlands in the PPR have been drained, mostly (> 80 %) to make way for agricultural crop production, and 34 % of the native upland habitats have been changed to cropland (Euliss *et al.*, 2006). The PPR is also characterized by dynamic inter-annual climate cycle where droughts are often followed by floods (Dahl, 2011; Balas *et al.*, 2012). Precipitation and temperature variability and extremes are predicted to be exacerbated by global climate change projections for the region (Henderson and Sauchyn, 2008).

Numerous hydrological studies (Meyboom, 1966; Sloan, 1972; Zebarth and De Jong, 1989; Woo and Rowsell, 1993; Labaugh *et al.*, 1998; van der Kamp and Hayashi, 1998; Winter, 1999, 2000; Winter and LaBaugh, 2003; Euliss *et al.*, 2004; Shaw *et al.*, 2012b; Nachshon *et al.*, 2013) and many others, conducted in the PPR of Canada and the United States have focused on understanding of hydrological functioning of the wetlands and solute exchanges by wetlands and their

surroundings. Some studies have addressed groundwater, in particular it's influence on pond chemistry, it's role in supplying water to surface depressions during periods of drought (Labaugh *et al.*, 1996, 1998; Winter, 2000; van der Kamp *et al.*, 2008), and recharge sources and mechanisms (Labaugh *et al.*, 1998; van der Kamp and Hayashi, 1998; Winter *et al.*, 2003). The studies depend largely on field measurement of water levels, water chemistry, hydraulic and application of numerical models. Studies on the hydrological functioning of prairie wetlands in the past were also either concentrated on groundwater or surface water (Brannen *et al.*, 2015). The traditional physical measurements (hydrometric) were important in providing real-time rainfall, runoff and groundwater level data, but this requires continuous monitoring and rigorous analysis. In recent times, prairie hydrological studies (Hayashi *et al.*, 1998; Berthold and Hayashi, 2004; Parsons *et al.*, 2004; Nachshon *et al.*, 2014; Pennock *et al.*, 2014) have been focused on the understanding the relationships between the surface and the shallow subsurface. The studies combined various methods including physical field measurements, water chemistry, numerical models, geophysical surveys and geographic information system (GIS) tools to analyze hydrological and chemical data in the region. Other studies have focused on the importance of hydrological connectivity in explaining prairie wetland hydrology and chemistry, pond water level and the catchment streamflow response in the wetland-dominated watershed (Leibowitz and Vining, 2003; Van Der Valk, 2005; Cook and Hauer, 2007; Brannen *et al.*, 2015; Leibowitz *et al.*, 2016). Groundwater recharge studies in the Prairies (Meyboom, 1967; Lissey, 1971; Hayashi *et al.*, 2003; Berthold and Hayashi, 2004) showed that the main sources of recharge to the shallow groundwater and possibly the deeper intertill aquifer in the Prairie region is from wetland depression ponds. This is termed as "depression-focused recharge".

The studies in the past have mostly concentrated on the shallow subsurface (~20 m depth) and also focused on groundwater contributions to wetland pond water balance. The conclusions were that groundwater contributions to wetland pond water balance are negligible and only significant in maintaining the salinity of permanent wetland ponds (van der Kamp & Hayashi, 2009). On the contrary, a recent study (Brannen *et al.*, 2015) showed that during extremely wet periods and high water levels, groundwater can contribute significantly to pond water volumes and streamflow in the Prairies. The studies (van der Kamp and Hayashi, 1998, 2009; Hayashi *et al.*, 2003) suggest the extent of groundwater influence on the surface water system in the region is poorly understood therefore further studies are required to evaluate these interactions.

Stable isotope studies of wetland ponds, surface waters and groundwater aquifers in the Prairies (Fritz *et al.*, 1974, 1987; Mcmonagle, 1987; Fortin *et al.*, 1991; Maule *et al.*, 1994; Grasby and Betcher, 2002; Jasechko *et al.*, 2017), however, have shown that stable isotope signatures of shallow groundwater and aquifers closely resemble cold-season precipitation events and not evaporitic surface pools. The question is, why is the aquifer water isotopically distinct from the enriched wetland pond waters that are understood to recharge the aquifer? Could it be that perhaps, the aquifer water was recharged under conditions little more "cold" than the water that has infiltrated during the last 100 years? The general concept of depression focus recharge to aquifers from wetland ponds or surface depressions cannot explain why the isotope compositions of these two water systems present different isotopic compositions. In Chapter 2, I have shown that wetland ponds of different permanency (i.e., permanent, semi-permanent and ephemeral wetland ponds) have significantly different isotopic signatures and contribute different amounts of recharge water to subsurface infiltration. There is, therefore, an urgent need for an integrated approach involving hydrometric and chemical measurements (including isotopes) provide an improved understanding of the interactions between the various wetland ponds and the subsurface units in the region.

The approach of combining stable isotopes and hydraulic/hydrometric measurements has been used to study the interactions between lake/river systems in semi-arid and arid regions (Kalbus *et al.*, 2006). Stable isotope compositions of initial water entering a system, subsequent additions and withdrawals, and the processes acting on that system are preserved in the water molecule (Hunt *et al.*, 1998, 2005). Groundwater infiltration is considered to come from a multi-year integration of seasonally weighted rainfall events, therefore, the isotopic composition of groundwater closely reflect the seasonally weighted long-term average inputs even in some of the aridest regions of the world (Wassenaar *et al.*, 2009). Evaporation produces characteristic heavy-isotope enrichment in surface waters due to enhanced kinetic fractionation of isotope molecules of water (Gibson *et al.*, 2005). Groundwater recharge from evaporated water sources such as permanent wetland ponds would, therefore, have isotopic compositions that closely reflect evaporated pond water isotope compositions. Similarly, groundwater recharged from preferential pathways with limited evaporation would reflect the isotope compositions of precipitation events in that region. Here

stable isotope compositions (^{2}H and ^{18}O) of precipitation, groundwater and surface waters from wetland ponds obtained from at St. Denis National Wildlife Area, Saskatchewan, Canada were used to determine the source(s) of water filling up the prairie wetland ponds, the shallow groundwater, aquitards and the confined intertill aquifer which underlie the site. Our objective is to investigate and determine which category of wetlands may play the dominant role in the recharge of the Prairie aquifers. More specifically, the interactions between various the ephemeral wetland ponds and the shallow groundwater, clay-rich aquitards, and intertill aquifer (> 50 m depth). We combined stable isotope data and hydrometric measurements from the site to further investigate the interactions between the wetland ponds and the groundwater units within the glacial till. Finally, high-precision tritium (H^{3}) concentrations from the groundwater samples were used to determine the approximate recharge periods for the various groundwater units. It is demonstrated in this study that combining water isotope data with minimal hydrometric data have helped to provide detail understanding of on the surface water-groundwater interactions between wetland ponds and the aquitard-aquifer in a system in a complex terrain as the Canadian Prairies.

3. 3. Study area

The study area, St. Denis National Wildlife Area (SDNWA), is located in the PPR of Canada on longitude 106˚069'W and latitude 52˚029'N. SDNWA was established in 1968 as a long-term study site for monitoring ecological changes and covers a total area of 3.85 km^2 (Heagle et al., 2013). The site is approximately 35 km east of the city of Saskatoon in the Province of Saskatchewan (Figure 2.1a). The areal extent of St Denis National Wildlife Area is shown in Figure 3.1a.

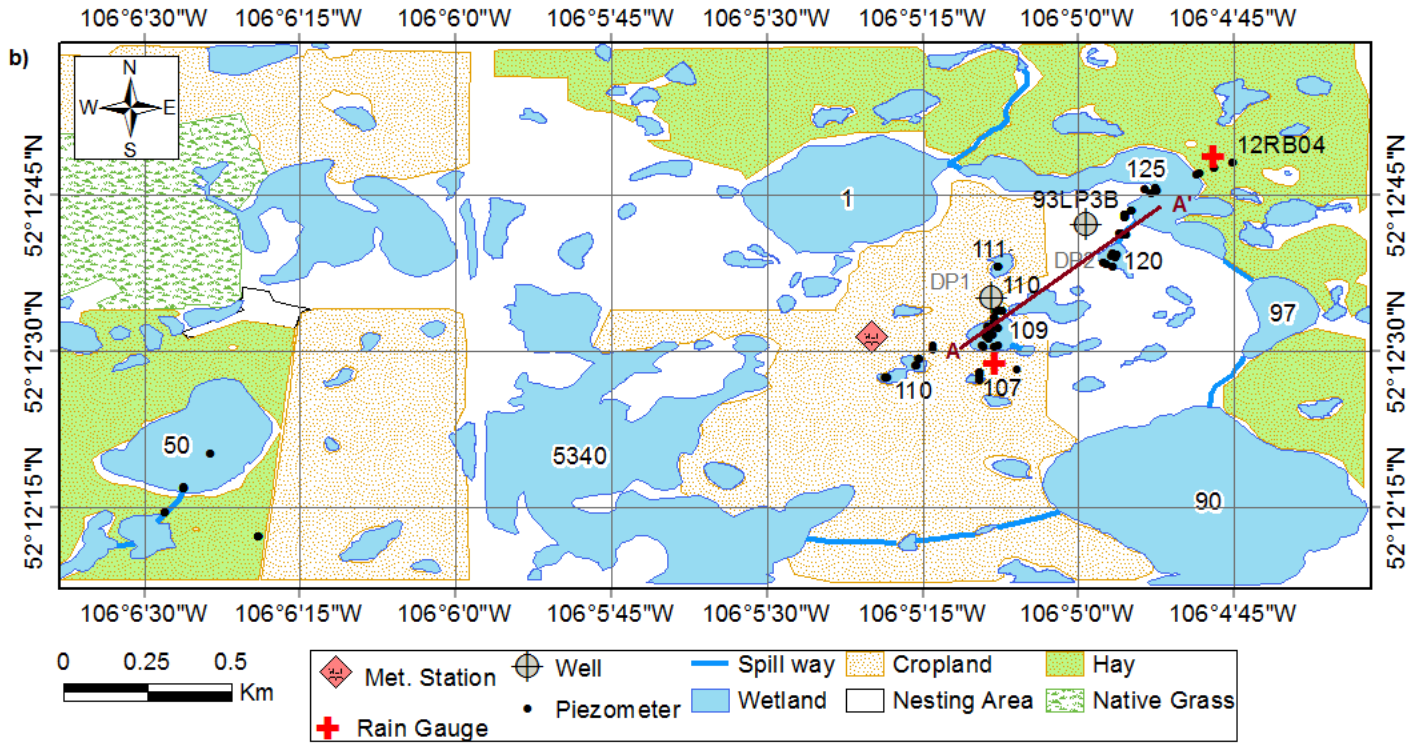

Figure 3. 1. a) The extent of the St Denis National Wildlife Area showing land use. The locations of piezometer, wells, and the wetlands (in numbers) are also shown. The piezometers for which Tritium samples have been collected are marked with names in red.

Much of the terrain is underlain by clay-rich glacial till and is poorly drained by regional flow systems, and as a result is dotted with hundreds of small depression ponds called "sloughs" or "potholes", typical of the northern glaciated plains (van der Kamp and Hayashi, 1998; Berthold and Hayashi, 2004). SDNWA soils are made up of low permeability stratified silty glaciolacustrine sediments and glacial till of the Battleford and Floral Formations of Middle to Late Wisconsin age (Hayashi *et al.*, 1998). The boundary between the two formations is not clearly visible and therefore not presented in the detailed geological cross-section (Hayashi *et al.*, 1998). The detailed geological cross-section shown here in Figure 3.1c, is based on two previous works (Miller *et al.*, 1985; Hayashi, 1996). The upper till layer, 0-6 m, is weathered, fractured and oxidized and below this depth is the unoxidized, less fractured till layer. Sands and gravels are encountered sporadically within these deposits, but the only sand layer that may have continuity across the site is the 1 to 2 m thick layer of sand encountered at a depth of about 40 m (Figure 3.2).

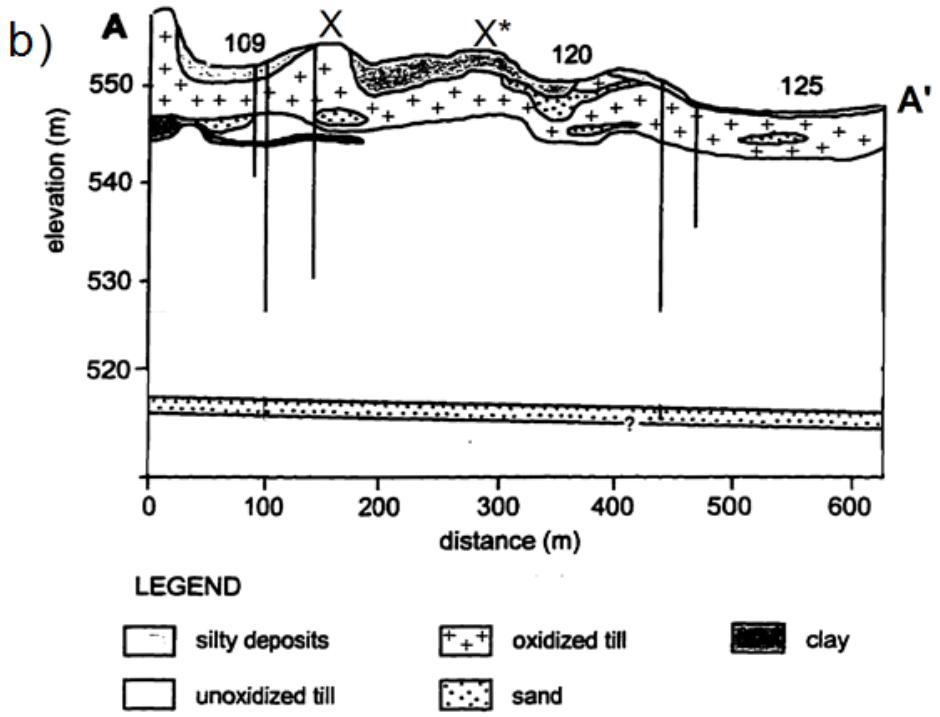

Figure 3.1. b) Geological cross-section of the transect A-A' in Figure 3.1b (modified from Miller et al., 1985; Hayashi, 1996). The approximate locations of new wells DP1 and DP2 are indicated as X and X*, respectively.

The soils comprise an Orthic Dark Brown Chernozems found in upland areas and on the mid-slopes. Orthic Regosols (Typic Ustorthents) and Calcareous Dark Brown Chernozems (Entic Haplustolls) occur on the knolls and the lower slopes, respectively (Miller *et al.*, 1985; van der Kamp *et al.*, 2003). The hydraulic conductivity of the till in the near surface (0-6 m depth) weathered zone reduces exponentially with depth, from as high as 10^{-5} ms^{-1} in the highly fractured surface to as low as $10^{-11}ms^{-1}$ in the deep, unfractured till layers [10 m-20 m] (van der Kamp and Hayashi, 2009). The very low hydraulic conductivity value of the deeper till has led to suggestions that the overall contribution of the intertill aquifer to annual water balance of surface water bodies (including ponds) is negligible (Brannen *et al.*, 2015). Intertill aquifer recharge source(s) and impacts on surface water have not been studied at this site as yet.

The vegetation at the site is diverse from cropped lands to natural grasslands at upland areas. Some ponds are surrounded by cat-tails (*Typha*) up to 1.5 m, 'willow rings' comprising balsam poplar

(*Populus balsamifera*), silver willow (*Salix spp*.) rising up to 8 m, and trembling aspen (*Populus tremuloides*) trees rising up to 10m (Nachshon *et al.*, 2014). The "willow rings" and other riparian zone plants around wetlands function as effective snow accumulators and in some cases reduce open water evaporation (Hayashi, 1996). Sedges (*Carex spp*.), spike rush (*Eleocharis pp.*), cattails (*Typha*) and other aquatic species grow within the center of the ephemeral and semi-permanent wetland ponds during the summer. Plant transpiration which occurs in the wetland margin induces infiltration and lateral flow of shallow groundwater from wetland ponds and this has a strong effect on the wetland water balance (van der Kamp and Hayashi, 2009; Nachshon *et al.*, 2014). During the study period, 2013 to 2016 some of the ponds were submerged with floating aquatic species.

At SDWA ponds are numbered (Figure 3.1b), and this numbering system is adopted in various studies, including this one. The study is focused on eight ponds (i.e., 50, 107, 108a, 109, 110, 117, 120, and 125) in reference to the terminal pond (Pond 5340) covering the years 1993 to 2016 where water levels records exist. The ponds water levels and sizes varied with seasons, vegetation cover, and permanence. In terms of persistence of ponds during the period of 2010 to 2016, three ponds (107,108a, and 117) are ephemeral ponds; two ponds (110 and 120) are semi-permanent, and three ponds (109, 125, 50 and 5340) are permanent according to Stewart and Kantrud (1971) classification of wetland ponds. In terms of surface-shallow groundwater interactions, pond 109 is considered a recharge wetland, pond 50 and pond 5340 are discharge ponds and pond 125 is a flow-through wetland (Hayashi *et al.*, 2003; Brannen *et al.*, 2015). In terms of surface -surface connections, ponds 50, 109 and 5340 are terminal ponds.

The climate is dry, sub-humid, and seasonally frozen with significant inter-annual variability in summer (April to September) and winter (October to March) precipitation. Monthly precipitation normal for the period 1981–2014 showed a general declining trend during the months of November to February (Wittrock and Beaulieu, 2015). The mean annual winter and summer precipitation between 1993 and 2012 was 78 mm and 282 mm respectively (Nachshon *et al.*, 2014). The observed monthly mean temperature varies between -20 °C (December to February) to 19 °C (July to August) (Wittrock & Beaulieu, 2015). The potential evaporation in the region also exceeds total annual precipitation and is estimated at 700-800 mm/y with annual open water (lake) evaporation at approximately 700 mm (Parsons *et al.*, 2004). Figure 3.3 shows precipitation and temperature recorded for Saskatoon, Saskatchewan (2013-2014) with 30-year normal values.

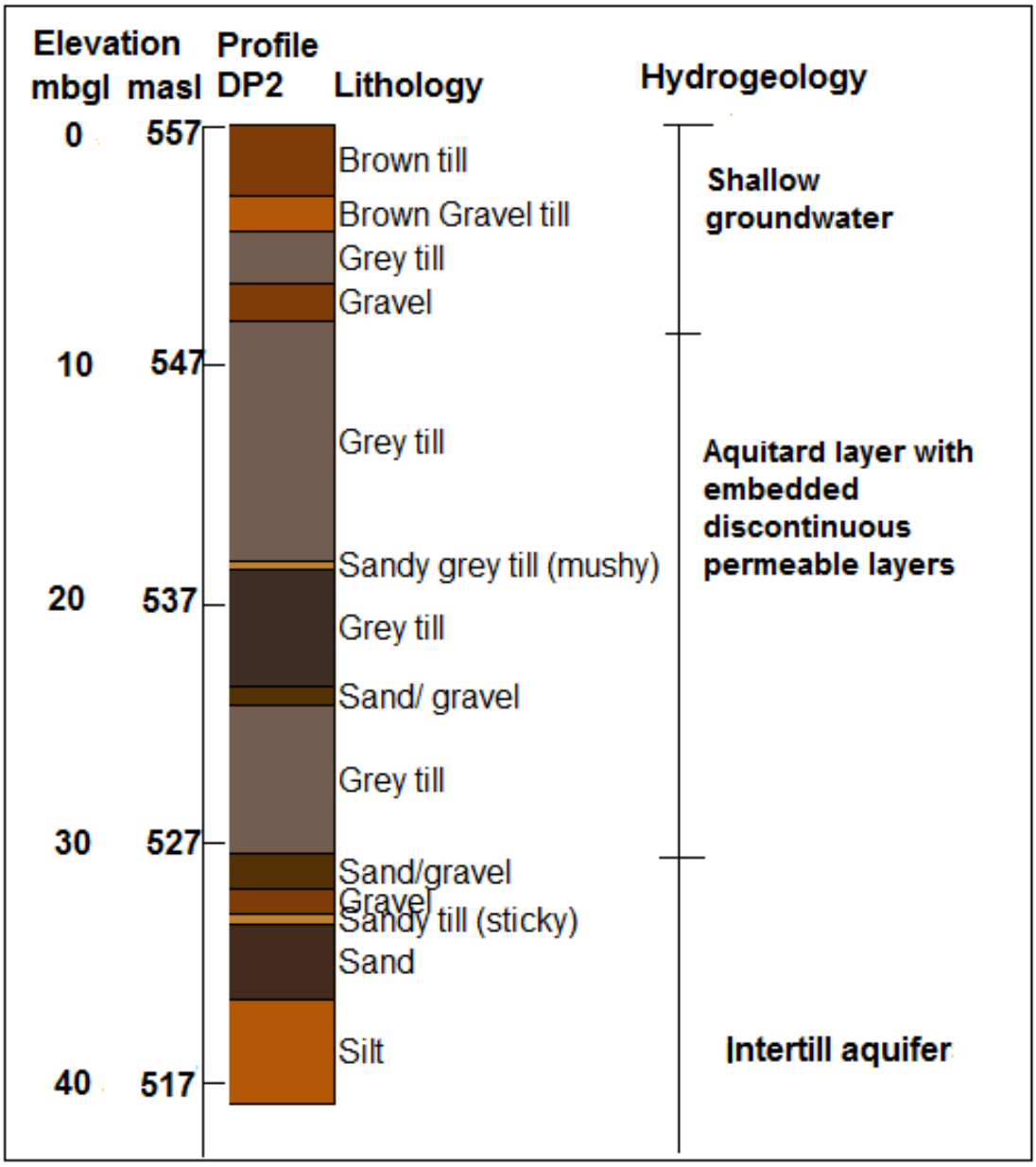

Figure 3.2. Stratigraphy of the new Well, DP2, shown in Figure 3.1b.

3. 4. Field and laboratory methods

3. 4. 1. Hydraulic data

Several piezometers have been installed at the SDNWA between 1982 and 2012. Hayashi et al. (1998a) reported discontinuous sand lenses of thickness 0.1-1.0 m, within which shallow groundwater is found throughout the till. Between 8-9 m, a thin (0.3 m) continuous layer of dense

clay occurred. Sand layer 1.5 m thick was discovered at 25 m below ground with a low yielding intertill aquifer.

During the course of this study, in October 2013, two deep piezometers 39 and 41m below ground were installed at the upland south-west of Pond 125 and northwest of Pond 109 using Reverse circulation drilling with pond water as drilling fluid. PVC pipes (5 cm in diameter) screened over at 37 and 32 m were installed in the intertill aquifer at DP1 and DP2, respectively. Sand packs were placed 24.5 m around each of the screens and a bentonite seal of thickness 12 to 16 m was placed above the screen intake zone. Water was pumped out of the intertill aquifer for about 3 hours until the electrical conductivities settled. The aquifer yield is estimated at 4 gallons/minute. The top of the Well casing was capped, and wells assigned the labels DP1 and DP2 and water level loggers installed on 1st November 2013.

In the course of the drilling, glacial deposits, consisting largely of clay-rich glacial till interbedded with thin sand and gravel with discrete intertill aquifer at elevations 521 and 519 meters above sea level (masl), respectively, were found in DP1 and DP2. The sand and gravel layer (intertill aquifer) is considered laterally extensive and is the same sand and gravel intertill aquifer that underlay the thick glacial till at elevations between 524 -537 masl elsewhere outside the site. The piezometer log for one of the two new holes is shown in Figure 3.2. The position and depth of the sand and gravel layer correspond with the "Qf-ms layer" on the G-G' cross-section of the Saskatoon well record (https://gis.wsask.ca/, Section 29, Township 37, Range 01, Meridian 3) indicating this aquifer is laterally extensive. A seismic test hole was drilled in 1991 between Pond 50 and 5340, to a depth of 45.7 m BGL (WSASK Ref, #031287). This well was likely completed in the sand/gravel intertill aquifer, and was artesian, which further supports the interpretation that this is an extensive aquifer in this region.

3. 4. 2. Hydrometric data

Archived manual and automatically logged long-term piezometer records, barometric pressures and pond levels of eight ponds from 1993 to 2012 were gathered. The head in the manually recorded piezometers was mostly measured on a sporadic basis at most twice in a year. The depth at the deepest point of all ponds was measured manually on a monthly basis during the summers from 2013 to 2016. Precipitation records from 1993 to 2014 for Saskatoon and geodetic measurements (2008) for SDNWA were obtained from the National Hydrology Research Centre

in Saskatoon. The geodetic survey was conducted between pond 109 and 125 in October 2014 to correct the hydraulic heads to meters above sea level (masl) where elevation data do not previously exist.

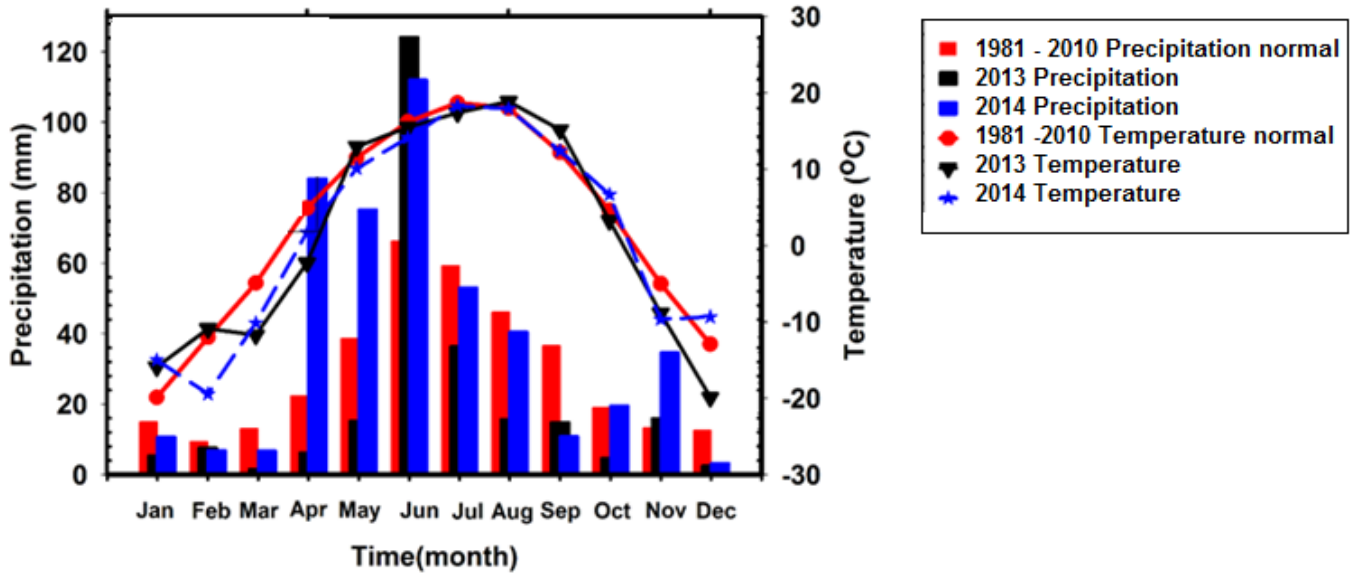

Figure 3.3. Precipitation amounts (P, black and blue bars) and temperature (T, black and blue lines with symbols) record for Saskatoon, Saskatchewan (2013 and 2014). Also shown are the 30 years normal for precipitation (red bar) and temperature (red line with a marker,) for 1981 to 2010 (Wittrock and Beaulieu, 2015).

3. 4. 3. Water samples

Water samples including unfiltered precipitation (snow and rainfall), pond water, pond ice, and groundwater were collected for isotopic analysis. The sampling locations (SDNWA) are illustrated in Figure 3.1b. The sampling details for the variety of ponds and water types are given below:

Precipitation: Onsite biweekly sample collection was done in August 2013 to October 2014 near Pond 109 in the south and Pond 125 in the north at the SDA site. The data from these sites were used to compare with the Saskatoon records. Archived snow and rainfall records and stable isotope values (δ^2H and $\delta^{18}O$) for Saskatoon were obtained for monthly integrated Samples collected from June 1990 to November 2014 from the National Hydrology Research Centre, Saskatoon. The collection station in Saskatoon is about 35 km from the SDNWA. Amount-weighted mean precipitation (W. mean) δ^2H and $\delta^{18}O$ values were obtained for the monthly integrated samples

using the precipitation amounts recorded by Environment Canada and Saskatchewan Research Council weather stations from event-based samples collected in Saskatoon (http://climate.weather.gc.ca/climateData/dailydata_e.html?StationID=47707&Month=11&Day=30&Year=2015&timeframe=2).

Surface (pond) water: pond water samples were collected bi-weekly in March-October 2014 at eight individual ponds excluding pond 5430 because this pond is flooded annually, and isotope signatures are not representative of this individual pond. The location of the ponds is shown in Figure 3.1b. Pond water samples were collected at depths well below the pond water surface into the narrow mouth 50 ml Polypropylene (PP) bottles and sealed. The archived surface water samples were collected monthly (where possible) from June 1993 to September 2013 and were also analyzed to supplement the data here.

Groundwater: Water level in each piezometer was recorded and the piezometers were purged by pumping water pumped out, recording field measurements for electrical conductance, pH, and temperature at approximately 5-minute intervals until the parameters become stable. Groundwater samples were collected from piezometers using a bailer or mechanical pump into narrow mouth 25 ml and 1000 ml Polypropylene (PP) bottles, which were then sealed and labeled. The locations of the piezometers are shown in Figure 3.1b. The groundwater samples were collected from the upland area, edge and beneath the Ponds 50, 107, 108a, 109, 110, 117, 120, and 125 where the piezometers were located in August 2013 and October 2014. The depth of the piezometers was between 1.82 to 41 m below ground surface. In addition, five groundwater samples at the depths of 5- and 41 m were collected into 1000 ml Polypropylene (PP) bottles from the edge (5 m) of Pond 109 to the upland area (300 m) near 125 on the 10th July 2016 for ^{3}H counting. The locations of these piezometers are shown in red labels in Figure 3.1b. The archived data set spanning from 1993 to 2012 and included fourteen piezometer records completed at various depths (1.2 and 25 m) between 1982 and 2012 within the till (Figure 3.1b) could not be sampled because they were either destroyed by farmers cultivating the land or flooded. A total of eighty-one groundwater samples were collected from piezometers installed in the shallow groundwater, aquitard and the intertill aquifer units were analyzed in this study.

3. 4. 4. Stable isotopes and tritium analyses

Water samples from ponds, groundwater from piezometers, and precipitation were analyzed for stable isotope ratios of hydrogen and oxygen (δ^2H and $\delta^{18}O$) at the NHRC in Saskatoon, Canada. Isotope measurements were conducted by laser spectroscopy using a Los Gatos Research DLT-100 liquid isotope water analyzer system coupled with a CTC LC-PAL liquid autosampler (Los Gatos Inc., California) using the methods described in (Lis *et al.*, 2008) and IAEA manual (2009). Laboratory standards, previously calibrated to the VSMOW2-SLAP2 reference waters were INV1 (δ^2H = -220.0‰, $\delta^{18}O$ = -28.5‰) and ROD3 (δ^2H = -8.0‰, $\delta^{18}O$ = -1.2‰). INV1 and ROD3 were used to normalize the results to the VSMOW-SLAP scale by assigning $\delta^{18}O$ and δ^2H values of -55.5‰ and -428.0‰, respectively, to the SLAP reference water. Samples, standards and control samples (river water) were analyzed repeatedly six times. The laboratory precision was ± 1.0‰ for δ^2H and ± 0.2‰ for $\delta^{18}O$ (Lis *et al.*, 2008). For ultra-low-level tritium analysis, five groundwater samples (1000 mL) were shipped to the Rafter Radiocarbon Laboratory at the National Isotope Centre of GNS Science in New Zealand. The ^3H concentrations are expressed in tritium units (TU); the precision at an average tritium concentration of New Zealand rain of 4 TU is ± 0.06 TU (98.5%) and the Rafter Radiocarbon Laboratory detection limit is ± 0.025 TU (Morgenstern and Taylor, 2009). Details of the analytical procedure are provided in Morgenstern and Taylor (2009).

3. 5. Results

3. 5. 1. Pond level and hydraulic head data

Long-term observations of the water level and hydraulic heads in all eight ponds are shown in Figure 3.4 for the period 1993 to 2015. The temporal characteristics of the different ponds are quite different. In the 1990s, ponds 107, 108a, 109, 110, 117 and 120 were empty at the end of most summers. Thus during dry periods, wetlands pond 109 and 120 behaved as seasonal wetlands because they retained water throughout most summers (i.e. through a season) and sometimes to the following years. However, the ephemeral ponds, 107, 108a 110 and 117 dried out every year usually by early summer. In the early 2000s, there was a significant drought and almost all the ponds were empty for a few years. Since 2005 ponds 50, 109, and 125 started filling and acting as permanent ponds. After 2010 the water levels in pond 50, 109, and 125 have been the highest on

record. In this entire record, pond 109 has not spilled in any measurable way. The behavior of pond 120 is similar to pond 109, but there is a maximum capacity, beyond which the pond spills. Pond 107, 108a, 110 and 117 are ephemeral, but Pond 110 is able to hold some amount of water and active vegetation throughout the summer after 2010. Pond 50 and 125 are large permanent ponds/lakes which are likely fed by groundwater (discussed below) and hence have a much more attenuated response to climate variability. Pond 50 does not spill but keeps filling up, because it is located in a large and deep valley. Pond 125 has a maximum capacity beyond which it spills. And pond 125 receives most of its water by surface spillage from other large ponds as pond 1 at higher elevations The spill from pond 125 makes its way to Pond 5340, which is the lowest point (below 546 meters above sea level) and terminal pond at the site. The observed characteristics of these eight ponds are similar across the landscape at SDNWA. More specifically, the large permanent ponds are associated with lower elevations and the small ephemeral ponds at the higher elevations as shown in Figure 3.4.

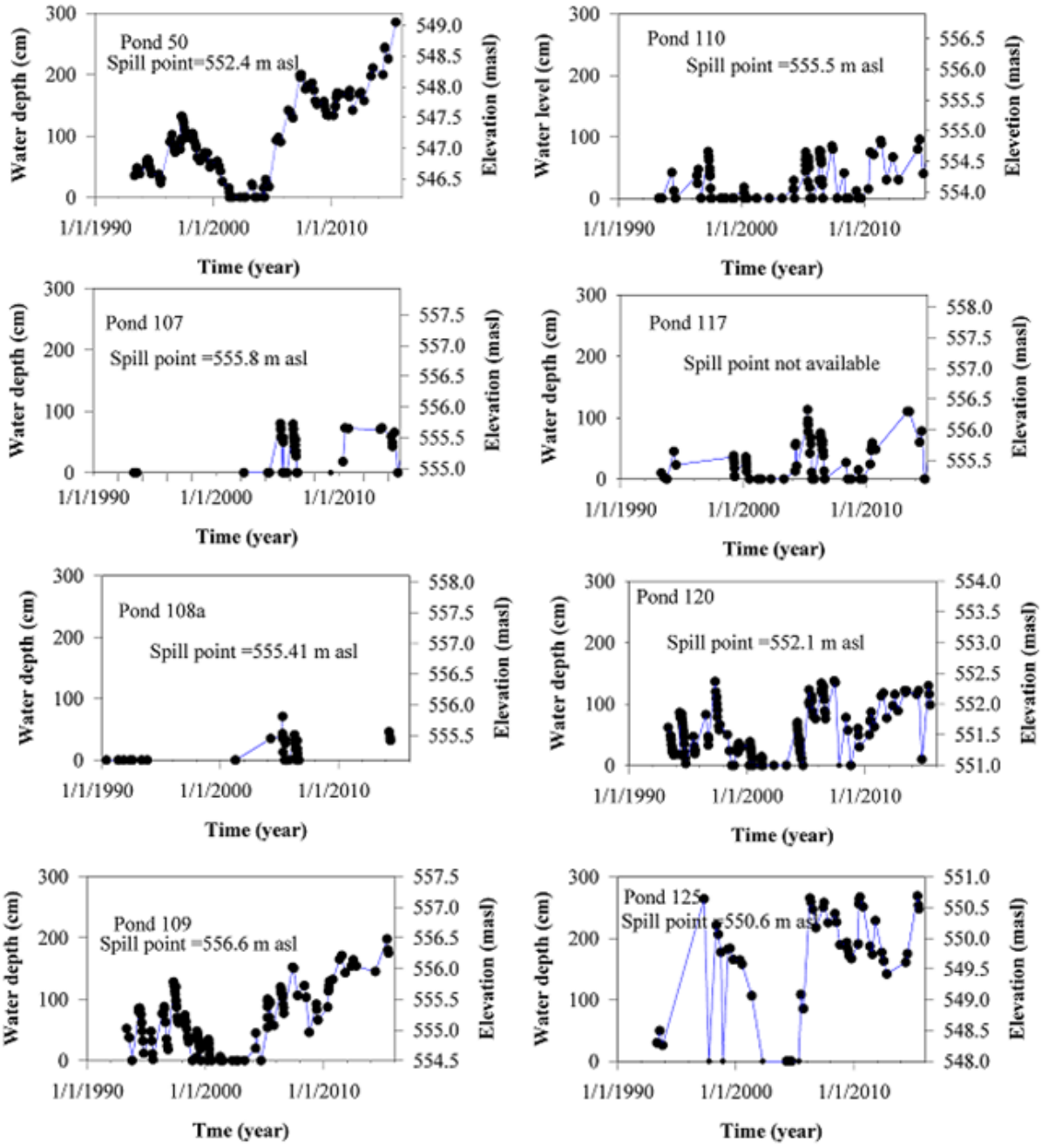

Figure 3.4. Pond water depths from 1993-2016 showing the shift in hydrologic conditions, showing how different types of pond function and the impact of climatic variability.

Observations of hydraulic head in the intertill aquifer and in ponds 50, 109, 125 and 5340, and the piezometers sampled for the tritium analyses are shown in Figure 3.5.

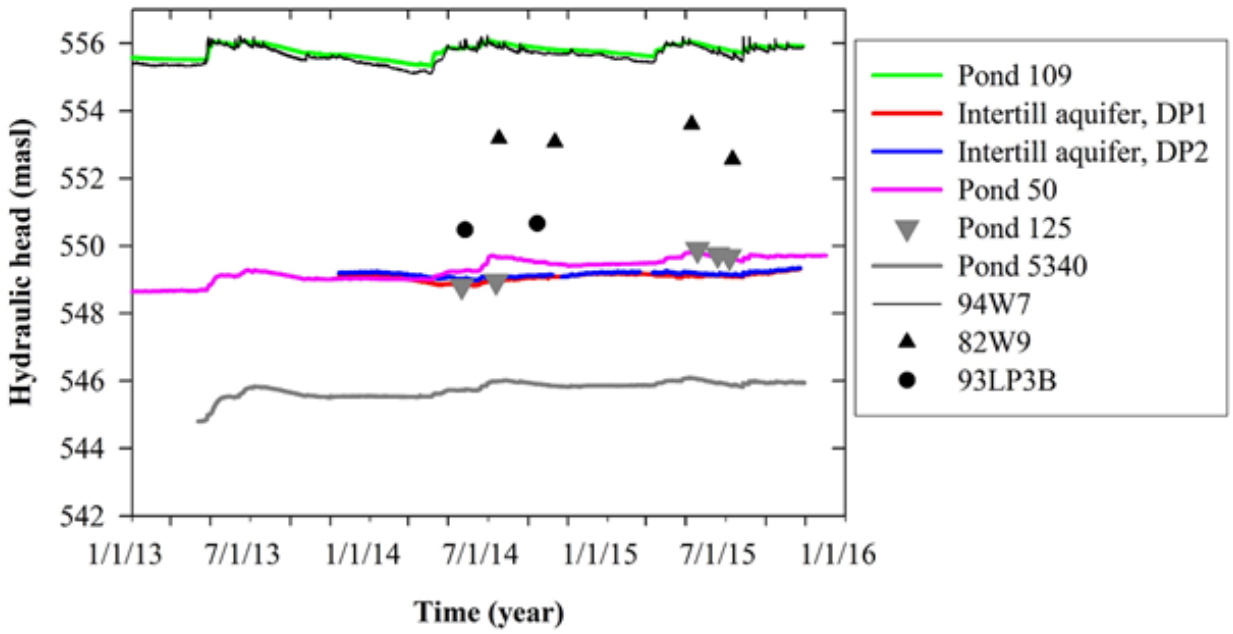

Figure 3.5. Plot of hydraulic heads in ponds 50, 109, 125, and 5340, intertill aquifer DP1 and DP2, and the piezometers for which tritium has been sampled at St Denis between January 2013 and December 2015.

The two piezometers in this intertill aquifer (DP1 and DP2 in Figure 3.1b) remain close to the same head stage with one another over the two-year monitoring period and do not show any strong seasonal response. For this period, the head in Pond 109 was more than 6 m higher than the other ponds and the intertill aquifer. Within the monitoring period, the shallowest piezometer 94W7 was at the same head stage with Pond 109. Ponds 50 and 125 were more or less at the same head stage with the intertill aquifer, and pond 5340 was 3 m lower. Despite the fact that these data are from an unusually wet period, the broad spatial patterns in heads are unlikely to change, although the magnitude of head gradients may become smaller and larger differences in head between the intertill aquifer and pond 50 and 125 might also develop in drier conditions. The head difference between piezometers 82W9 and 93LP3B and the intertill aquifer are 4 m and 2 m, respectively.

3. 5. 2. Landscape - pond aerial analysis

Computing possible contribution from uplands and ponds from the estimated land area of the confined intertill aquifer catchment, a simple catchment landscape analysis done. The areal analysis showed that 75% of the catchment was dry uplands without ponds. About 73% of the dry

upland area was above the potentiometric surface of the confined intertill aquifer and the remaining 27% discharge area. In catchment wide analysis, total area from dry upland areas and ponds areas capable of contributing recharge to the aquifer is 92% and 8%, respectively. It is therefore suggested that if recharge were uniform from ponds and uplands, then the isotope signatures of water samples from upland areas would dominate the aquifer. Also since gradients were elevated in both the ponds at higher elevations and in most piezometers found upland, this effect could be even be further exaggerated beyond a factor of 10.

In terms of hydraulic conductivity of the soil, the sediment under the wetland may have higher hydraulic conductivity values than the weathered till in the uplands. The hydraulic conductivity in the aquitards (i.e., below 5 m depth from the ground) to approximately the $10^{-9}ms^{-1}$ or less (van der Kamp and Hayashi, 2009) thus the recharge flux that reaches the confined aquifer from both below the ponds and uplands are of the same magnitude.

3. 5. 3. Tritium, ^{3}H

Tritium samples were collected from water sampled from five groundwater sources shown in Table 3.1. All samples were tritiated, except in the case of DP1 where it is difficult to eliminate contamination as a source of the very low TU value. All samples were tritiated, except in the case of DP1 where the lower very low TU value may be considered non-tritiated. The presence of Tritium suggests that groundwater in the St Denis intertill aquifer has been recharged by precipitation that fell sometime after the 1950s (Gleeson *et al.*, 2015). Shallow groundwater at 5.3 and 6.0 m depth had tritium values that were the highest (4.89 to 5.94 TU). Since the cessation of atmospheric nuclear tests, tritium concentrations in the region have dropped to an average of 10 TU although nuclear power plants may add small concentrations (Wassenaar, 1995; Gleeson *et al.*, 2015). The values found in the shallow groundwater are consistent with water that is 10 to 20 years old. Considering a piston displacement in the interpretation of the observations of TU with depth, this suggests a slow advective flow in the till at pore water velocities in the range of 0.27 to 0.6 m/year. Fracture flow within the weathered till could delivered water at flow velocities greater than reported for piston flow. The groundwater at 21.5 m depth is in an aquitard and has 1.27 TU, approximately another two half-lives below the shallow measurements, consistent with a piston displacement travel time of an additional 25 years, and a pore water velocity of 0.6 m/year. This pore water velocity is highly uncertain, however, as the Tritium concentrations could be subject

varying degrees of diffusion/dispersion. The deepest measurements (39.1 to 41.5 m) are from the intertill aquifer and were < 0.025 and 0.22 TU.

3. 5. 4. Stable isotopes of water

The isotope compositions of precipitation, snowmelt, groundwater and the eight ponds are presented in Table 3.2 and Figure 3.6a. The Figure 3.6b is a box-whisker plot that compares the range of $\delta^{18}O$ distribution in the various water types. The Figures 3.6a and 3.6b show distinct differences between the different units. The precipitation data from SDNWA fall on the Saskatoon local meteoric water line (SKMWL), but showed distinct seasonal variability, with winter measurements (snow) being more depleted. The surface water data plot along a pond evaporation line with a slope of 5.7, starting on or close to the MWL in the spring and becoming progressively enriched through the summer months.

Table 3.1. Tritium and associated stable isotopes of water from water samples collected at St Denis National Wildlife Area. *SigTU is one-sigma statistical certainty in the standard deviation of measurements.

Sample ID	Water type	Date	Intake depth (m)	δ^2H (‰)	^3H (TU)	sigTU*
DP1	Intertill aquifer	10/7/2016	39.6	-155.13	0.01	0.02
DP2	Intertill aquifer	10/7/2016	41.5	-155.12	0.22	0.02
94W7	Shallow groundwater	10/7/2016	5.3	-139.82	5.94	0.08
82W9	Shallow groundwater	10/07/16	6.0	-140.42	4.89	0.06
93LP3B	Aquitard	10/11/13	21.5	-149.10	1.27	0.04

The shallow groundwater data are fairly similar to the pond data but subject to less evaporation. Variability in the shallow groundwater data is predominantly due to spatial variation, as will be shown. The aquitard and intertill aquifer data plot on the MWL and biased towards the snow end of the spectrum of precipitation.

Table 3.2. Summary of isotopic concentrations in various water pools at St Denis National Wildlife Area, Saskatchewan.

	Pond water		Shallow groundwater		Aquitard		Inter Till aquifer	
	$\delta^{18}O$, ‰	$\delta^{2}H$, ‰	$\delta^{18}O$, ‰	$\delta^{2}H$, ‰	$\delta^{18}O$, ‰	$\delta^{2}H$, ‰	$\delta^{18}O$, ‰	$\delta^{2}H$, ‰
Min	-22.2	-173.1	-20.0	-157.8	-21.5	-162.2	-19.7	-155.1
Max	-2.0	-52.9	-11.1	-104.7	-16.9	-134.4	-19.4	-155.1
Range	20.1	120.2	8.9	53.1	4.6	27.8	0.4	0.0
Mean	-10.6	-102.4	-15.2	-125.2	-18.5	-146.7	-19.6	-155.1
Median	-10.1	-96.1	-15.1	-123.8	-18.3	-147.8	N/A	N/A
SD	4.3	24.5	2.3	14.9	1.1	7.0	0.2	0.0
Count	163	163	50	50	24	24	2	2

Figure 3.7 shows the variations in the isotope composition of the ponds, and in groundwater samples collected at the edges, upland and beneath the ponds. The intertill aquifer is also shown in each plot. The pond waters plot off the SKMWL to varying degrees. Pond 50 and pond 125 (which are in the same head stage with the intertill aquifer) are the most enriched and are consistently enriched, never intersecting the SKMWL. Meteoric rainfall and snowmelt enter the ponds and mix with the enriched water, resulting in seasonal movement along the pond evaporation line, but since the pond never empties (in the period of isotope records here), the isotopic signature is never fully returned to the SKMWL, as in other ponds. Since the water in the intertill aquifer is meteoric (Figure 3.6a), these data confirm that pond 50 and 125 cannot be a source of water to the intertill aquifer and leaves open the possibility that the intertill aquifer feeds the ponds. The remaining ponds in Figure 3.7 are all elevated above the potentiometric surface in the intertill aquifer (Figure 3.4), and hence have the potential to function as recharge ponds. In all cases, the pond waters intersect the intertill aquifer waters, but with a strong bias towards the depleted end of the pond water. This suggests that if these ponds are indeed recharging the intertill aquifer, then the recharge is taking place preferentially in the spring snowmelt period when the pond isotopic signature is depleted, and not from the enriched pond waters in the summer/fall.

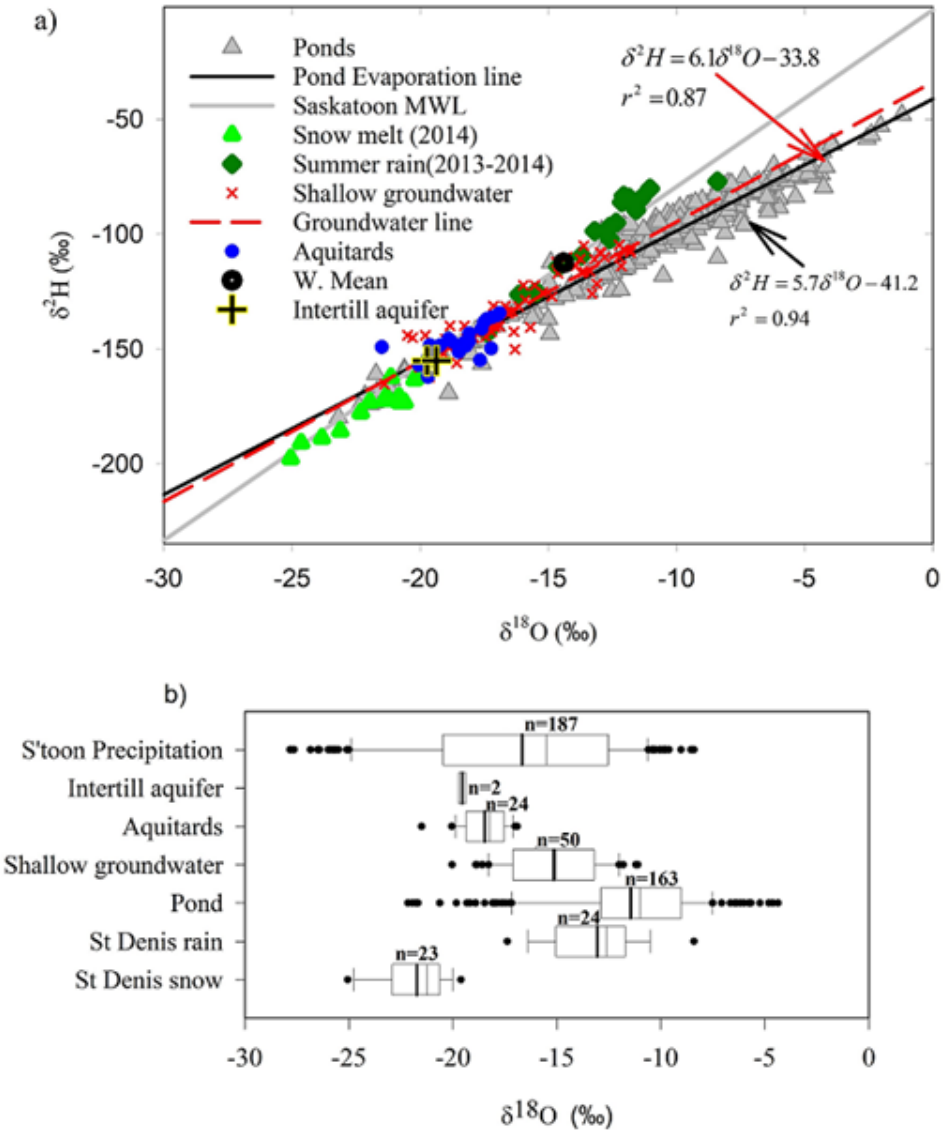

Figure 3.6. a) Scatter plot of dual isotopes (δ^2H-δ^{18}O) for spring–fall pond water (1993-2014), rainfall (2013-2014) and snowmelt water (2014), and b) box plot of δ^{18}O isotopes values of the various water types at St Denis National Wildlife Research Site at Saskatchewan. The boxes in Figure 3.6b mark the 25th–75th percentile range of data, whiskers mark the 10th–90th percentile range of data, and vertical black and gray lines are the mean and median isotope compositions, respectively for all samples.

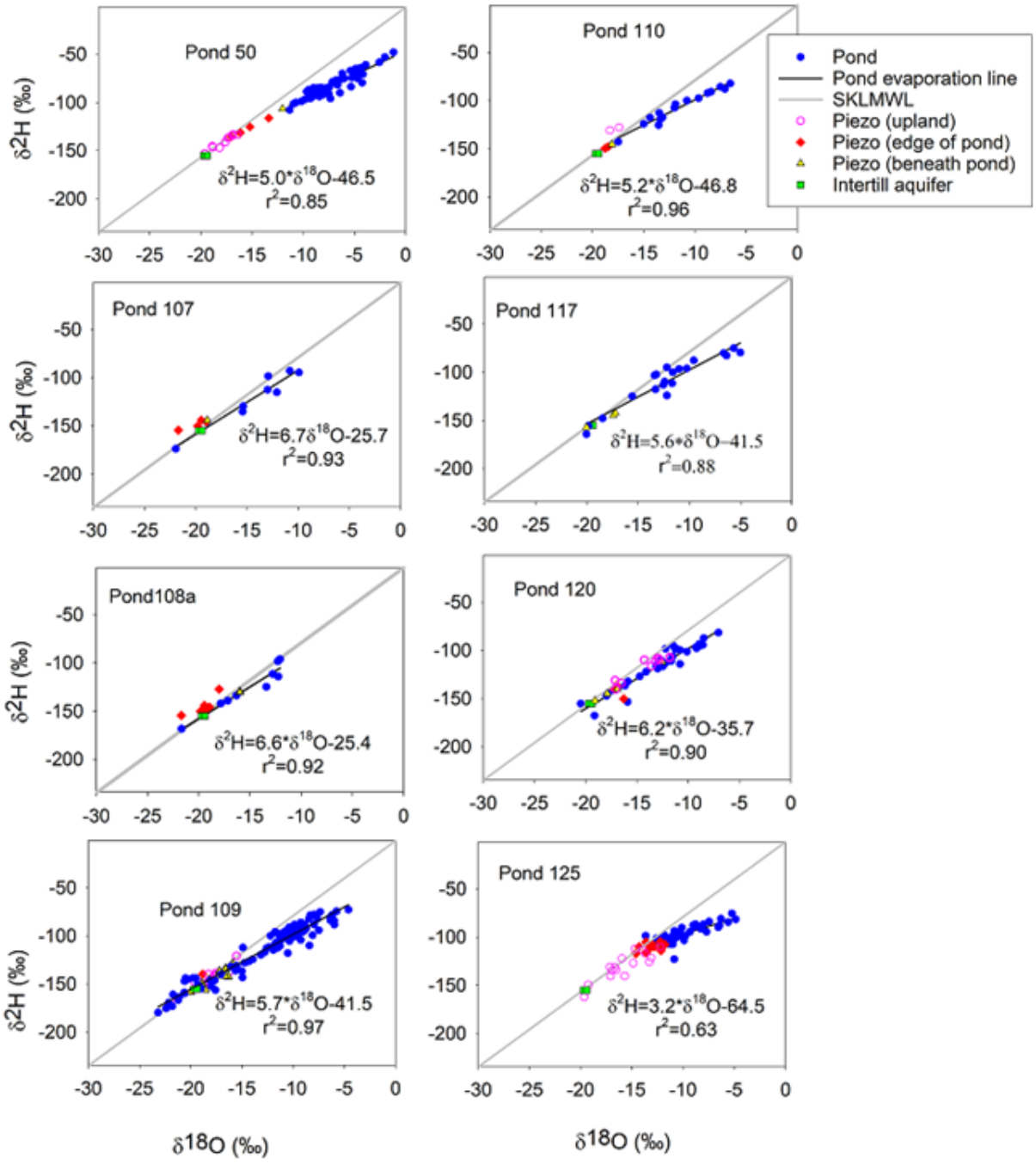

Figure 3.7. Dual isotopic plot to deduce the relationship between individual ponds (50, 107, 108a, 109, 110, 117, 120 and 125), and the subsurface units at St Denis National Wildlife Area.

Figure 3.8 (a and b) shows the isotope data for pond 109 separated into data prior to 2009, and since 2009, when the pond water levels have been the highest on record (Figure 3.4). In the recent period pond 109 has been behaving as a permanent pond, with a consistently enriched isotopic signature (similar to the normal behavior of pond 50 and 125). This signature is distinct from that of the intertill aquifer. This shows that caution must be taken in interpreting these data, since in the absence of the pre-2009 observations, one might conclude that the pond is not recharging the intertill aquifer.

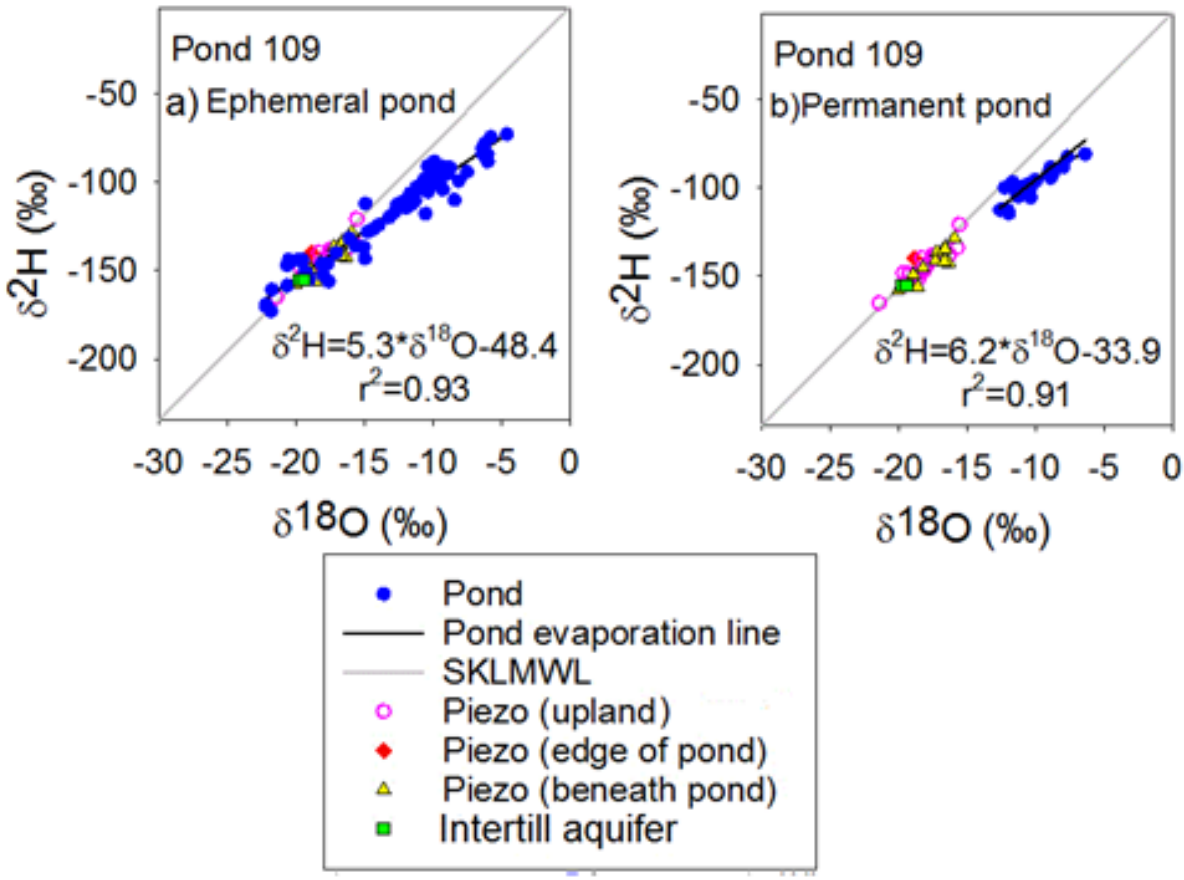

Figure 3.8. The long-term evolution in pond isotope composition of the recharge Pond 109 for the period between (a) 1993 and 2009 and (b) between 2010 and 2016 where the pond acted as an ephemeral /semi-permanent pond and as a permanent pond, respectively.

3. 6. Discussion

Two piezometers were installed in this intertill aquifer for the first time (DP1 and DP2 in Figure 3.1b) at the SDNWA. The small differences in head between the two wells (Figure 3.5) is consistent with the intertill aquifer being a highly conductive and laterally extensive unit. The small seasonal variations in the head, implying that recharge to this intertill aquifer is heavily attenuated by the aquitards. The Tritium data suggest that the confined intertill aquifer is recharged with modern (i.e. since 1950) water, and it is very unlikely that this is connate water. In other words, the surface system is considered to be actively interacting with the intertill aquifer, albeit slowly. This is also consistent with other lines of evidence that showed significant tritium values in the North American Pleistocene glacial till aquifers at depths of 20 to 60 m below ground (Fortin *et al.*, 1991; Bacon and Keller, 1998; Gleeson *et al.*, 2015). On the other hand, studies (Keller *et al.*, 1988; Hendry and Wassenaar, 1999; van der Kamp and Hayashi, 2009) reported that groundwater at similar depths within thick aquitards in the prairies were of Holocene and connate Pleistocene ages. This, however, could be due to differences that exist from site to site (e.g. the depth and permeability of the aquitards) in the case of Keller *et al.*, (1988) and Hendry and Wassenaar, (1999). However, the findings of Keller *et al.*, (1988) predated the time tritium isotopes were observed at greater depths in the till (Bacon and Keller, 1998).

The potentiometric level in the confined intertill aquifer is understood to be an important control on pond-subsurface flow exchanges and pond salinity (Nachshon *et al.*, 2013). The head differences between ponds and the intertill aquifer (shown in Figure 3.4 and 3.5) clearly suggest that pond 109 is a recharge pond (as others have reported, e.g., Nachshon *et al.*, (2013). However, pond 50 has been reported to be a discharge pond (Heagle *et al.*, 2013; Nachshon *et al.*, 2013; Pennock *et al.*, 2014), due to the high salinity in the pond. This is inconsistent with head observations in the intertill aquifer (Figure 3.5), which show that for the period of record, pond 50 is at the same head stage with the intertill aquifer. It is concluded therefore, conclude that pond 50 is a discharge pond, but this discharge is likely local groundwater recharged in the shallow transmission intertill aquifer surrounding the pond, and is not water from the intertill aquifer (as in the conceptual model of Nachshon *et al.*, (2013). Examination of the head profiles shown by (Heagle *et al.*, 2013) suggests that the area around Pond 50 is better interpreted as a classical upland-lowland lateral exchange regime, than as an upward flow of groundwater from below the

pond. Pond 5340, on the other hand, is likely a classical discharge pond, where water from the intertill aquifer is slowly discharged to the pond, via the aquitards between the two units.

It should be noted that this area has been subject to extreme climate variability in the past 20 years, as shown in Figure 3.4. During an extreme drought in 2001-2003, Pond 50 and 109 dried out completely, and the head in a piezometer below Pond 109 fell to the lowest level on record, slightly above 549 m (Hayashi *et al.*, 2016). This is roughly the same as the heads in the intertill aquifer in the period studied here, suggesting that recharge to the intertill aquifer may have stalled at this time. On the other hand, the period of detailed study here, 2014 to 2016, is a period of extreme wetness, with water levels unprecedentedly high. There is the need, therefore, to be careful when interpreting the head data in this period (2013 to 2015) as representative of longer-term conditions. Lake level data for the past 200 years in this region showed that wet conditions, similar to our current observation period, prevailed during the late 19th century (van der Kamp *et al.*, 2008). This long-term variability potentially confounds interpretations based on relatively short-term data sets.

The reported isotope values of surface water and groundwater at SDNWA (Table 3.1.) were similar to isotope values of water taken from surface ponds and glacial deposits throughout southern Saskatchewan and the central Canada (Fritz *et al.*, 1974, 1987; Wallick, 1981; Hendry, 1983; Mcmonagle, 1987; Fortin *et al.*, 1991; Hendry and Wassenaar, 1999, 2000, 2004; Kelley and Holmden, 2001; Grasby and Betcher, 2002; Harrington *et al.*, 2007; Grasby *et al.*, 2010; Jasechko *et al.*, 2014, 2017, Hendry *et al.*, 2015a, 2015b). The seasonal variations in the isotope composition of precipitation and ponds showed that isotope composition (^{18}O and ^{2}H) of pond water varied with season within and between the wetland ponds in the Prairies and that this variability cannot be simply be explained by the seasonal cycle of rain and evaporation, but the permanence of the ponds must also be taken into account (see Chapter 2 Figure 2.2 and 2.3). The larger permanent ponds, 50 and 109, had less variable isotope contents and were generally more enriched than the ephemeral ponds. The isotope data was used to interpret the relationship between the various ponds of varying permanence and subsurface groundwater recharge. In terms of the shallow groundwater (Figure 3.6a and 3.6b), the isotopes are generally more depleted than the mean weighted precipitation of Saskatoon and fall between the summer rainfall and the spring snowmelt water signatures. The isotopes cluster around the local meteoric water line with few deviations showing evaporitic water signals. The evaporitic signals are attributed to mixing of shallow groundwater with evaporitic pond water. The data suggest that the shallow groundwater is recharged year-round

by precipitation and in some cases mixes with local pond water. The spread of the isotope signatures of the aquitards and intertill aquifer along the SKMWL, however, was quite different from that of the shallow groundwater isotopes. They all plot on the MWL, suggesting little or no influence of evaporated pond water and also no effect of evaporation before recharge. They were also more depleted in $\delta^{18}O$ and $\delta^{2}H$ and biased towards snowmelt water suggesting cold season recharge (Figure 3.6a, and 3.6b). This raises the question: how/where is the intertill aquifer recharged? The isotope data from pond 50 and 125 (Figure 3.7) rule out the possibility that these ponds recharge the intertill aquifer, further corroborating our interpretation based on the hydraulic head data above. Since rainfall are generally more enriched than the aquitards and the intertill aquifer the possibility of recharge from direct infiltration of rainfall is also ruled out. This is likely because rainfall that infiltrates is largely lost to evapotranspiration in this semi-arid environment. However, a credible recharge water source that is consistent with our isotope observations came from the direct infiltration of snowmelt to recharge the aquifer. This could be facilitated by desiccation cracking of the soils on the uplands and below the ephemeral ponds in the summer (Heagle *et al.*, 2013), which would enhance infiltration during the subsequent melt, and would also shut infiltration down as the soils become wetter in late spring and the cracks seal up. This wet–dry-cycle repeated over hundreds of times, causes the snowmelt water to be transported downward through the desiccation cracks in the wetland to the intertill aquifer. However, it does not appear to be strong evidence for widespread desiccation cracking at St Denis, other than beneath the ephemeral ponds. If recharge is "depression-focused" (Lissey, 1971; Woo and Rowsell, 1993; van der Kamp and Hayashi, 1998, 2009) from recharge ponds (including ephemeral depressions) then it must occur preferentially in the spring snowmelt period when the pond isotopic signature is much depleted, and not from the enriched pond waters or the summer/fall rainfall. This raises the question: why is pond infiltration causing deeper recharge so much more significant during the melt/early summer period? It is the case that pond infiltration should be maximum following melt, as, most years, this is the largest injection of water into the system and pond levels are at their seasonal maximum (Nachshon *et al.*, 2014). However, in permanent ponds, the head in the ponds which drives recharge should not be very different between the spring and summer/fall period. In ephemeral ponds, on the other hand, the water level, and hence driving head, would dissipate into the summer, as the water levels drop below the base of the

pond and the ponds dry out. In Chapter 2, I showed that ephemeral and seasonal ponds lose approximately 87% of their water volume to infiltration during the spring-summer season. Thus, it is possible that the significance of small ephemeral ponds, which are widespread over the landscape but disappear shortly after the melt period, has been underestimated, and that these ponds deliver a disproportionate amount of recharge.

The role of large permanent ponds, like 50, 109, and 125 to aquifer recharge is questionable. These ponds are enriched for significant periods of time, and this signature is neither present in the aquitards nor the intertill aquifer, which casts doubt that they provide significant recharge. On the other hand, it is possible that over the past several decades, prior to 2009 (Figure 3.8), Pond 109 was itself functioning as an ephemeral pond. In this case, Pond 109 does provide recharge, in spite of the recent wet conditions that transitioned the pond into a permanent one. However, the current condition is not usual from historic trends where these ponds could go dry presumably due to evaporation and recharge to groundwater, and at that stage the ponds are reset. Thus, the current isotopic value in the intermediate aquifer is a mix of historical values (during the time since these ponds last went dry) and acted like ephemeral wetland ponds. Furthermore, pond 125 routinely spills and receives spilled water from upland ponds, also affecting the time-averaged isotopic value.

3. 7. Conclusions

Data on the hydraulic head, tritium and stable isotopes of water were collected at St Denis to understand groundwater-surface water interactions, and to test the existing conceptual model for the Prairie groundwater recharge. Tritium data indicate that the intertill aquifer is most likely recharged by modern water (since the 1950s). The head and isotope data show that some ponds do not provide recharge to the deeper groundwater systems and may indeed receive a discharge from those systems. Furthermore, the head data suggested other ponds could function as recharge ponds – that is they have higher heads than the aquifer, but stable isotope data show that not all of them do supply recharge water to the aquifers. The aquitards and intertill aquifers are recharged by meteoric, snowmelt water, which is distinct from the water in many ponds for much of the time, including the previously identified recharge ponds. It is concluded that it is most likely that

depression-focused recharge is a good conceptual model for this system, but that ephemeral ponds play a more important role than the permanent recharge ponds. It is easy to overlook these ponds because they are typically gone within weeks of the snowmelt period, and this suggests that their importance as a source of groundwater recharge needs to be considered more carefully in this, and other snowmelt dominated environments.

3. 8. Transition statement

In Chapter 3, a distinct perspective of the hydrological setting at St Denis was presented to improve our understanding of the hydrological processes linking wetland ponds and groundwater in the prairie pothole region. By examining a variety of ponds in terms of permanence and relation to groundwater, the wetland ponds capable of delivering of groundwater recharge water to intertill aquifers in the PPR. The evidence further supports the already existing depression-focused groundwater recharge conceptual model for the region. It has been shown in Chapter 3 that small ephemeral ponds especially those found uplands are critically important to the Prairie groundwater recharge and must be given attention in groundwater recharge studies. The evidence does not preclude recharge from the uplands but the literature on upland groundwater study in the glacial till PPR is rare and those that exist are limited to shallow zones. Our key next step is to examine recharge pathways from the uplands, lowlands, and the ponds and determine whether or not fractures in the till at upland areas can also be important conduits for groundwater recharge in this semi-arid –seasonally frozen climate. Chapter 4 draws on the multi-tracer profiles from the soils upland and lowland including a recharge pond to examine the role of the uplands and the mechanism of water flow and solute transport to the intertill aquifer systems in the glaciated North American Prairie Pothole region.

3. 9. Acknowledgements

This project was funded in part by the University of Saskatchewan Dean's scholarship, Government of Saskatchewan's Innovation and Opportunity Scholarship, and the Global Institute for Water Security. Professor Jeffery J. McDonnell is acknowledged for helpful advice during the formulation of the project and manuscript review comments. Dr. Melkamu Ali for his thoughts

and assistance during fieldwork. Thanks are also extended to Randy Smith, Dr. Dawn Keim, and Heather Wilson for field assistance and Geoff Koehler for giving us access to archived stable isotopes data and carrying out current isotope analysis. Special thanks to hydrologist from the National Hydrology Research Centre and the Global Institute for Water Security who have installed equipment and measured various parameters at the St Denis Site.

3. 10. Author contributions

E.K.P.B. designed the study and field work, compiled each data set, did the geographic information system work, and wrote the paper. A.M.I supervised and funded the research, G.V. provided archived isotope and water level data, A.M.I, G.V., and M.J.H, discussed the results, commented on the manuscript and contributed to the text.

CHAPTER 4: HIGH-RESOLUTION MULTI-TRACER STUDY OF WATER FLOW AND SOLUTE TRANSPORT IN GLACIAL TILL

Status: In preparation

4. 1. Abstract

In this paper, high-resolution vertical profiles of a stable isotope of water ($\delta^{18}O$, $\delta^{2}H$, and deuterium offset), dissolved ions (SO_4^{2-} and Cl^-), and measurements of till hydraulic properties were used to investigate groundwater recharge processes in the North American glacial till. The stable isotopes and lc-excess data showed that evaporated waters were present to a depth of 5 m and within the weathered till. In the saturated zone, water resembles isotopically depleted cold season precipitation water, not subject to evaporation. The dissolved ion concentrations show increases from the till surface to 3 and 6 m above the water table within the weathered till and decreased afterward. The lc-excess and dissolved ion concentrations data suggest downward leaching, evaporation, plant water uptake, and dilution from geological sources of water and solute. This complex combination of processes means that it is hard to make useful inferences about the flow processes from observed ion profiles in this environment. The observations suggest that groundwater recharge is recharge is predominantly due to fracture flow in the shallow weathered zone, and that this meteoric water penetrates below the root zone before enrichment in the matrix. On the other hand, water that is imbibed into the matrix within the weathered zone is captured by evapotranspiration and does not contribute significantly to groundwater recharge. Below the weathered zone, flow and transport are through the poorly fractured till matrix where the hydraulic conductivity is of the order 10^{-2} and 10^{-1} m/y culminates into a slow recharge to the intertill aquifer.

4. 2. Introduction

Assessment of groundwater recharge, that is the flux of water into the saturated zone, is essential for management and protection of water resources from over-exploitation and contamination. Understanding groundwater recharge includes the estimation of flow rates and analysis of the pathways (i.e. Matrix and or macropore) through which recharge occurs (Sophocleous, 2005; Manna *et al.*, 2017). Water can travel in macropores from the soil surface to groundwater with minimal resistance in a process termed as macropore flow. Macropore flow processes can be rapid, and fluids and solutes may be subject to minimal evaporation. Water flow through the matrix of soil or porous rock occurs more slowly and uniformly (Scanlon *et al.*, 2001; Manna *et al.*, 2017). Water held on the matrix in shallow soil depths can be subject to evaporation and transpiration (i.e. root water uptake). The amount of evaporation from a water pool can be assessed by the enrichment of stable isotopes, and this can thus provide insights into the pathways through which that water travelled (Hsieh *et al.*, 1998; Stumpp and Hendry, 2012; Mueller *et al.*, 2014a; Hendry *et al.*, 2015a, 2015b). Stable isotope tracers of water ($\delta^{18}O$ and $\delta^{2}H$) which are part of the water molecule preserve the initial isotope composition of the water entering the system (soil or pond), subsequent additions and withdrawals, and the processes acting on the system (Hunt et al., 1998; Mueller et al., 2014). Distinct isotopic patterns observed in different soil profiles, particularly when successive precipitation (rainfall and snow) events are isotopically different, make them useful in providing understanding on surface and subsurface hydrologic processes, estimate soil water fluxes and transport parameters at different landscapes and scales (Remenda *et al.*, 1996; Garvelmann *et al.*, 2011; Mueller *et al.*, 2014; David *et al.*, 2015; Hendry *et al.*, 2015a; Sprenger *et al.*, 2015, 2016b). Soil water abstraction for vegetation transpiration processes do not produce isotopic fractionation (Jasechko *et al.*, 2013; Huang *et al.*, 2015) and hence stable isotope tracers have been used to study soil evaporation processes (Allison and Hughes, 1983; Liu *et al.*, 2006), mechanism of soil salinization (Phillips *et al.*, 2003) and to partition evapotranspiration fluxes in soils (Yakir and Wang, 1996; Wang and Yakir, 2000; Rothfuss *et al.*, 2010; Wenninger *et al.*, 2010; Sutanto *et al.*, 2012). Critical to any useful quantification of groundwater recharge is the qualitative understanding of the flow processes that lead to groundwater recharge. However,

understanding groundwater recharge processes with respect to the characteristics of soil unsaturated zone is still a challenging scientific issue in catchment hydrology (Manna *et al.*, 2017). In the North American glacial till, quantification of groundwater recharge remains a challenge. This is complicated by the combination of a semi-arid climate, hummocky topography shaped by the last glaciations, and the highly variable hydraulic conductivity of the clay-rich sediments within which sequences of aquifers and aquitards are found (Zebarth *et al.*, 1989; Hayashi *et al.*, 1997; Winter and Rosenberry, 1998). Bulk hydraulic conductivity measurements (Hayashi *et al.*, 1997; van der Kamp and Hayashi, 2009; Ireson *et al.*, 2013) indicate that the till hydraulic conductivity decreases exponentially with depth until it becomes equal to that of till matrix in greater depths. Fractures or macropores in the till which may strongly influence the system response to water fluxes and exhibit a range of behavior, depending on both the characteristics of the porous matrix and the fractures and the climatic conditions to which they are subject (Ireson et al., 2013). Zebarth *et al.*, (1989) showed that the soil water is spatially redistributed in a hummocky terrain due the influence of topography, making flow highly variable in time and space in a local catchment area.

For a region, where the potential evapotranspiration exceeds precipitation, so groundwater recharge is mostly associated with areas only where soil moisture penetrates below the root zone before it is lost to evapotranspiration (Fortin *et al.*, 1991; van der Kamp and Hayashi, 1998). Groundwater recharge is, therefore, associated with depressions (wetland ponds) where snowmelt accumulates in the spring, and the soil moisture exceeds retention capacity. This is referred to as "depression focussed recharge" (Lissey, 1971; Fortin *et al.*, 1991; Woo and Rowsell, 1993; van der Kamp and Hayashi, 1998). Studies (e.g., Hayashi *et al.*, 2003) have shown that depression-focused recharge is facilitated by the rapid thawing of soil under depressions to enable infiltration of snowmelt water. But estimates (Millar, 1971; van der Kamp *et al.*, 2003; Parsons *et al.*, 2004)(Millar, 1971; van der Kamp *et al.*, 2003; Parsons *et al.*, 2004; van der Kamp and Hayashi, 2009; Nachshon *et al.*, 2013) suggest that about 60-70% of infiltrating water is lost to evaporation from depression surfaces and transpiration by riparian vegetation and plant water uptakes. Such losses may significantly reduce the contribution of depressions to recharge aquifers.

Despite significant progress in understanding groundwater recharge processes from surface depressions to the shallow surficial groundwater (0 to 25 m depth), little is known about the

contribution of upland and other lowland water transport from the soil surface to relatively deep intertill aquifers (~40 m). Over the past six decades, mainly physical measurements, and groundwater modelling techniques and few tracer methods (Meyboom, 1966; Lissey, 1971; Woo and Rowsell, 1993; Hayashi *et al.*, 1998a, 1998b, 2003, 2016; van der Kamp and Hayashi, 1998; van der Kamp *et al.*, 2003; Berthold and Hayashi, 2004; Parsons *et al.*, 2004) have been employed to study flow processes in the glacial till with regards to the wetlands. The studies provided detailed qualitative accounts on the flow and transport of solutes and in some cases, quantified recharge rates between wetland ponds and shallow groundwater. Within the findings of these studies, the contribution of snowmelt water and summer rainfall infiltrations to groundwater recharge is limited in the upland areas of the till (Lissey, 1971; Woo and Rowsell, 1993). Other studies (Keller *et al.*, 1985; Bacon and Keller, 1998; Joshi and Maule, 1999; Kelln *et al.*, 2007; Stumpp and Hendry, 2012) showed, however, that highly conductive fractures found in the till at lowland and upland areas transmit snowmelt water and tritium isotope into greater depths in the till. Recent works on groundwater (Jasechko *et al.*, 2017; Pavlovskii *et al.*, 2017) also points to groundwater recharge waters that come from cold season snowmelt waters. These studies suggest that the role of the secondary porosities in the till from both the uplands and lowlands areas, in transmitting recharge water to the groundwater may be poorly understood and hence require further investigation.

Studies involving stable isotopes ($\delta^{18}O$ and $\delta^{2}H$), and water chemistry (SO_4^{2-} and Cl^-) in the saturated zone and surface water systems are numerous. To date, however, most hydrogeological studies that use stable isotopes and/or water chemistry in the till have focused on either water flow and solute transport in saturated, non-fractured till or unsaturated, fractured soils covering the till (Hendry and Wassenaar, 2009; Hendry et al., 2004, 2011, 2015a; Keller et al., 1986; Remenda et al., 1996; Stumpp and Hendry, 2012). The challenges associated with the use of stable water isotope tracers in studying hydrological processes in seasonal climates where wide temporal and spatial variations exist in the initial isotope composition of precipitation entering the catchments (e.g., evaporation effect) (Peng *et al.*, 2004; Berman *et al.*, 2009; Huang and Pang, 2012) has also not been adequately addressed. Based on water stable isotope data, deuterium offset ("line condition, lc excess", Landwehr and Coplen, (2004)) can be evaluated to study the effect of evaporation or condensation processes on precipitation water in soils and surface waters, which

may recharge groundwater systems at the local level. The lc excess value (Landwehr *et al.*, 2014), defines the offset between a local meteoric water line and water samples associated with evaporation, condensation or mixing processes. The local meteoric water line is an equation defined by the mean relationship between hydrogen and oxygen isotope ratios in natural precipitation waters, expressed as a local mean for at least three years (IAEA, 1992). Unlike, deuteruim excess (d-excess) (Dansgard, 1964) which defines the effects of meteorological conditions and processes such as evaporation and condensation on global isotopes in precipitation, lc-excess is a local measure (Gat, 1996; Landwehr and Coplen, 2004). Lc-excess values of zero (0) indicate direct precipitation with no evaporation; negative values indicate evaporative isotopic fractionation; and positive values suggest sample arising from several sources including relatively newly evaporated vapour reflux and condensation. The lc-excess is calculated and used here to provide insights and bridge the gap between what happens to water molecules before and after it enters the soil, transverse the unsaturated zone and/or reach the water table.

The objective of this study is to provide a mechanistic understanding of water flow and solute transport from the soil surface (i.e., 0.2 m depth below ground) through the unsaturated zone to the underlying aquitards and intertill aquifers (~40 m depth BGL) covering upland and lowland landscape positions of the hummocky terrain. High-resolution tracer profiles of a stable isotope of water ($\delta^{18}O$, and lc-excess), dissolved ions, SO_4^{2-} and Cl^-, and soil hydraulic properties were combined to understand the pathways of water and solute in the till. Pore water isotope and dissolved ion concentrations were obtained from three soil profiles between the soil surface, 0.2 m and 14 m depth in upland and lowland areas of the St Denis National Wildlife Area in southern Saskatchewan. The data were integrated with stable isotopes and water chemistry data from a known groundwater recharge pond and piezometer groundwater samples obtained at 1 and 40 m depth BGL from the same site. The study is important for water resource management in glacial till and the Canadian prairies where farmers and majority of the rural population depend on groundwater. The semi-arid SDNWA National Wildlife Research Area in central southeastern Saskatchewan, Canada is used as an example to illustrate possible mechanisms of water flow and solute transport at various places of the hummocky terrain of the glacial till.

4. 3. The study area

Fieldwork was conducted between May 2013 and May 2017 at the 385-ha SDNWA National Wildlife Area, SDNWA (52˚ N, 106˚ W), located 40 km east of Saskatoon, Saskatchewan, Canada (Figure 3.1a). The SDNWA was established in 1968 as a long-term study site for the ecological monitoring of a wetland complex (Hogan and Conly, 2002). There are 100 wetlands of varying size and hydrological seasonality on the SDNWA (van der Kamp and Hayashi, 2009).

The region has seasonally frozen semi-arid climate with significant interannual variability in summer (April–September) and winter (October–March) precipitation. The monthly mean temperature for varies between -20 °C (December- February) to 19 °C (July-August) (Wittrock and Beaulieu, 2015). The annual open-water evaporation in the region exceeds the total annual precipitation (Parsons *et al.*, 2004). The site has climate and landscape typical of the North American PPR (Hayashi *et al.*, 2016). The area is underlain by stratified silty glaciolacustrine sediments and further underlain by the glacial till of the Battleford and Floral Formations of Middle to Late Wisconsin age (Hayashi et al., 1998a). The upper till layer, 0-6 m, is weathered, fractured and oxidized. Below this depth is the un-oxidized layer sometimes with fractures at deeper depths (Keller *et al.*, 1985; Harrington and Hendry, 2005; Harrington *et al.*, 2007; van der Kamp and Hayashi, 2009). The water table fluctuates between 2 to 3 m according to seasons and in some cases act as artesian wells in the ponds after snowmelt recharge and summer –fall (van der Kamp and Hayashi, 2009; Hayashi *et al.*, 2016). Typically, water tables are found measured between 0.6 m below ground level near the ponds and 7 m in the uplands. The water table in the pond and the shallow piezometers (that is shallow piezometers located at the edge of wetland) frequently reversed direction between inward and outward flow and typically inward during spring and early summer after snowmelt recharge and outward in late summer and fall (Woo and Rowsell, 1993; Rosenberry and Winter, 1997; Hayashi *et al.*, 1998; Heagle *et al.*, 2013).

The three profiles (EB1, EB2, and EB3) considered were taken from a plot of 100 m^2. Profiles depths ranged from the soil surface to the depths of 11.5 m (EB1), 8.0 m (EB2) and 13.5 m (EB3) (Figure 4.2). The distances between the soil profile locations EB1, EB2, EB3 and the reference pond 109 (Figure 4.2) are 40 m, 60 m, and 330 m, respectively. The distances between soil profile EB1 and EB2, EB1 and EB3, and EB2 and EB3 are 20 m, 290 m, and 270 m, respectively. The distances from the profiles to the various piezometers ranged from 0 to 70 m (Figure 4.2). The

second and third profiles EB2 and EB3 (Figure 4.2) were located at higher elevation areas close to the piezometer installed within the intertill aquifer well, DP1 and DP2. These are taken as of water transport mechanisms in upland areas. Soil profile EB1 is closest to Pond 109 and is chosen to test depression-focused recharge conceptual model. Pond 109 is considered a recharge wetland (Hayashi *et al.*, 1998; Parsons *et al.*, 2004) which interacts laterally with the shallow groundwater within its margin.

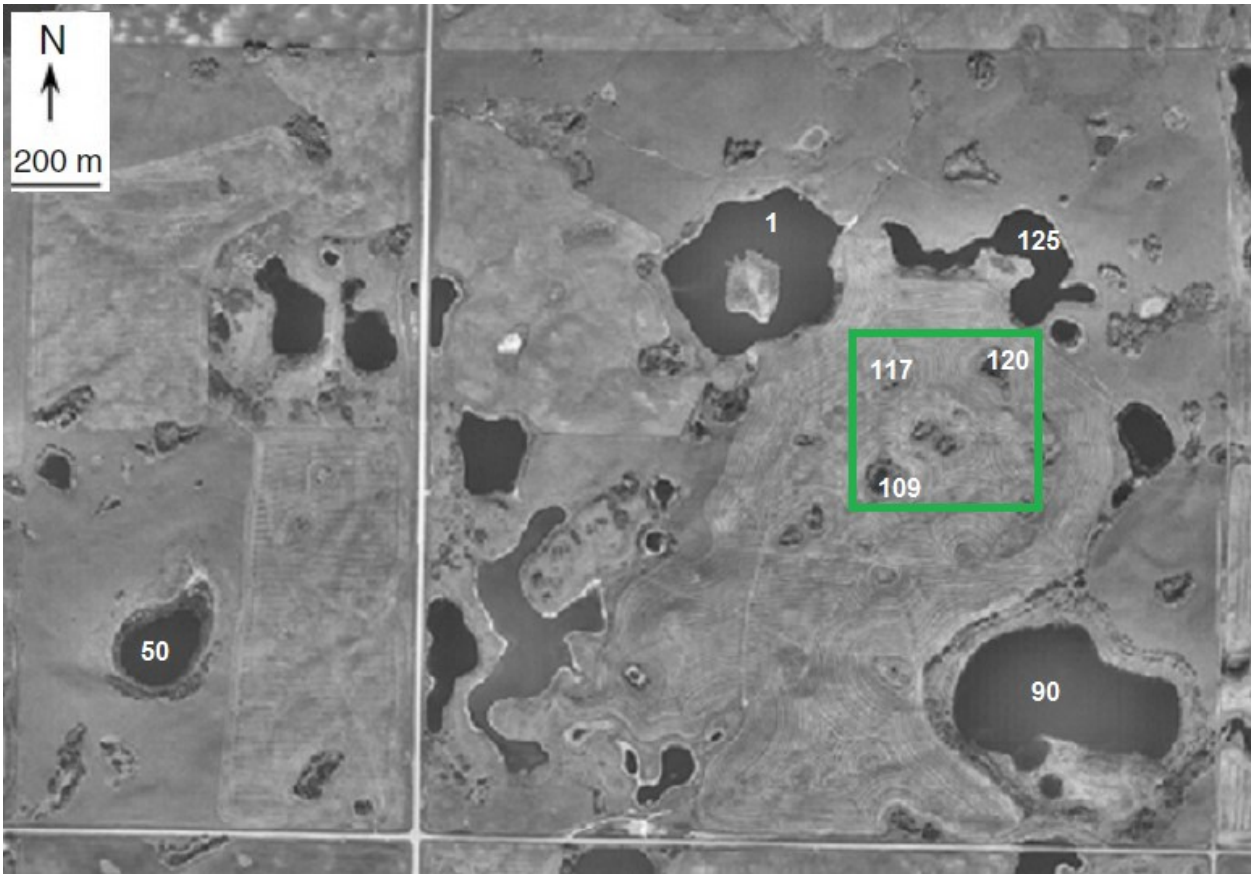

Figure 4.1. An aerial photograph of the SDNWA taken October 1997 (van der Kamp and Hayashi, 2009) and showing is the location of the study area in the green square and wetland ponds 50, 90, 109, 117, 120, and 125, and other wetlands.

4. 4. Field and laboratory methods

4. 4. 1. Soil cores sampling

In November 2014, continuous soil cores (127) were collected at EB1, EB2 and EB3 (Figure 4.2) using Failing 1250 TD rotary drilling rig and a 1.52 m x 75 mm diameter core barrel. Repeated

cores of 1.5 m were collected between approximately 0.2 and 11.5 m, 0.15 to 8.0 m and 0.15 to 13.5 m depths at locations EB1, EB2 and EB3, respectively. The core barrel was split open, and the soil core was cut into sections of approximately 10 to 30 cm length depending on the suitability of the core to stable isotope and chemical analysis or bulk density and soil physical properties analysis. In total, 39, 41, and 47 soil core samples were collected from profiles EB1, EB2, and EB3, respectively. Forty-three soil cores (13 from EB1, 14 from EB2, and 16 from EB3) were collected for bulk density, water content, and porosity measurements. Thirty-one core samples

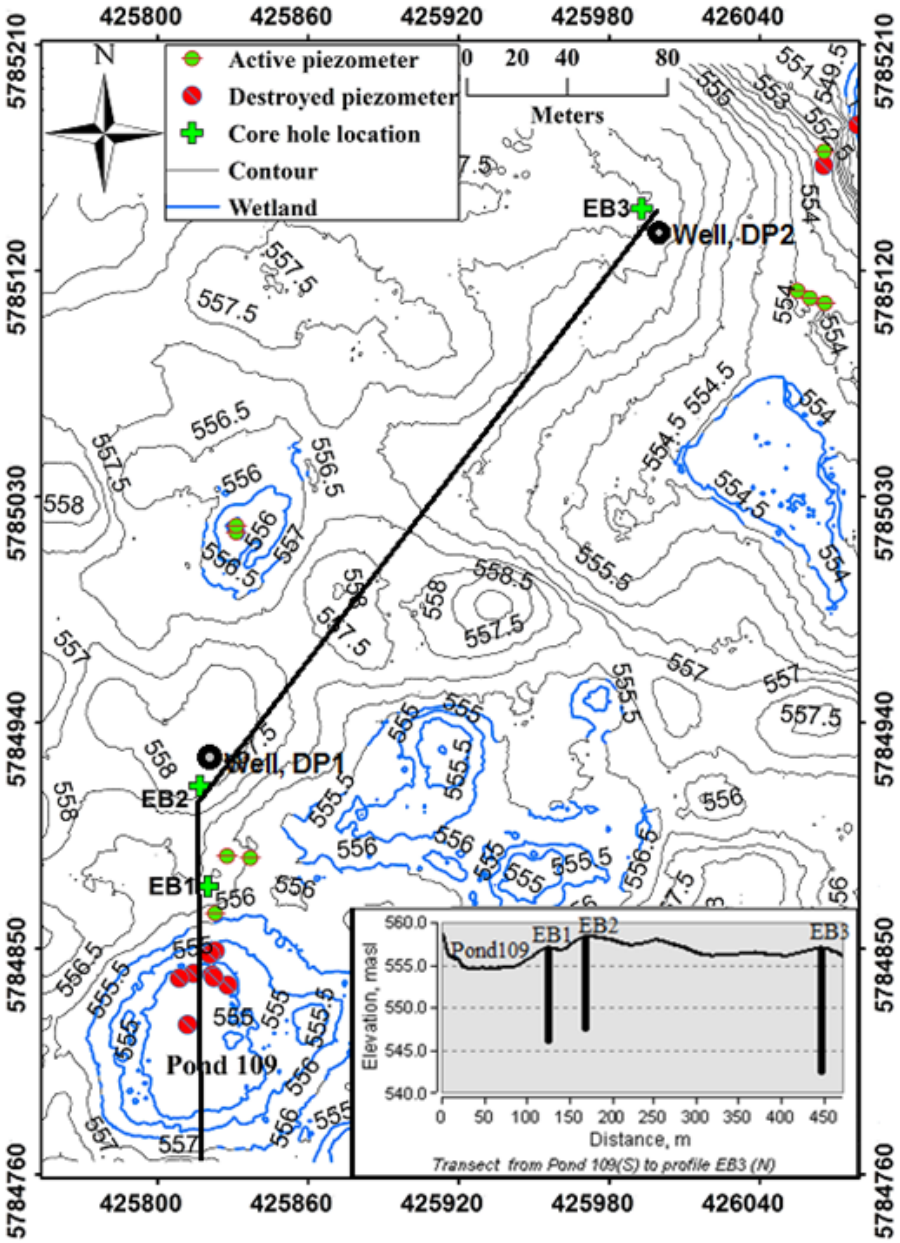

Figure 4.2. Contour map of the study area (green in Figure 4.1) with Pond 109 and surrounding wetlands, Wells, soil core and piezometers locations. The insert is the vertically exaggerated transect from Pond 109 to the upland profile EB3.

were collected for stable isotope analysis by vapor-equilibration and forty-three for squeezing and stable isotope and chemical analyses. Sample preparation and preservation procedures follow those of Hendry et al. (2013). Thus, immediately after the retrieval of the 10 to 30 cm length soil core from the core barrel, the outer 2 to 5 mm of each core sample was removed to minimize contamination from the drilling mud. The samples were then placed in labeled medium-sized, double seal Ziploc^{TM} bags, and atmospheric air removed by squeezing the air out of the bags, which were then sealed. Each bagged sample was then placed inside a larger Ziploc double seal bag, with the air again squeezed out before sealing and labeling. The bagged cores were placed in coolers and kept at ambient temperature (5 to 10 ˚C) until transported to the Department of Geological Sciences at the University of Saskatchewan where they were kept in the coolers at room temperature until analysis. All of the holes from which the core samples were obtained were later backfilled with bentonite chips.

4. 4. 2. Soil property analysis

Dry bulk density (ρ_b, gcm^{-3}) was determined on the 43 core samples using the American Society for Testing and Materials ASTM D7263-09 (ASTM, 2009) and ASTM D854-10 (ASTM, 2010) procedures, respectively. These data were used to calculate total porosity ($n_T, \%$) of the samples. The weight of water, determined as the difference between the weight of the sample and its weight after oven drying at 110- 150 ˚C for 24 h, was used to estimate the gravimetric moisture content. Gravimetric moisture content was converted to volumetric moisture content ($\theta, \%$) using the mean soil bulk density determined for each core sample.

4. 4. 3. Pore Water Squeezing and Analyses

The forty-three soil core samples selected for chemical and stable isotopes analyses were squeezed in a high-pressure mechanical squeezer to obtain pore waters (Hendry *et al.*, 2013, 2015b). The samples, before squeezing, were reduced in size, to fit into the squeezing cylinder, by scraping with a knife and immediately packed as tightly as possible into the squeeze cylinder (316 L

stainless steel; 50 mm diameter by 80 mm long). A piston was inserted into the cylinder and the cylinder placed in the hydraulic press where the pressure was increased to between 50 and 70 MPa. This pressure range was selected for squeezing because it has no measurable effects on SO_4^{2-} and Cl^- ion concentrations as well as on $\delta^{18}O$ and δ^2H isotope values (Fernández *et al.*, 2014; Hendry *et al.*, 2015b). The samples were maintained under pressure for 3-5 days. During squeezing, pore water passed through a 0.45 μm stainless steel filter before exiting via a port at the base of the cylinder where it was collected in a clean 60 cm^3 plastic syringe. The pore water samples, which ranged in volume from 3 to 50 cm^3, were subsequently transferred to 50 ml polypropylene bottles, and tightly sealed until analysis. Before analysis, each sample was split into two portions, a 2 ml aliquot for stable isotope analysis and the remainder for dissolved ion analysis.

For $\delta^{18}O$ and δ^2H analysis, the 2-ml aliquot pore water samples were used to fill a 1.5 ml glass for laser absorption spectroscopy analysis. The samples were then analyzed using a Los Gatos Research DLT-100 liquid isotope water analyzer system coupled with a CTC LC-PAL liquid autosampler (Los Gatos Inc., California) at the National Hydrology Research Centre, Saskatoon. Two water standards with $\delta^{18}O$ and δ^2H values that bracketed those of the precipitation values in the study area were prepared and used in analyzing the pore water samples. The precision of the analytical method tested on laboratory standard waters has been estimated to be less than ± 2‰ for $\delta^{18}O$ and ± 0.4‰ for δ^2H, which is comparable to modern continuous flow isotope ratio mass spectrometer methods and better than those reported for physical water extractions (Lis *et al.*, 2008). The second portion of the split pore water samples was retained at four degrees Celsius for analyses of dissolved ions (SO_4^{2-} and Cl^-) using an inductively coupled plasma optical emission spectrometry (ICP-OES) analytical technique. The analysis was carried out at the Department of Geological Sciences, University of Saskatchewan. It was estimated that the analytical error for the ions was better than ± 5%.

4. 4. 4. Soil core vapor – equilibration and analysis

Stable isotopes of water (δ^2H and $\delta^{18}O$) were measured from water vapor from for thirty-one (31) subsamples of cores. Vapour –equilibration for the δ^2H and $\delta^{18}O$ analysis followed the methods described in earlier studies (Wassenaar *et al.*, 2008; Hendry *et al.*, 2015b) Thus, before isotope analysis, medium-size double seal Ziploc™ bags containing the cores were inflated with H_2O-free dry air and resealed to create a sample equilibration and headspace sampling volume. Each inflated

bag was placed back into the large Ziploc bag from which it came and resealed to prevent leakage. Samples were allowed to equilibrate isothermally to 100% relative humidity at room temperature for 5 days before analysis. The water vapor developed from the core samples in the filled were then collected with a syringe and analyzed using $H_2O_{(liquid)}$-$H_2O_{(vapor)}$ analyzer Picarro L1102-i isotopic water liquid analyzer (Picarro Inc. Sunnyvale, CA). Like liquid-water isotope analysis, two aliquots of known water standards with $\delta^{18}O$ and $\delta^{2}H$ values that bracketed those of precipitation values in the study area were equilibrated as core samples but at reduced time and used in analyzing the samples. The standards were equilibrated in the same way as the core samples but with a shorted equilibration time (1 h). These standards were run to correct for instrument drift and to normalize the results to the VSMOW scale. Testing for accuracy and precision on the $H_2O_{(liquid)}$-$H_2O_{(vapor)}$ equilibration method showed that the equilibration times provided optimum results for $\delta^{2}H$ and $\delta^{18}O$ (Hendry *et al.*, 2015b).

4. 4. 5. Archived data

Data obtained during the investigations, as described above, were supplemented with data on piezometer depth, groundwater level and chemistry, pond water, and stable isotope data from Environment and Climate Change Canada (ECCC), Saskatoon. The dataset spanned from 1993 to 2010 and included fourteen piezometer records completed at various depths (1.2 and 25 m) between 1982 and 2012 within the till (Figure 4.2). These could not be sampled because they were either destroyed by farmers cultivating the land or flood or inaccessible. Archived hydraulic conductivity data (K) was obtained from slug test data at SDNWA reported in Hayashi (1996) and van der Kamp and Hayashi (2009). The isotope results from pond 109, the piezometers (groundwater) and the aquifer used here were previously used in Chapters (that is Chapter 2, and 3) but combined here with chemical data to understand the flow of water and transport of solutes through the till.

4. 4. 6. Data processing

Because plant transpiration and salt dissolution does not affect isotope composition of water and the subsequent lc-excess values (Goldsmith et al., 2012; Herve-Fernandez et al., 2016; Huang et al., 2015; Landwehr et al., 2014; Brooks et al., 2010), we characterized all water isotopic signatures using the deviations of $\delta^{2}H$ and $\delta^{18}O$ from the SKLMWL, and lc-excesses of the different water

types from different locations as well as lc-excess to depth at which water is obtained. By comparing isotope values of meteoric water, pore water and groundwater, and lc-excess values, it is possible to assess the extent of transport of evaporated water and evaporation in the soil and determine the source and processes acting on water recharging the groundwater. We adopted the lc-excess value calculated previously (Landwehr and Coplen, 2004) as:

$$lc - excess = [\delta^2 H_s - a * \delta^{18} O_s - b]/S, \quad (4.1)$$

where the subscript,'s', stands for the sample, 'a' and 'b' are the slope and intercept, respectively of the LMWL and 'S' is the standard error associated with instrumental measurement of δ^2H and δ^{18}O. The standard error of the all liquid water isotope analysis using the Los Gatos Laser Liquid water analyzer is 0.2‰ for δ^{18}O and 1.0‰ for δ^2H. The $lc - excess$ is used to assess significant departures of the various water types from meteoric conditions and to provide a comparison between water sources and the local precipitation (Landwehr and Coplen, 2004). In general, the slopes and intercepts of the local evaporation lines (with regards to pore water, piezometer groundwater, and pond water were estimated using the ordinary least square linear regression method (Crawford *et al.*, 2014). The isotope compositions obtained from the two isotope analysis methods (i.e., vapour equilibration and squeezing) were combined since there was no significant variations in the two data sets. Hendry *et al.*, (2015b) and Orlowski *et al.*, (2016) showed that the results of water isotope compositions measured in soil with water content between 20 to 30% by direct vapour equilibration and squeezing using lasers and mass spectrometer methods are comparable. A very strong linear correlation (R^2 = 0.92 and R^2 = 0.93) exist between our squeeze samples and the vapour-equilibrated data for δ^{18}O and δ^2H, respectively.

4. 5. Results

4. 5. 1. Soil properties

Figures 4.3 and 4.4 shows the properties of the soil at the SDNWA. Dry bulk density for all the core samples was 1.99 ± 0.06 g cm^3 (n = 43). The dry bulk density was relatively low (1.8 g cm^3) in the shallow (< 2 m) sediment. This was attributed to weathering, the presence of macropores (e.g., fractures) and high organic content in the top layer of the soil. Soil porosity was 24.89 ± 2.49% (n = 43) and were mostly higher values at shallow depths than the deeper depths of each profile (Figure 4.3). Soil particle distributions (results not shown) were variable within each

profile. The particle distributions are given Table 4.1. Soil volumetric water content was 24.57 ± 2.27% (n = 43). The volumetric water content at the bottom 8 to 15 m (not reported here) of EB1 and EB3 exceeds the porosity – which is not possible. However, anomalous data such as these are common for deep cores and are likely due to compaction and errors in cored volume calculations (Reynolds, 1970). The variability in the soil water content is attributed to the soil heterogeneity with depth in the soil profiles.

Figure 4.4 shows the soil saturated hydraulic conductivity (K) measured by slug tests on piezometers (Hayashi et al. 1998a), permeameter tests on soil cores (Parsons et al. 2004) and ring infiltrometers (van der Kamp et al. 2003) at the St Denis National Wildlife Area from the soil surface to 25 m depth (van der Kamp and Hayashi, 2009). The K values in the upper 2 m depth were variable from a low of 1 to 1000 m/y. Below 2 m depth, the K values decrease exponentially with depth. More specifically, the K values were low and lie between 10^0 to 10^2 m/y at 2 to 5 m depth and decreased gradually to less variable values of 10^{-1} and 10^{-2} m/y at 5 to 25 m. The presence of fractures in the shallow weathered and more fractured till (0 to 5 m depth BGL) and the continuous decrease in the fractures in the non-weathered (> 5 m) till at deeper depths explains the Ksat values (Keller *et al.*, 1985; van der Kamp and Hayashi, 2009; Hendry *et al.*, 2015a).

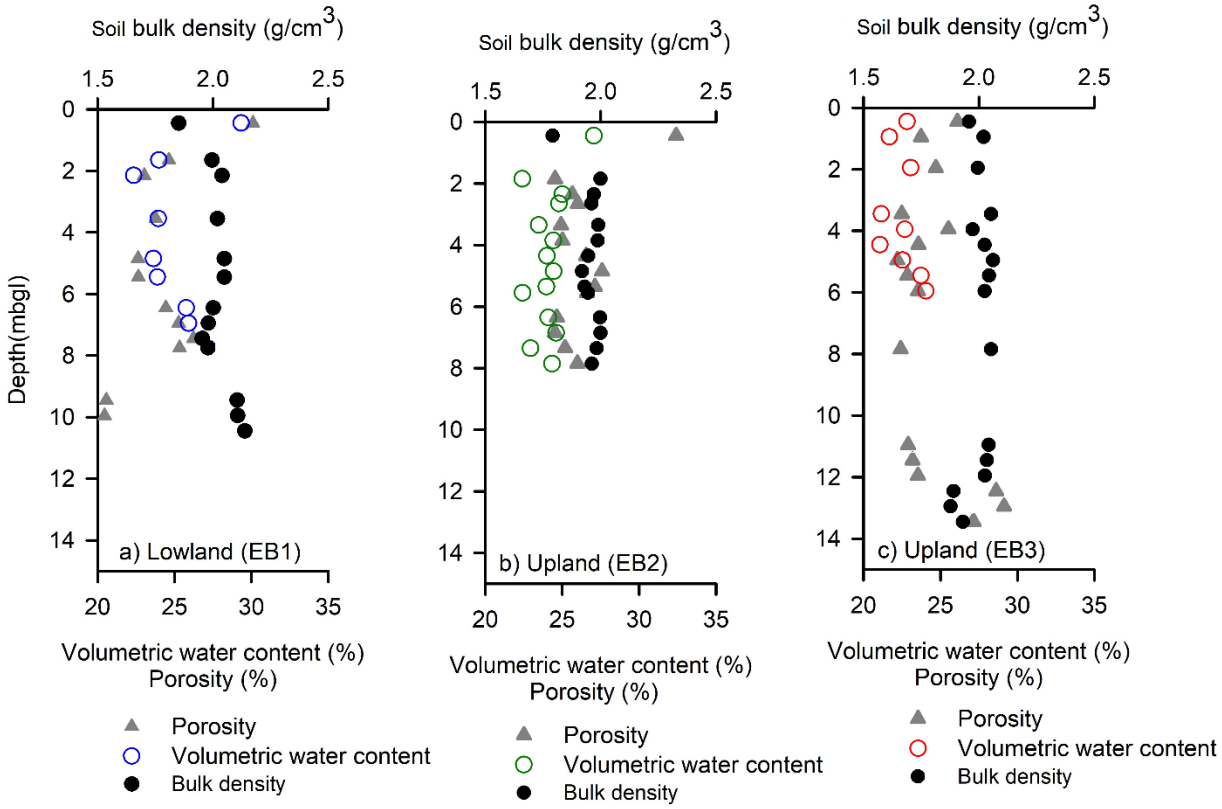

Figure 4.3. Porosity, volumetric water content and dry bulk density of soil samples from three profiles in the riparian (EB1) and uplands (EB2 and EB3).

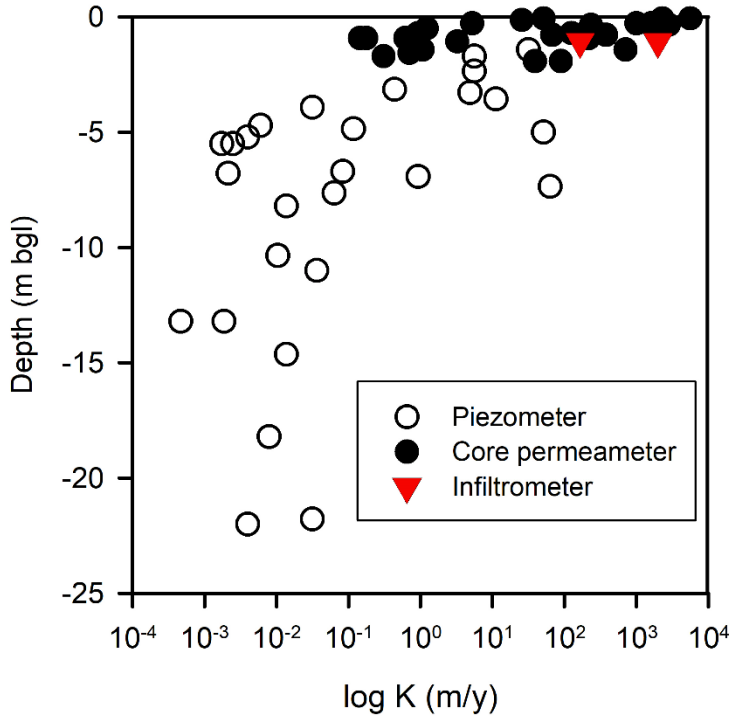

Figure 4.4. Soil hydraulic conductivity obtained from the slug test on piezometers, permeameter tests on soil cores and ring infiltrometers at St. Denis National Wildlife Area (reported in van der Kamp and Hayashi, 2009).

Table 4.1. Soil properties as measured from auger cored samples at St. Denis National Wildlife Area laser diffraction.

Location	Property	Mean	Standard Deviation	Minimum	Maximum	Count
Lowland (EB1)	n_T (%)	23.73	2.83	19.31	30.11	13
	θ (%)	25.14	2.10	22.35	29.33	13
	ρ_b (g/cm3)	2.02	0.08	1.85	2.14	13
	Clay (%)	1.45	0.48	0.97	2.16	13
	Silt (%)	58.54	7.16	49.98	74.71	13
	Sand (%)	40.01	7.55	23.18	49.03	13
Upland (EB2)	n_T (%)	26.20	2.04	24.53	32.40	14
	θ (%)	24.14	1.17	22.42	27.06	14
	ρ_b (g/cm3)	1.96	0.05	1.79	2.00	14
	Clay (%)	1.01	0.21	0.61	1.28	14
	Silt (%)	51.65	6.58	37.13	58.41	14
	Sand (%)	47.35	6.74	40.34	62.24	14
Upland (EB3)	n_T (%)	24.49	2.20	22.20	29.14	16
	θ (%)	24.49	3.11	21.07	31.06	16
	ρ_b (g/cm3)	2.00	0.06	1.88	2.06	16
	Clay (%)	1.31	0.25	0.84	1.72	16
	Silt (%)	57.76	3.26	50.80	64.98	16
	Sand (%)	40.93	3.45	33.47	48.17	16

4. 5. 2. Stable isotopes (δ2H, δ18O) and lc-excess

Figure 4.5 shows the monthly weighted isotope compositions of precipitation water (δ^2H, $\delta^{18}O$) and lc-excess in Saskatoon for the period January 2013 to Oct 2014. The isotope values of varied from -27.8 to -8.6‰ (mean -16.9‰), and -216.7 to -79.0‰ (mean of -133.7‰) for $\delta^{18}O$ and δ^2H respectively (Figure 4.5a). The lc-excess values vary between -7.3‰ to 3.0‰, with a mean of –2.0‰ (Figure 4.5b, Table 4.2). The temporal variations in the precipitation isotope values are attributed to seasonal changes in temperature and moisture sources to the region. The variability would make it difficult to adequately study water flow and solute transport processes in the till

using the raw isotope values since it will be impossible to know which water molecule in the soil is enriched as a result of evaporation or seasonal change. The lc-excess values indicate the degree of evaporation or reflux that the water sample has undergone after precipitation fall (Landwehr and Coplen, 2004). Lc-excess values reflect the processes of evaporation and condensation on water samples coming from the same source. The greater the deviation of an lc-excess value (i.e., more negative) from the local precipitation lc-excess value, the more evaporated the water sample.

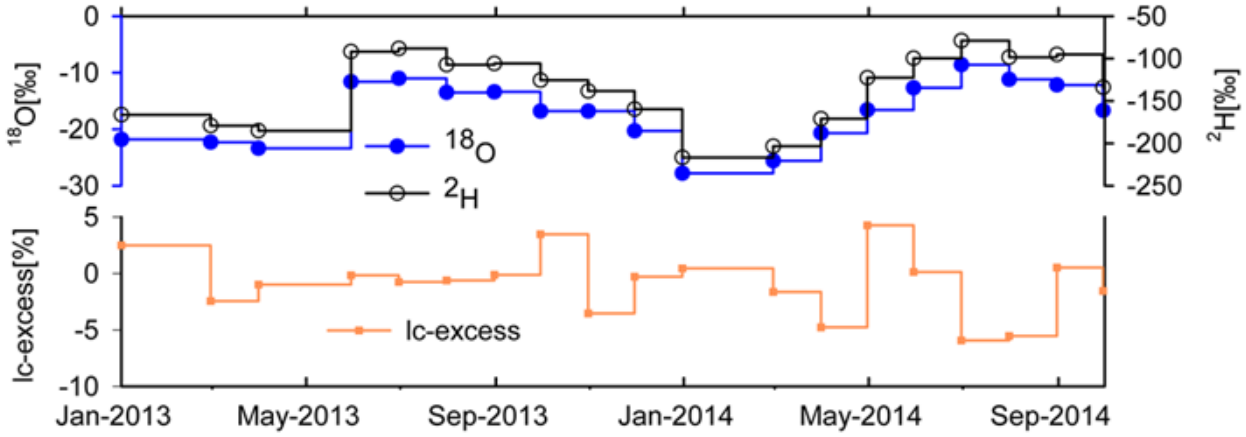

Figure 4.5. Monthly weighted isotopic signal (δ^2H, $\delta^{18}O$, and lc-excess) of precipitation between January 2013 and Oct 2014 at St Denis National Wildlife Area.

Figure 4.6 shows the dual isotope and box plot of Pond109, piezometer groundwater (i.e, shallow groundwater and aquitard), intertill aquifer, and pore water from the three soil profiles EB1, EB2, and EB3. The aquitard and the intertill aquifer clustered around the local meteoric water line indicating direct recharge with meteoric water. The pore waters from the three profiles (EB1, EB2, and EB3) and the pond water plot below and deviated to the right of the local meteoric water line indicating the evaporation signals.

Table 4.2 is a statistical summary of the precipitation and the samples isotope compositions of water ($\delta^{18}O$ and δ^2H) and lc-excess from the Pond 109, the piezometer groundwater, the aquifer, and the pore water from profiles EB1, EB2, and EB3 at the SDNWA. The intertill aquifer has the most depleted mean isotope composition and the smallest mean lc-excess value of all the water samples analyzed (Figure 4.6, Table 4.2). The mean isotope values ($\delta^{18}O$ and δ^2H) of the aquifer is 19.8 ± 0.2‰ and 154.4‰ with an lc-excess of -1.0 ± 0.1‰. The mean isotope values ($\delta^{18}O$ and

δ^2H) of the three soil profiles were slightly more depleted in the lowland porewater (EB1) compared to the upland porewater (EB2 and EB3) but more enriched than the intertill aquifer. The isotope compositions of pore water in the riparian zone profile (EB1) has the least variability and variability increased in the upland profiles (EB2 and EB3). The riparian zone profile (EB1) has the most depleted $\delta^{18}O$ isotope values with a mean of -16.3 ± 1.1‰, followed by the upland EB2 (-13.7 ± 1.8‰) and EB3 (-14.47 ± 2.0‰). The deuterium offsets lc-excess) values decreased slightly between pore waters of the three profiles. The lc-excess mean values were -4.2 ± 2.5‰ (EB1), -5.0 ± 2.0‰ (EB2) and -4.0 ± 2.5‰ (EB3) for, respectively (Table 4.2). Decreased (i.e., more negative values) in deuterium offset values in soils and groundwater is common in dry climates and is as a result of evaporation of water at the soil surface (Huang and Pang, 2012; Sprenger et al., 2016). The stable isotopes of shallow groundwater varied widely from -21.4‰ to -11.1‰ for $\delta^{18}O$ and -165.3‰ to -104.7‰ for δ^2H, respectively (Table 4.2., Figure 4. 6). The mean lc-excess value for shallow ground waters was -4.48 ± 4.1‰ (n = 31). The lc-excess (Table 4.2) showed slight enrichment to variations between the shallow groundwater samples.

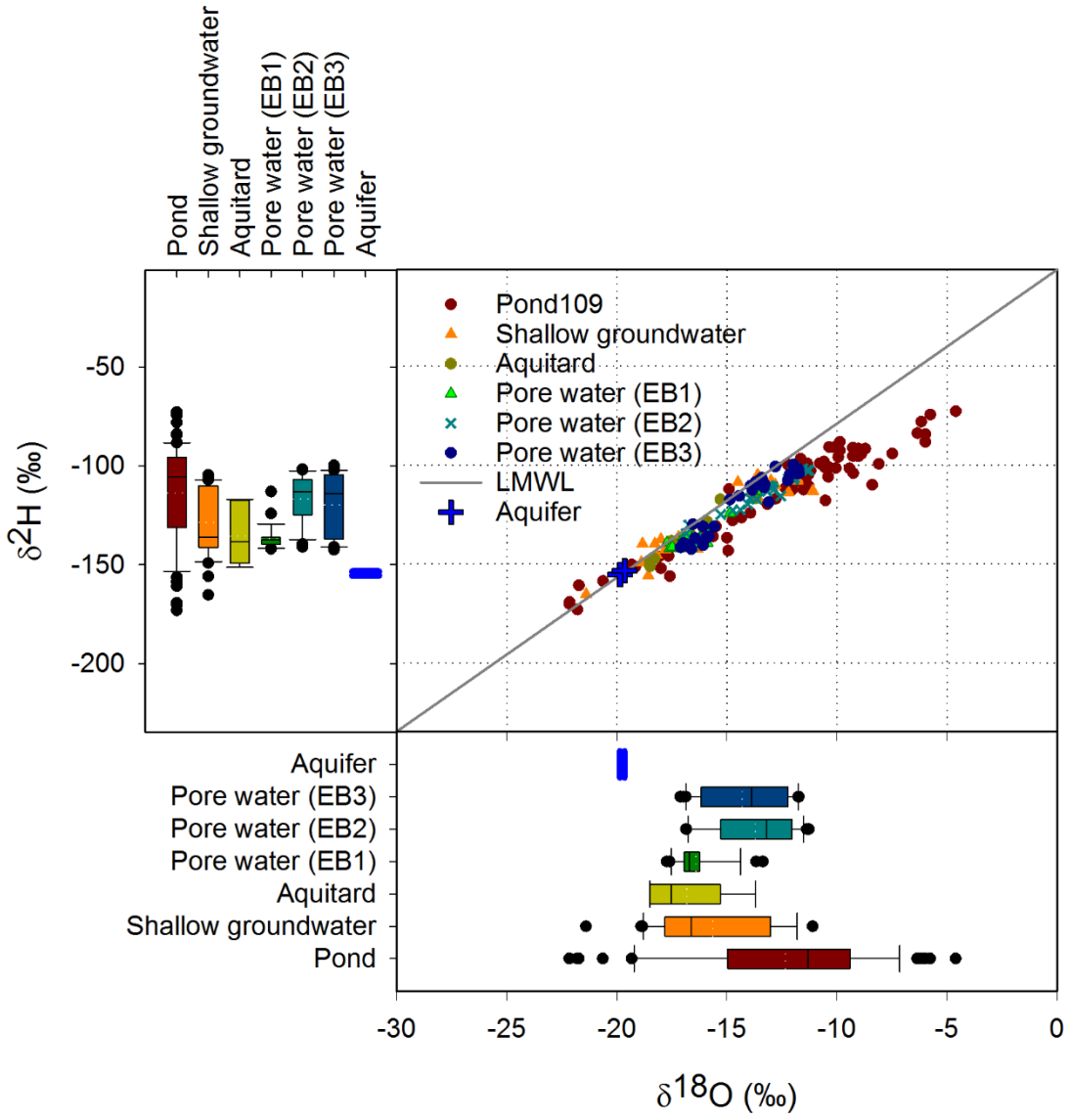

Figure 4.6. Multiplot of dual isotopes δ^2H and $\delta^{18}O$ for water samples from Pond 109, intertill aquifer, pore waters (EB1, EB2, and EB3), and piezometer groundwater (shallow groundwater and aquitard).

The $\delta^{18}O$ and δ^2H in the aquitards were homogeneous with no significant outliers in the data (Table 4.2, Figure 4.6) with the mean isotope value of -16.8 ± 1.9‰ for $\delta^{18}O$ and 135.6 ± 4.8‰ for δ^2H. The isotope composition of water from the Pond 109 varied the most. The Pond 109 water isotopes ranged from -22.2 to -4.6‰ with a mean of -12.3 ± 4.3‰ for $\delta^{18}O$, and -173.1 to -72.9‰, with a

Table 4.2. Statistical summary of isotope compositions, and lc-excess of all water types at St Denis National Wildlife Area.

Sample name	Property, [‰]	Mean	Median	SD	Min	Max	Sample total
Pore water (EB1)	$\delta^{18}O$	-16.3	-16.7	1.1	-17.7	-13.4	26
	$\delta^{2}H$	-135.8	-137.3	6.9	-142	-113.1	26
	lc-excess	-4.2	-4.1	2.5	-13.3	-0.1	26
Upland (EB2)	$\delta^{18}O$	-13.7	-13.2	1.8	-16.9	-11.3	27
	$\delta^{2}H$	-116.9	-113.3	12.2	-141.1	-101.8	27
	lc-excess	-5	-5.2	2	-9.3	0.6	27
Upland (EB3)	$\delta^{18}O$	-14.4	-13.9	2	-17.1	-11.7	31
	$\delta^{2}H$	-120.3	-115.7	15.5	-142.5	-99.9	31
	lc-excess	-4	-4.3	2.5	-8.7	0	31
Precipitation	$\delta^{18}O$	-16.9	-16.7	5.4	-27.8	-8.6	20
	$\delta^{2}H$	-133.7	-124.1	41.5	-216.7	-79	20
	lc-excess	-2	-1.8	2.9	-7.3	3	20
Pond 109	$\delta^{18}O$	-12.3	-11.3	4.3	-22.2	-4.6	66
	$\delta^{2}H$	-113.7	-105.5	25.1	-173.1	-72.9	66
	lc-excess	-10.4	-10.1	6.3	-25.1	3.8	66
Piezometer (Shallow groundwater)	$\delta^{18}O$	-15.6	-16.6	2.7	-21.4	-11.1	31
	$\delta^{2}H$	-128.6	-136.1	17.5	-165.3	-104.7	31
	lc-excess	-4.5	-3.8	4.1	-15.3	3	31
Piezometer (Aquitard)	$\delta^{18}O$	-16.8	-17.5	1.9	-18.5	-13.7	7
	$\delta^{2}H$	-135.6	-138.4	14.8	-151.3	-116.9	7
	lc-excess	-3.3	-3.4	2.1	-6.3	0.2	7
Intertill aquifer	$\delta^{18}O$	-19.8	N/A	0.2	-19.7	-19.9	2
	$\delta^{2}H$	-154.4	N/A	0	-153.4	-155.4	2
	lc-excess	-1.0	N/A	0.1	-1.1	-0.9	2

more negative than that of the piezometer groundwater and the intertill aquifer. The variation of the stable isotope compositions of $\delta^{18}O$ and lc –excess values with depth is shown Figures 4.8 and 4.9.

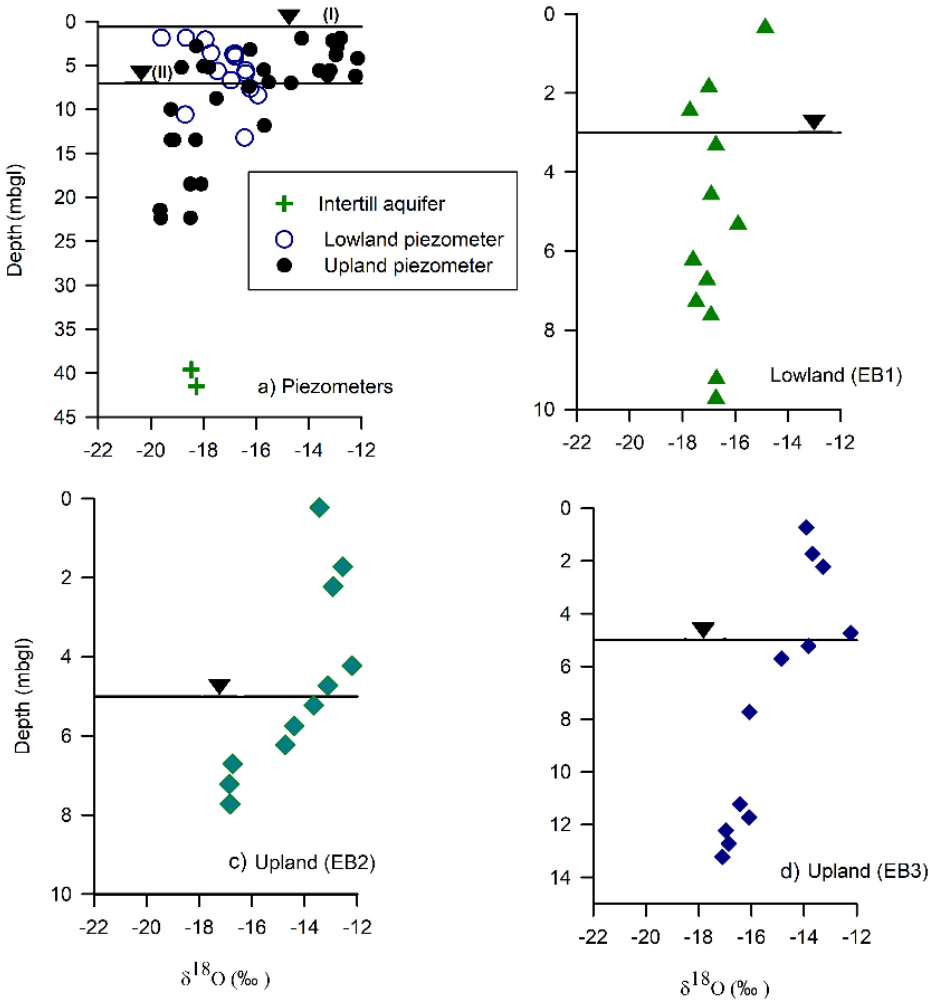

Figure 4.7. Stable isotope ($\delta^{18}O$) and depth profiles of piezometer groundwater, intertill aquifer, and pore waters from the till with approximate water table depths at St Denis National Wildlife Area, Saskatchewan.

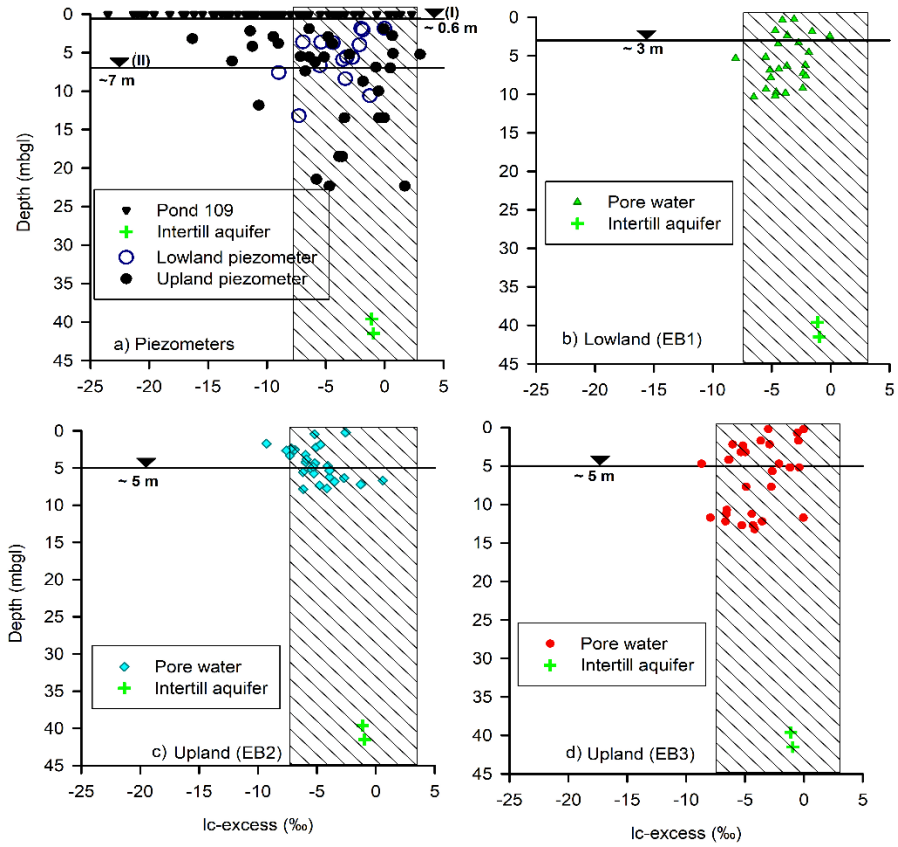

Figure 4.8. Line condition-excess profiles of piezometer groundwater, and pore waters from the glacial till at the St Denis National Wildlife Area, Saskatchewan. The precipitation lc-excess range of Saskatoon (shaded area) and approximate water tables near the pond (I) and the deepest water table at the site (II) are shown.

Table 4.3 shows the slopes and intersection values of $\delta^{18}O$ and $\delta^{2}H$ for local evaporation lines obtained from pond water, soil pore waters and piezometer groundwater with the Saskatoon meteoric water line. The intersection points indicate the initial source water for soil, piezometer groundwater, and pond water in the catchment (Gibson *et al.*, 2005). The slopes of the various ranged from 5.3 ± 0.6 to 7.6 ± 0.4 and were lower than the slope of the local meteoric water line of 7.78 ± 0.11 obtained from the 24 year record Saskatoon (see Chapter 2 Figure 2.2d) . The isotope values at the points of intersection were between -18.1 ‰ to -20.4 ‰ for $\delta^{18}O$ and -141.8 ‰ to -159.9‰ for $\delta^{2}H$, respectively. The values were similar to the isotope values in the aquifer and precipitation in Saskatoon and the Canadian Prairies (Fritz *et al.*, 1974, 1987; Peng *et al.*, 2004a) and in Chapter 3.

Table 4.3. Slope and intersections values of pore waters, piezometer groundwater, and pond at St Denis National Wildlife Area.

Location	Slope	d-excess (‰)	Intersection with LMWL	
			δ18O (‰)	δ2H (‰)
EB1	5.33 (± 0.66)	-48.84 (± 10.86)	-19.41	-152.23
EB2	6.44 (± 0.29)	-28.58 (± 4.05)	-20.40	-159.95
EB3	7.63 (± 0.43)	-10.60 (± 6.16)	-18.07	-141.83
Pond109	5.60 (± 0.19)	-44.63 (± 2.53)	-19.94	-156.35
Shallow groundwater	6.05 (± 0.40)	-34.02 (± 6.28)	-18.95	-148.66
Aquitards	6.81 (± 0.77)	-20.58 (± 13.65)	-19.91	-156.14
Precipitation (LMWL)	7.78 (± 0.11)	-1.23 (± 1.91)	-	-
Intertill aquifer, DP1	-	-	-19.7	-155.1
Intertill aquifer, DP2	-	-	-19.4	-155.1

4. 5. 3. Water chemistry of SO_4^{2-} and Cl^-

Figure 4.9 and Figure 4.10 show dissolved ion concentrations of SO_4^{2-} and Cl^- in pore waters from three soil profiles EB1, EB2 and EB3, as well as the piezometer groundwater, and the intertill aquifer, respectively. Pore water had relatively high SO_4^{2-} concentrations ranging from 50 to 350 mmol/L. The SO_4^{2-} concentrations of shallow piezometer (lowland and upland) groundwater samples were highly variable and ranged between 0.29 to 236.04 mmol/l (Figure 4. 9). The SO_4^{2-} ion concentration in all of the upland shallow groundwater samples were greater than the levels measured beneath the pond (0.01 to 1.00 mmol/l). Higher SO_4^{2-} ion concentrations were also observed in the uplands (EB2 and EB3) compared to those measured in the lowland (wetland margin, EB1). The measured SO_4^{2-} concentrations in the upper (2.5 m depth) of the lowland profile near the pond margin (EB1) were greater than concentrations measured in the upland cores (EB2 and EB3). The SO_4^{2-} ion concentrations measured in the profiles EB2 and EB3 (uplands) ranged between 9.02 to 239.53 mmol/l and increased with depth between the soil surface 0.15 m and about 4 m. The SO_4^{2-} ion concentrations decreased with depth within the profile EB 3 from below 4 m to 12 m (Figure 4.9) and no significant variations was observed in the SO_4^{2-} ion concentrations of

piezometer groundwater samples with depth between 5 and 41 m. The SO_4^{2-} ion concentrations in the lowland profile (EB1) was near constant and ranged between 24.53 to 130.42 mmol/l. Sulfate ion concentrations in the pond were lower than the concentrations measured in the piezometer groundwater samples and are between 0.01 and 0.1 mmol/l.

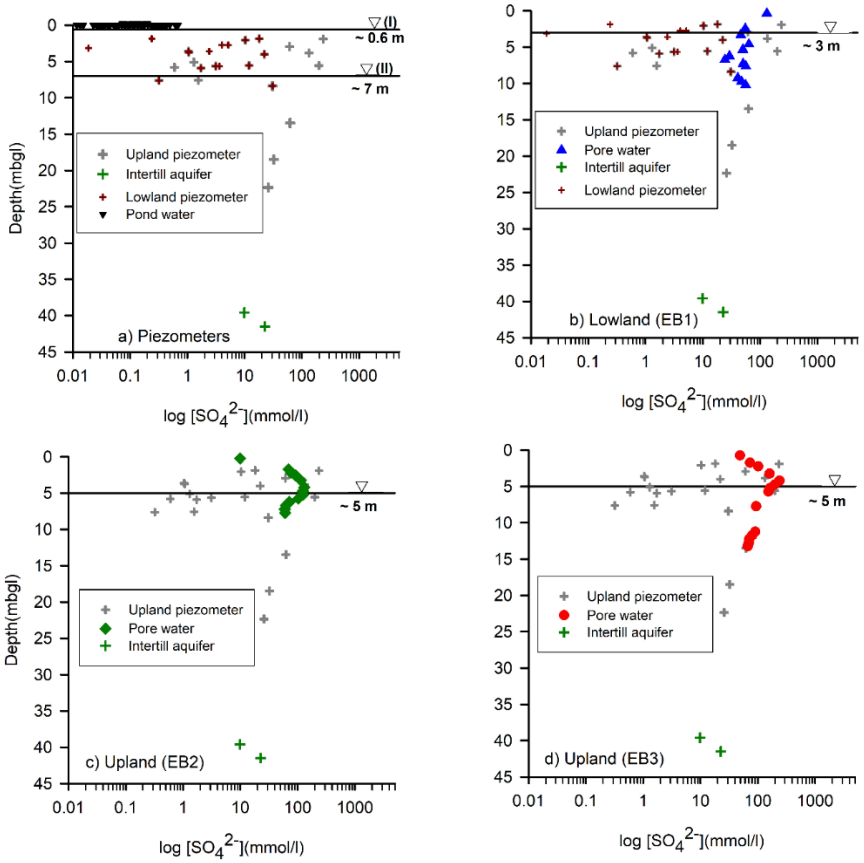

Figure 4.9. Concentration depth profiles of dissolved SO_4^{2-} ions measured in the lowlands - and uplands of the till from piezometer groundwater and pore waters, Pond 109, and the intertill aquifer. The approximate water tables near the pond (I) and the deepest water table at the site (II) are shown.

The SO_4^{2-} ion concentrations in the intertill aquifer is between 9.88 and 22.71 mmol/l and falls within the range of values observed for the three soil profile samples and the piezometer groundwater samples from the upland.

The pond water Cl^- ion concentrations were between 0.001 to 1.00 mmol/l (Figure 4.10). The Cl^- ion distribution in the shallow piezometer groundwater is scattered and ranged between 0.1 to 10.0 mmol/l. The chloride ion concentrations in the pore water samples ranged between 0.38 to 9.4 mmol/l. The pore water Cl^- ion concentrations increased with depth between 1 and 6 m in the profiles (EB1 and EB3). The concentrations peak at 6 m depth and begin to decrease. The Cl^- ion concentrations in the intertill aquifer are between 0.12 and 0.93 mmol/l and fall within the range of values observed for the pond and the piezometer groundwater samples. There were no significant variations in the chloride concentrations observed for profile EB1, compared with measured values from the other pore water profiles, EB2 and EB3. The Cl^- ion concentrations in the lowland profile, EB1, was almost constant with depth and ranged between 0.38 to 0.89 mmol/l. The Cl^- ion concentrations from the three soil profiles (EB1, EB2, and EB3) were greater than the concentrations measured in the pond water.

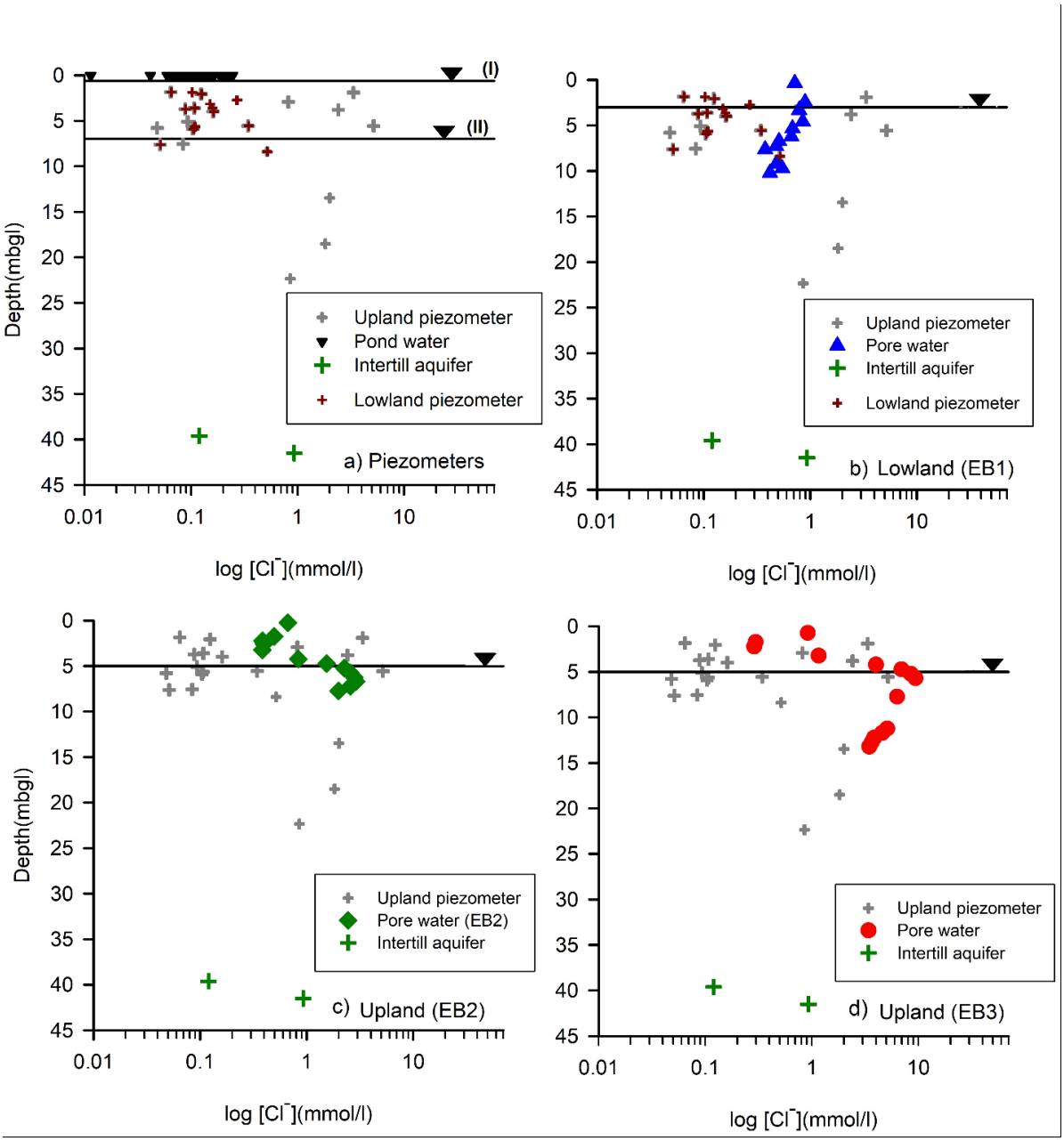

Figure 4.10. Concentration depth profiles of dissolved chloride ions measured in the lowlands-and uplands of the till from piezometer groundwater and pore waters, Pond 109, and the intertill aquifer. The approximate water tables locations at the each profile site near the pond (I) and the upland (II) are shown as black triangle.

Figure 4.11 is a contour plot of measured SO_4^{2-} and Cl^- ion concentrations in piezometers groundwater, pore- and pond- water in the top 13 m BGL along the cross-section from the Pond 109 to the upland profile EB3 (Figure 4.2) to explain the process of evapoconcentration in

dissolved ions accumulation in the shallow 4 to 6 m depth below ground. The water table and the water fluxes are also indicated.

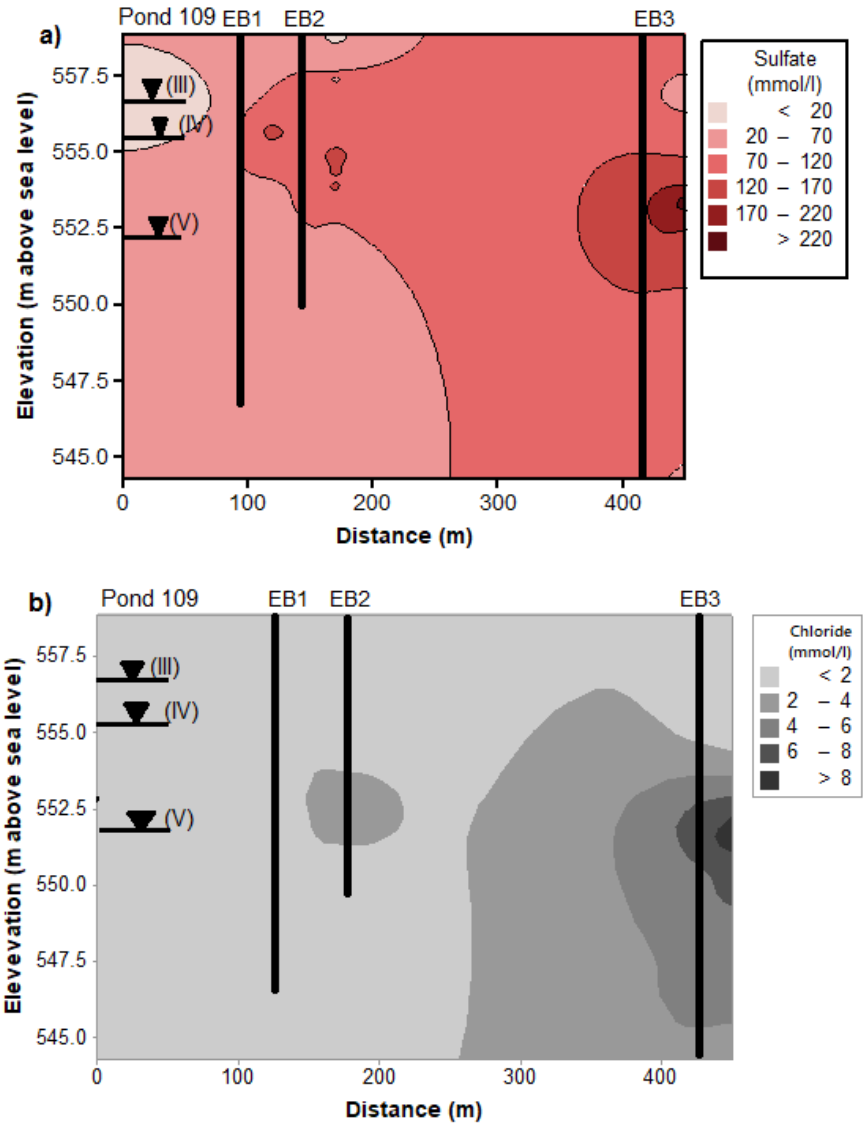

Figure 4.11. Measured SO_4^{2-} and Cl^- ion concentrations (mmol/l) in piezometer groundwater, pore water, and pond water along the cross-section from Pond 109 to the upland profile EB3 indicated in Figure 4.2. Straight horizontal back lines with triangles are the approximate water tables in the Pond (III), lowland EB1 (IV) and Uplands EB2 and EB3 (V), respectively. Soil profiles are indicated with black vertical lines.

When a water pool has undergone evaporation, the dissolved solute concentrations increase and the lc-excess values decrease. However, solute concentrations increase can be as a result of geochemical processes such as mineral dissolution, and/or plant transpiration (where solutes are not taken up by the plant roots), both of which do not affect the lc-excess. Therefore, the relationship between lc-excess and dissolved ion concentrations resulting from evapoconcentration is inversely proportional, whilst the contributions from mineral dissolution and/or transpiration are constant. Figure 4.12 shows the relationship between the lc-excess and the chloride ion concentrations for the water types in the catchment. The relationship between lc-excess of waters and corresponding dissolved chloride ions is shown in Figure 4.12 will help determine, the mechanisms of dissolved ions accumulation in the prairies soils and water samples.

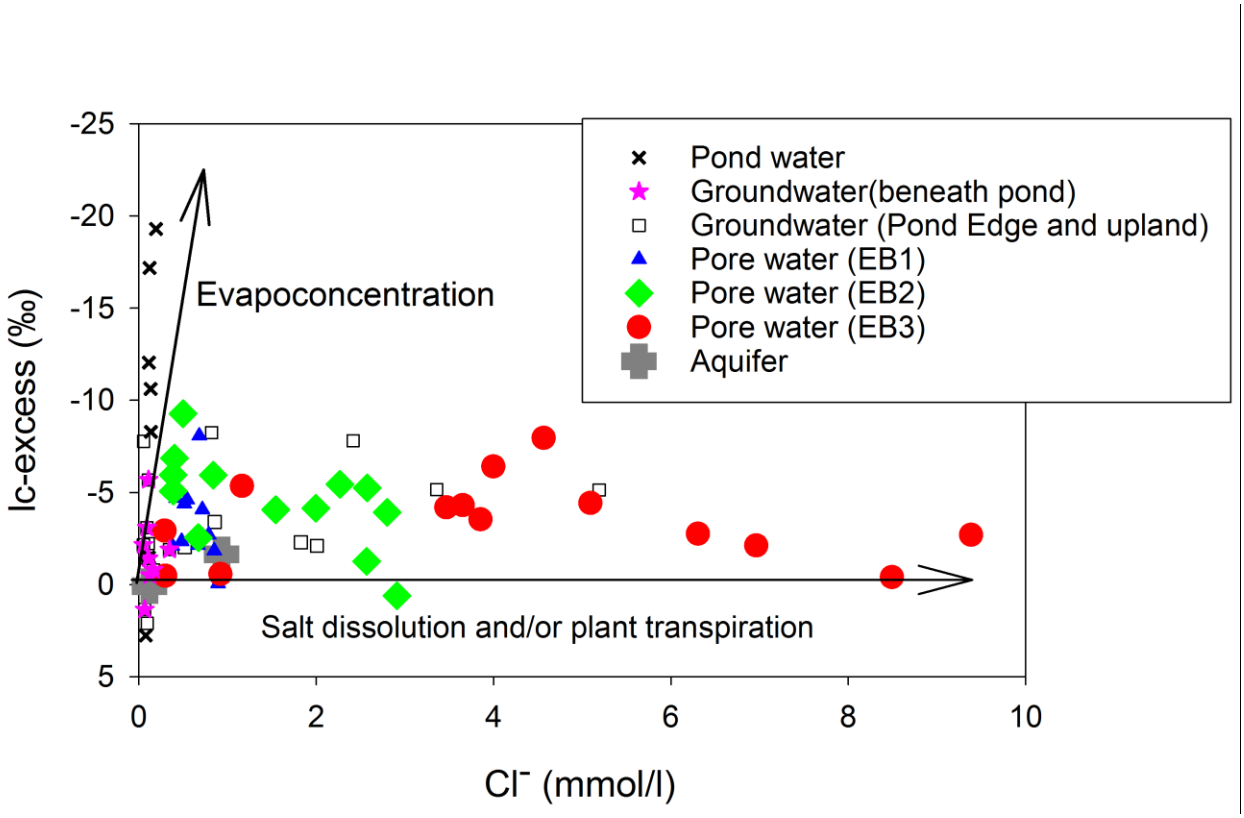

Figure 4.12. Sources of dissolved ions accumulation shown by the relationship between lc-excess and chloride in water.

4. 6. Discussion

4. 6. 1. Soil properties – moisture content, porosity and bulk density

The relatively low dry bulk density of core samples in the shallow (< 2 m) sediment is a consistent property of the weathered till. Heagle *et al.* (2013) attributed the property low dry bulk density in the till to high organic matter content and the presence of macropores (e.g., fractures) at this depth. The low bulk densities may be the attributed to the observed high porosity and water content values at the shallow depths of the soil profiles. The observations thus explain the high saturated hydraulic conductivity values reported near the ground surface (0-2 m depth) in Figure 4.4. Studies (Hayashi *et al.*, 1998; Labaugh *et al.*, 1998; van der Kamp and Hayashi, 2009; Nachshon *et al.*, 2013; Brannen *et al.*, 2015) suggest that the weathered nature of the till results in high K-values in shallow depths creating high conductive zones which could enhance strong lateral flow of shallow groundwater which could be carried to wetland edges where the water table is low. Such high conductive zones exist throughout the glacial weathered till whether upland or lowland (Keller *et al.*, 1985; Hendry *et al.*, 1986, 2015a; McKay *et al.*, 1993; van der Kamp and Hayashi, 1998, 2009; Hendry and Wassenaar, 2004).and may allow for rapid infiltration of precipitation (snowmelt water and summer rains) into the shallow groundwater

4. 6. 2. Insights from high-resolution water isotope profiles

The temporal variations in the precipitation isotope compositions reflect the changing meteorological conditions that are associated with precipitation amount, season, temperature and wind carrying moisture to the region. The negative lc-excess values show the precipitation has undergone some level evaporation, especially in the summer months. The relatively enriched isotopes and negative lc-excess values of the pond and pore water samples (Table 4.2, Figure 4.7. and Figure 4.8b) suggest these waters were evaporated either before infiltration at the soil surface and in the pond, or within the shallow (0.7 m depth, Maule *et al.*, 1994) soil following infiltration. The negative lc-excess values observed at shallow depths in the three pore water profiles and the slopes of the soil evaporation lines suggest evaporation at the soil surface and this is commonly observed in dry climates regions (Huang and Pang, 2012; Sprenger *et al.*, 2016b). The negative lc-excess values observed between 0.7 m and 3 m depth in the profiles is attributed to the transport of evaporated enriched isotope waters through the soil matrix.

The stable isotopes and lc-excess values measured in some shallow groundwater piezometers indicated the water undergone evaporation and this may occur before recharge water infiltrates the soil. At greater depths (~8 to 41m, Figure 4.7a), the stable isotope compositions of the piezometer groundwater, and the intertill aquifer water samples are depleted with near zero lc-excess values. The observation suggests that these waters may not have undergone any significant evaporation at the soil surface or within the soil or in the pond before groundwater recharge is true.

The location of the water isotopes on the δ^2H- $\delta^{18}O$ -plot (Figure 4.6) and the intersection values of the water evaporation lines from the pore waters, the pond, and the piezometer groundwater (Table 4.3) with the local meteoric water line showed the waters are of meteoric origin and the influence of geochemical exchanges between rocks minerals and /or very old soil water within the system is negligible. Mixing and geochemical/mineral exchange processes, alter the position of the water isotopes with regards to the meteoric water line (Hendry and Wassenaar, 1999, 2000; Karolytė *et al.*, 2017). The intersection values of the pore and pond water isotopes with the local meteoric water line are similar to the isotope compositions of the intertill aquifer and cold season precipitation in the Canadian Prairies (Fritz *et al.*, 1974, 1987; Peng *et al.*, 2004). The observation suggests that these waters were replenished from the same source –meteoric precipitation. A previous study involving tritium isotope (Bacon and Keller, 1998) also suggest that water in the till at the depths used in this study were not very old and have been recharged within the last 100 years from precipitation. The question is, by what mechanism/process could the precipitation water that is subjected to little or evaporation get into the saturated zone considering that the till has poor hydraulic conductivity?

The high resolution vertical depth - isotope stables and dissolved ion concentrations measured in the soil unsaturated and saturated zones are useful in providing some insights on the pathways the transport of water and solute (David et al., 2015; Garvelmann et al., 2011; Hendry et al., 2015a; Mueller et al., 2014; Remenda et al., 1996; Sprenger et al., 2015, 2016a). The stable isotope profiles obtained from the piezometers and the soil cores in the glacial till define a curvilinear shape that approaches straight lines from the soil surface to the intertill aquifer (Figure 4.7a, c, and d). The profiles patterns are characteristic of conservative tracer profiles observed in non- or poorly fractured fine-textured deposits of the till and been attributed to slow matrix flow of water and transport of solutes (Desaulniers et al., 1981; Hendry et al., 2015a; Hendry and Wassenaar, 1999).

In the weathered-fractured zone (0 to ~7 m BGL) the piezometer groundwater samples are evaporated. The evaporation signals were less pronounced in the upland profiles (Figure 4.7c and d) at 4 and 5 m BGL. Within the less fractured, or non-weathered (~6 to 41 m BGL) zone, the isotopes values are depleted. The observed enriched isotope signals down to ~3 m depth in the uplands (EB2 and EB3, Figure 4.7c and d) are attributed to the slow matrix flow of evaporated soil water. The isotope values in the piezometers between 6 to 41 m depth (Figure 4.7) was depleted with no variations. Similarly, the uplands (EB2 and EB3) show no little variations in isotopes values between 7 and 14 m BGL. The lc-excess values were near zero at greater depths (Figure 4.8). It is suggested that the depleted waters found at greater depths, which have much-depleted isotope values than in the soil matrix were most probably introduced into the till by macropore flow through the fractures that exist in the weathered and sometimes the poorly weathered till. Rapid advective macropore flow of water (vertical and horizontal) in the weathered and fractured till has been suggested to carry depleted precipitation water to greater depths (Keller *et al.*, 1985; Joshi and Maule, 1999; Joshi and Maulé, 2000; Kelln *et al.*, 2007; Stumpp and Hendry, 2012). Thus, it is possible for snow-melt water flowing through fractures in the weathered till to escape evaporation at the soil surface (i.e., from lowlands and uplands) and enter into the till at greater depths. The isotopically depleted water could then be transported laterally and vertically into the non-fractured till. The vertical transport of this water through the till matrix flow (possibly by matrix diffusion, Hendry *et al.*, 2015a) would eventually serve as the recharge water to the intertill aquifer. The till hydraulic conductivity values reported in relation to depth (Figure 4.4) for the weathered upper (0 to 6 m) and the deeper non- or poorly fractured unoxidized clay till permits the different flow velocities described above. Porewater isotopes obtained from soil core sampling may only capture flow and other hydrological processes representative of the matrix within which water flow or is stored. Though fractures do not hold water by themselves their presence in a soil can reflect on the isotopic nature of water soil especially at deeper levels where the water captured by them escapes evaporation

4. 6. 3. Solute transport in the till

Sulfate concentration

The differences in spatial variation of SO_4^{2-} concentrations within the wetland complex could be attributed to several processes: i) the depletion of soluble SO_4^{2-} in the shallow parts of the

weathered upland areas as a result of lateral transport by surface runoff water; ii) pond-to-sediment transfer of SO_4^{2-} and subsequent accumulation of gypsum during drying episodes at wetland sediment (Heagle *et al.*, 2013; Pennock *et al.*, 2014); and iii) downward leaching followed by evapotranspiration aided by changing season and plant water uptake (Nachshon *et al.*, 2013). In the Prairies, isolated root hairs were observed in soil cores to a depth of about 4 to 5 m (Joshi and Maule, 1999), thus root abstraction can take water and concentrate solutes between the soil surface and the 5 m depth. The variability in SO_4^{2-}concentrations with depth in pore water is consistent with sulfate behaviour in the prairie soils and attributed to variability in solid-phase SO_4^{2-} amount (Heagle *et al.*, 2013). The total SO_4^{2-} content measured in the soil (not reported here) is much higher in upland areas than measured in the pore waters and piezometer groundwater. Total sulphur content observed in sediments and soil cores at both SDNWA and nearby study areas Warman and Dalmeny, located 60 km west of SDNWA (Keller *et al.*, 1988; Van Stempvoort *et al.*, 1994) and at SDNWA (Heagle *et al.*, 2013; Nachshon *et al.*, 2013) also showed low sulphur content values in the poorly fractured deeper glacial till (0.25–0.3%) below the 6 and 7 m depth. The bulge with the peak of SO_4^{2-} at ~4 m depth reflects the in situ SO4 concentration of the immobile salt in the oxidized till (Keller *et al.*, 1991; Nachshon *et al.*, 2013) which has not been leached by the relatively slow vertical and lateral subsurface flow rates at the uplands as shown in Figure 4.12). Hayashi et al., (1998b) indicated that this peak is strongly suggestive of the zero flux boundary between the root zone and the unsaturated zone. The decrease in the SO_4^{2-} concentrations in the profiles EB2 and EB3 (Figure 4.9) with depth between the soil surface (0.15 m) and ~4 m is as a result of flushing of the SO_4^{2-} ions in the shallow soil layers and subsequent release of SO_4^{2-} ions into solution as result of chemical weathering and this can be aided by the fluctuating water table. The decreasing SO_4^{2-} ion concentrations between 5 -14 m is be attributed to slow velocity matrix transport of the SO_4^{2-} peak at ~4 m from the water table through the poorly fractured till.

The extremely low SO_4^{2-} concentrations (0.01 to 0.9 mmol/l) observed in the pond water have been attributed to: i) leaching into groundwater and subsequent removal and deposition in the wetland margin; ii) bacterial reduction to pyrite in wetland sediments, and /or iii) gypsum precipitation (Heagle *et al.*, 2007, 2013; Goldhaber *et al.*, 2014). Bacterial reduction and pond-sediment deposition have been identified as the dominant factors for sulfate reduction in the ponds in the Prairies (Heagle *et al.*, 2007, 2013; Nachshon *et al.*, 2013). The SO_4^{2-} concentrations in the shallow piezometer groundwater near the pond and in upland soil profiles were substantial (Figure 4.5a)

and suggests pond-sediment transfer of SO_4^{2-} ions and subsequent concentration by evapotranspiration. Nachshon *et al (*2014) observed that during the wet season, the surface runoff generated by snowmelt washes soluble accumulated salts, including SO_4^{2-}, at uplands into the depressions-ponds. Also lateral subsurface flows of groundwater from ponds into the shallow groundwater water table in the upland areas and the wetland riparian zones, is capable of concentrating these salts at depths where most water losses occur during the dry season by evapotranspiration (Millar, 1971; Berthold and Hayashi, 2004; Nachshon *et al.*, 2013). Active lateral groundwater flows from the pond into the groundwater is confined within the shallow saturated zone, called the active transmission zone, and takes place at ~5 m depth between the pond water table and the bottom of the highly fractured till (van der Kamp and Hayashi, 2009). The SO_4^{2-} ion concentrations in the aquifer were similar to values observed for the pore water samples and upland groundwater. This suggests the aquifer may not be very old (paleo-aquifer), and the SO_4^{2-} ions may have come from slow matrix transport through the poorly fractured till or dissolution from the geological materials.

Chloride ion concentration

The spatial variations in the Cl^- ion concentrations similar to those observed in sulfate ions obtained from the pore water, groundwater, pond and intertill aquifer (Figure 4.11). The variations are attributed to the influence of hydrologic activities that take place at the locations.

Chloride ion concentrations measured at the lowlands and in the pond water are generally low and scattered with some relatively large concentrations at greater depths suggesting the presence of preferential pathways. Chloride concentration is generally large in the upland piezometer groundwater samples and soil profiles (EB2 and EB3). The concentrations increase with depth and peaks at ~5 and 7 m suggesting that the chloride ions may be flushed downward from the soil surface and the water table into deeper depths in the till. The chloride accumulation peaks such as observed between ~5 and 7 m at the interface between weathered -fractured and the non-weathered –poorly fractured till interface could also be attributed to the presence of chloride ions in the parent rock material that has undergone little or no weathering as in the case of sulfate ions. However, studies (Hayashi *et al.*, 1998; Hendry and Wassenaar, 2000; Harrington *et al.*, 2007) have shown that no significant geologic source of chloride has been identified in the till. In 2007, Harrington *et al.*, (2007) proposed that such chloride peaks in the till (though at more greater depth) could

reflect the impact of the sand deposit, which could allow for contamination somewhere off-site to be transported laterally along sand layers interbedded in the till. Such a proposal may require an extensive lateral layer of sand and long timescales to be transported to our site. The stratigraphic vertical cross-section of SDNWA (Miller *et al.*, 1985; Hayashi, 1996) shows no existent of sand bed at ~5 to 7 m that could allow off-site transport of contamination at depths. The possibility of salinity stratification in connate water tapped at such depths (Harrington *et al.*, 2007) is also not possible. Several studies (Hayashi *et al.*, 1998; Joshi and Maule, 1999) show that the till has no known chloride-rich minerals and the glaciolacustrine sediments have no chloride of marine origin and depositional water chemistries measured in the till are homogeneous (Hendry and Wassenaar, 2000; Hendry *et al.*, 2000; Harrington *et al.*, 2007). Solute accumulation by evapotranspiration enrichment of chloride ions deposited by infiltrating rainfall and snowmelt water during the wet-dry cycles is another way by which such peaks could develop (Scanlon, 1991; Nachshon *et al.*, 2013). In these processes, the infiltrating rainfall and snowmelt water leach salt downwards especially during rainfall events, while between the rainfall events, capillary flows draw saline water upwards to satisfy evapotranspiration demands. This would mean, however, that higher concentration of the chloride is concentrated near the surface (Figure 4.6). Evapotranspirative enrichment which is commonly associated with salt belt region of wetlands; where vertical and lateral subsurface flow rates are high and the salts are relatively mobile (Nachshon *et al.*, 2013). In the case the soil profiles EB2 and EB3 (uplands), we do not expect that vertical and lateral subsurface flow rates would be high to enable the easy transport of wetland chloride to those regions to be further concentrated. The presence of fluctuating water table which is located in the region could enhance such peaks. Hayashi et al., (1998b) indicated that this peak could be strongly suggestive of the zero flux boundary between the root zone and the unsaturated zone

The mechanism of evapotranspiration enrichment of chloride ions in the depths reported has been further investigated using the lc-excess data of all water types and chloride ion concentrations. The chloride and sulfate ion accumulation peaks (Figure 4.12) were further examined by studying the effect of evaporation on the waters. The lc-excess–sulfate plot suggests same as the chloride, so only the chloride result chloride is shown here. The Figure 4.12 shows that the Cl^- ions found in the pore waters EB2 and EB3, groundwater was mostly concentrated by evaporation and salt dissolution and/or plant water uptake via transpiration. In the North American glacial till, Cl^- ions

are deposited by rain and snowfall and there no other known major sources or sinks in the landscape (Hayashi *et al.*, 1998; Hendry *et al.*, 2000; Hendry and Harrington, 2014), thus the possibility of salt dissolution associated with parent rock material is ruled out. The use of Cl^- containing fertilizers did not occur at our study area, and the nearest paved road is 3 km south of the area so the effects of road salt (NaCl) applied in winter would be negligible. This leads to one conclusion that the chloride peak is because of evapotranspiration enrichment, which could be enhanced by the fluctuating water table in the region. Chloride ions concentrations measured in the pond water, the pore water of the profile EB1 and piezometer groundwater show that they are as a result of evapotranspiration as seen in (Figure 4.12). The considerable differences both in the shape and magnitude of the chloride concentrations in the three profiles could be explained as likely related to climatic changes and flow processes involved in their transport within the till.

4. 7. Conclusions

This paper provided analyses of water flow and solute transport from the soil surface through the deep unsaturated into the saturated zone in the glacial till. The high-resolution data of soil properties and multiple tracers show that groundwater recharge and solute transport at various parts of the prairies landscape is subject to two mechanisms – macropore and matrix flow processes. Pore water isotope profiles showed evaporated water at the shallow depth and depleted water at greater depths. Sulfate and chloride concentrations showed that dissolved ions were leached at the shallow depths leading to peak enrichment at the near surface and at depths of ~ 3 and 6 m, close to the water table. The lc-excess values showed that sulfate and chloride accumulation peaks observed at ~ 3 to 6 m depth, respectively were the result of evapotranspiration and also water table fluctuations induced by seasonal changes and hydrologic flow processes at the landscape. Evaporation and plant water uptake enhance the upward and lateral flow and accumulation of dissolved ions at shallow depths. At greater depths (~ > 7 m below ground) in the till slow matrix flow dominates the water flow and solute transport. It is concluded that groundwater recharge can occur at both uplands and lowlands (including ponds), where fractures in the shallow weathered and poorly weathered till play the essential role in allowing snowmelt water (and rainfall) infiltration to go beyond the root capture zone. On the other hand, water held up in the matrix of the shallow unsaturated zone which becomes enriched, does not have a

significant impact on deeper saturated zone water recharge. Below the weathered zone, flow and transport are through the matrix of the poorly weathered till which culminates into a slow recharge to the intertill aquifer.

4. 8. Acknowledgements

This project was funded in part by the University of Saskatchewan Dean's scholarship, Government of Saskatchewan's Innovation and Opportunity Scholarship, and the Global Institute for Water Security. The author wishes to acknowledge Dr. Andrew Ireson for financial support towards the field work and for reviewing the manuscript, Professor Jim M. Hendry for allowing us to use his laboratory to analyze soil properties, soil water chemistry, and stable isotope samples, as well as his helpful advice in discussing of the results. Emeritus Research Scientist, Dr. Van Der Kamp is acknowledged for reviewing this manuscript and Professor Jeffrey J. McDonnell for his suggestions during committee meetings. Thanks are also is extended all laboratory managers Ms. Erin Schmeling and Ms. Fina Nelson of the Geological Sciences Department, University of Saskatchewan and Geoff Khoeler of National Hydrology Research Centre, Saskatoon for field and laboratory assistance.

4. 9. Author contributions

J.M.H proposed the study, E.K.P.B. and A.M.I designed fieldwork and collected core samples. E.K.P.B carried out laboratory analysis, compiled each data set, did the geographic information system work, and wrote the paper. A.M.I, supervised and funded the research and make suggestions for consideration in result discussion, and M.J.H reviewed the results, commented on the manuscript.

CHAPTER 5: CONCLUSIONS AND FURTHER WORK

5. 1. Conclusions

The goal of this Ph.D. thesis is to quantify wetland hydrological fluxes, and explain how water and solutes are transported from the surface (uplands and wetland ponds) to the shallow groundwater, aquitards and deep confined intertill aquifers in the North American Prairie Pothole Region. An integrated approach was applied involving hydrometric and hydraulic measurements, water chemistry, stable and radioactive isotopes of water, and the development of a stable isotope-based water balance model. The pathways of water and solutes and the approximate contributions of water from the upland and lowland areas across the landscape to the intertill aquifer have also been understood. Also the approximate contributions of water balance fluxes from wetland ponds across the landscape to the atmosphere (as evaporation) and the subsurface (infiltration) has been quantified. The wetland pond water balance fluxes were determined to be comparable to measurements obtained by other methods. In addition, the specific types of wetland ponds that serve as dominant sources of groundwater recharge to the relatively deep intertill aquifer (~ 40 m bgl) were identified and the individual relationships between various wetland ponds and the relatively deep intertill aquifers were also established. Water flow and solute transport processes in the till from ponds, uplands, and lowlands through the unsaturated zone to the intertill aquifer at the St Denis National Wildlife Area has also been explained.

In Chapter 2, the study showed that the water balance of wetland ponds is controlled by interactions with the subsurface and the climatic conditions. Further, it is established that spatial variability in hydrological fluxes (that is infiltration and evaporation) can be quantified across landscapes using stable isotope-water-mass balance model. It is shown in this thesis that the infiltration fluxes (the water loss to groundwater recharge, plant transpiration and riparian zone soil evaporation) from ephemeral/seasonal wetland ponds exceed evaporation in larger permanent ponds.

The results from the new isotope-water -mass balance model demonstrated that the isotopic regime of prairie wetland ponds can be reasonably predicted. Where climate data and pond geometries are available, the model can serve as a good approximation for evaporation and infiltration flux estimates for small water bodies anywhere across the globe (as seen in Rosenberry *et al*., 2004). The independent flux estimates obtained from the isotope data are consistent with field observations and estimates based on hydrological data using other methods (Millar, 1971; Stewart and Kantrud, 1971; Hayashi *et al.*, 1998, 2016; Parsons *et al.*, 2004). The variations in evaporation and infiltration flux estimates for individual wetland ponds suggest that care should be taken in generalizing evaporation rates. One limitation of the new model is that it requires more data to compute and could be subjected to considerable error if underlying assumptions are not met.

Chapter 3 also showed that depression-focused groundwater recharge occurs mostly from seasonal and ephemeral/temporary wetland ponds. It is easy to overlook these ponds because they are typically dry out within weeks after the snowmelt period or the summer. This thesis showed that the isotopic composition of the deep intertill aquifer groundwater (~ 40 m bgl) is inconsistent with the ponds in various ways: i) the groundwater is completely distinct from permanent ponds (like pond 50); ii) the isotopic composition of the intertill aquifer more depleted than most pond waters and is not equal to the average isotopic composition of water of the recharge ponds (e.g., Pond 109), though both originate from meteoric precipitation; and iii) the intertill aquifer water is biased towards early season/snowmelt portion and water found in most ephemeral and seasonal ponds in the spring season. For a permanent recharge pond (Figure 5.1a and b), there is no logical reason that recharge should be biased to snowmelt, since there is an almost constant hydraulic head difference between the pond and the aquifer (Figure 5c). Thus, the rate of downward flow to the aquifer (recharge to the aquifer) remains almost steady year-round. Therefore the recharge is not taking place only preferentially in the springtime and there must be some other explanation of why the evaporated-enriched pond water is not a major contributor to the groundwater in the aquifer. For ephemeral ponds that dry out quickly by summer (Figure 5.1b), however, vegetation in the pond area could intercept much of the evaporitic water from below the pond preventing such water from reaching the aquifer. Furthermore, the absence of evaporitic isotopic water signals in the shallow groundwater at few meters depth beneath the ponds confirms the idea of vegetation uptake of evaporated water from the ephemeral ponds. It should be emphasized that the isotope

composition water beneath the ponds were similar to the isotope composition of the intertill aquifer water. The fact that the ephemeral ponds are numerous and occupy more of the landscape area than the permanent recharge ponds (Figure 5.1a and b) suggests that the enriched isotope signals from the permanent ponds is eclipsed and diminished in much of the recharge water that reaches the intertill aquifer. It is suggested that the wet-dry cycle and associated impact on the pond water isotope compositions and hydraulic conductivity of ephemeral and seasonal ponds has great implications for groundwater recharge in the prairies. The dry-wet cycle repeated many times since the deglaciation of the region *ca*. 12 ka (Heagle *et al.*, 2013) is suggested has allowed the subsurface snowmelt runoff water to infiltrate the ephemeral wetland basins and weathered oxidized till to recharge the confined aquifer. This hypothesis is consistent with the observed depleted isotope signatures in the ephemeral ponds and the aquifer.

In Chapter 4 , the three unsaturated zone profiles from the uplands and near a depression showed that soil water near the till surface were evaporated, but water from deeper depths (i.e., below 5 m depth in aquitards) were not and but biased toward snowmelt. This suggests that the spring melt pulse is transmitted through fractures in the near surface from both the upland and low-land areas into the aquitards. Though water held in the soil matrix near the till surface and in the aquitards are meteoric water same as water found in the groundwater aquifer, water in the aquifer is non-evaporitic. Water stored in the soil matrix near the surface can be accessed for evaporation and vegetation transpiration resulting less infiltration as indicated in Chapter 3. Thus, for the till aquitards and aquifer water to remain depleted, there must be a highly conductive macropores units that allows for preferential flow of spring meltwater into deeper depths of the till that cannot be accessed by evaporation. In the till, these macropores occur as fractures in upland areas and desiccation cracks in wetland ponds that dries up during the summer. It is concluded therefore, that the major process responsible for enhancing deep vertical water flow and solute transport between the soil surface and the aquifer is macropore flow.

In summary, this thesis has shown from water isotope, hydrometric and hydraulic data that small wetland ponds are the predominant source of depression-focused groundwater recharge in the prairies. The time series of pond levels and isotope data show that these ponds, which are also numerous in the prairies of North America, are crucial especially during dry periods when their

behaviour is important for groundwater recharge. The science of these findings is summarized in a refined conceptual diagram, Figure 5.1, below. Between the uplands and ponds, more spring infiltration is observed beneath ephemeral ponds during the spring–summer period. However recharge under permanent ponds continuous throughout the year, but the recharge is partly attenuated by the presence of large organic matter deposits under permanent ponds. The result is that the more water come from the ephemeral ponds to recharge the confined aquifer than from the permanent ponds. The phenomena enables the isotope signal of water from ephemeral ponds to dominate the water isotope signal of the confined aquifer. The implication of this finding is that more careful consideration has to be applied when draining or changing the land use activities regarding small temporary wetlands for agriculture and other purposes in the prairies and snowmelt dominated environments.

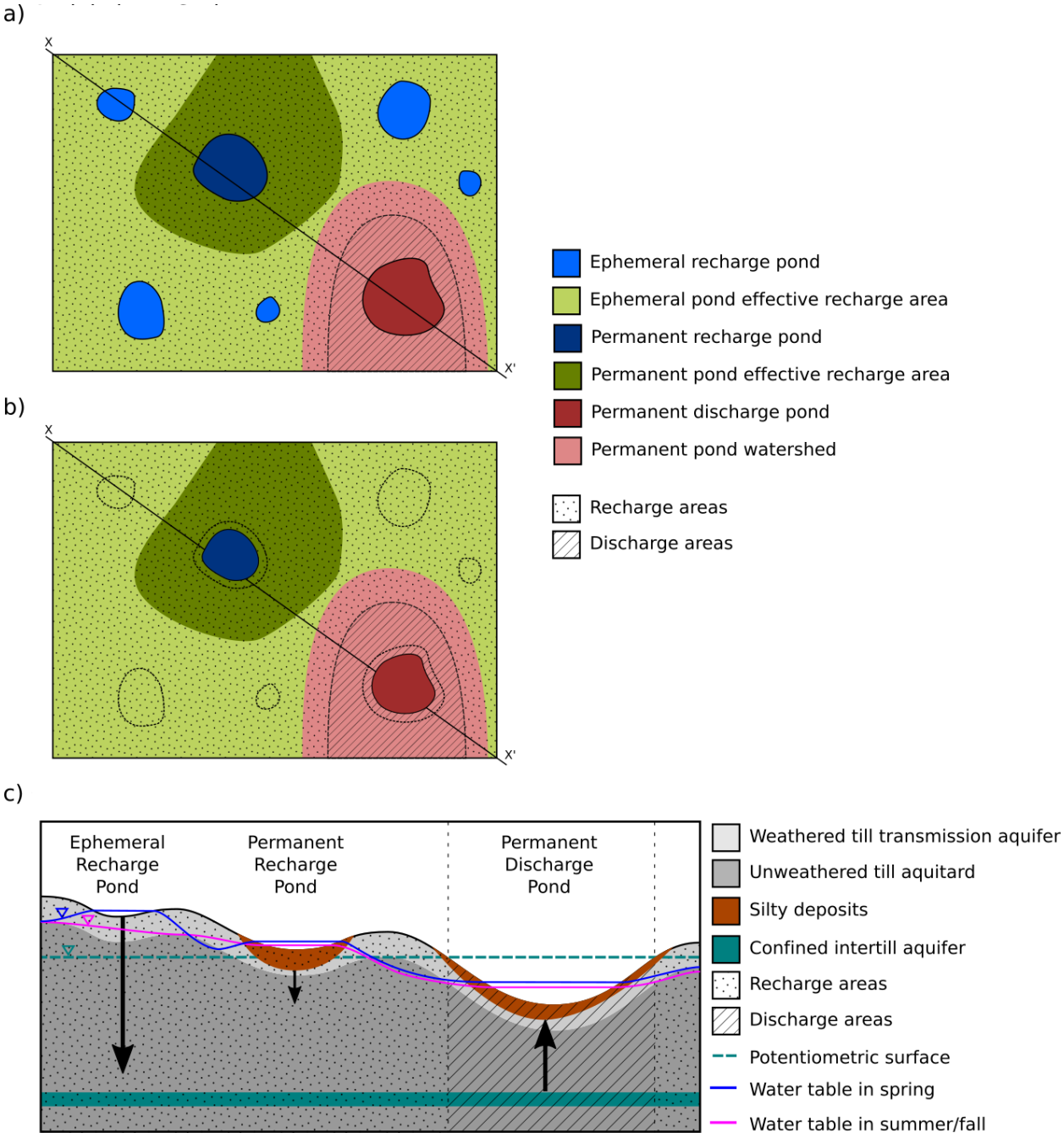

Figure 5.1: Schematic diagrams showing pond –aquifer interactions in the Prairies glacial till. a) Aerial view of the landscape after major snowmelt runoff (i.e., water depleted in heavy water isotopes) into raising pond and shallow ground-water tables. b) Aerial view of the landscape after summer and fall seasons. Gradual decline of pond and shallow ground-water table. c) Cross-section through X-X' with seasonal water tables. Note that the overall hydraulic gradient in the ephemeral and the permanent recharge wetland pond are towards

the confined intertill aquifer, but the matrix flow rate of pond water to and from deep groundwater is very small due to the low hydraulic conductivity of the unweathered till.

5. 2. Recommendations for further Work

1. One limitation of the new isotope model is that it requires more data to compute and the results can be subjected to considerable error if the underlying assumptions are not met and climate data is limited. Care must be taken to measure every parameter in the field as accurately as possible to reduce errors in flux estimates. It is also recommended that this work be extended by combining this modeling approach with evapotranspiration measurement and /or solute balance method within the region to partition the infiltration flux into transpiration and groundwater recharge. The model needs to be extended if possible to cover full hydrological cycle (i.e., wet and dry cycles).
2. The changes observed in pond isotope compositions as a result of the ability of some ponds to transition between one pond type to another (i.e., from seasonal to permanent pond or vice versa) during extreme climate events suggests that the absence of long-term observations could lead to misleading conclusions. This may impact on the identification of which ponds can/not provide recharge water to the intertill aquifer. It is recommended, therefore, that prairies recharge studies involving stable isotopes be carried out using long term data.
3. The importance of ultra-low level tritium isotope data is essential for interpretation of the relationships between the intertill confined aquifer and the surface wetland ponds. It is recommended that more water samples be collected from the deep wells after a much longer term pumping test across seasons and tritium isotopes measured. The fact that tritium values keep decreasing and the cost of analyses is high, it will be useful to use other environmental isotopes to compliment tritium in future studies.
4. The long-term impact of climate variability on ground and surface water resources in the region needs to be studied further.

REFERENCES

Abtew W, Assefa M. 2013. *Evaporation and Evapotranspiration Measurements and Estimations*. Springer Scienec+Business Media Dordrecht: New York.

Allen RG, Pereira LS, Raes D, Smith M. 1998. Crop evapotranspiration: Guidelines for computing crop requirements. 56. Rome, Italy. DOI: 10.1016/j.eja.2010.12.001

Allison GB, Hughes MW. 1983. The use of natural tracers as indicators of soil-water movement in a temperate semi-arid region. *Journal of Hydrology* **60**: 157–173

Araguas-Araguas L, Froehlich K, Rozanski K. 2000. Deuterium and oxygen-18 isotope composition of precipitation and atmospheric moisture. *Hydrological Processes* **14** (2000): 1341–1355

Bacon DH, Keller CK. 1998. Carbon dioxide respiration in the deep vadose zone: Implications for groundwater age dating. *Water Resources Research* **34** (11): 3069 DOI: 10.1029/98WR02045

Balas CJ, Euliss NH, Mushet DM. 2012. Influence of conservation programs on amphibians using seasonal wetlands in the prairie pothole region. *Wetlands* **32** (2): 333–345 DOI: 10.1007/s13157-012-0269-9

Barr G, County S. 1996. Hydrogeology of the surficial and intermediate aquifer systems in Sarasota and adjacent counties, Florida

Bennett KE, Gibson JJ, McEachern PM. 2008. Water-yield estimates for critical loadings assessment: comparisons of gauging methods versus an isotopic approach. *Canadian Journal of Fisheries and Aquatic Sciences* **65** (1): 83–99 DOI: 10.1139/f07-155

Benson L V., Paillet FL. 1989. The use of total lake-surface area as an indicator of climatic change: Examples from the Lahontan basin. *Quaternary Research* **32** (3): 262–275 DOI: 10.1016/0033-5894(89)90093-8

Berman ESF, Gupta M, Gabrielli C, Garland T, McDonnell JJ. 2009. High-frequency field-deployable isotope analyzer for hydrological applications. *Water Resources Research* **45** (10): 1–7 DOI: 10.1029/2009WR008265

Berthold S, Hayashi M. 2004. Integrated hydrogeological and geophysical study of depression-focused groundwater recharge in the Canadian prairies. *Water Resources Research* **40** (6) DOI: 10.1029/2003WR002982

Bortolotti LE, Clark RG, Wassenaar LI. 2013. Hydrogen isotope variability in prairie wetland

systems: Implications for studies of migratory connectivity. *Ecological Applications* **23** (1): 110–121 DOI: 10.1890/12-0232.1

Brannen R, Spence C, Ireson A. 2015. Influence of shallow groundwater-surface water interactions on the hydrological connectivity and water budget of a wetland complex. *Hydrological Processes* **29** (18): 3862–3877 DOI: 10.1002/hyp.10563

Bullock A, Acreman M. 2003. The role of wetlands in the hydrological cycle. *Hydrology and Earth System Sciences* **7** (3): 358–389 DOI: 10.5194/hess-7-358-2003

Clark I. 2015. *Groundwater Geochemistry and Isotopes*. Taylor & Francis Group, LLC: Boca Raton,. DOI: 10.1111/gwat.12377

Clark I, Fritz P. 1997. *Environmental isotopes in hydrogeology*. Lewis Publishers, New York.

Coles AE, McConkey BG, McDonnell JJ. 2017. Climate change impacts on hillslope runoff on the northern Great Plains, 1962–2013. *Journal of Hydrology* **550**: 538–548 DOI: 10.1016/j.jhydrol.2017.05.023

Conly FM, Su M, Kamp G van der, Millar JB. 2004. A practical approach to monitoring water levels in prairie wetlands. *Wetlands* **24** (1): 219–226 DOI: 10.1672/0277-5212(2004)024[0219:apatmw]2.0.co;2

Cook BJ, Hauer FR. 2007. Effects of hydrologic connectivity on water chemistry, soils, and vegetation structure and function in an intermontane depressional wetland landscape. *Wetlands* **27** (3): 719–738 DOI: 10.1672/0277-5212(2007)27[719:EOHCOW]2.0.CO;2

Craig H, Gordon LI. 1965. Deuterium and oxygen 18 variations in the ocean and the marine atmosphere. *In: Tongiorgi, E (Editor), Stable Isotopes in Oceanographic studies and Paleotemperatures, SPOLETO*: 9–130

Craig H, Gordon LI, Horibe Y. 1963. Isotopic exchange effects in the evaporation of water. *Journal of Geophysical Research* **68** (17): 5079–5087 DOI: 10.1029/JZ068i017p05079

Crawford J, Hughes CE, Lykoudis S. 2014. Alternative least squares methods for determining the meteoric water line, demonstrated using GNIP data. *Journal of Hydrology* **519** (PB): 2331–2340 DOI: 10.1016/j.jhydrol.2014.10.033

Cressey RL, Austin JE, Stafford JD. 2016. Three Responses of Wetland Conditions to Climatic Extremes in the Prairie Pothole Region. *Wetlands* **36**: 357–370 DOI: 10.1007/s13157-016-0818-8

Dahl T. 2011. Status and Trends of Wetlands in the Conterminous United States 2004 to 2009.

U.S. Department of the Interior; Fish and Wildlife Service, Washington, D.C. (November): 108

Dansgard W. 1964. Stable isotopes in precipitation. *Tellus* **4** (XVI): 436–467 DOI: 10.1111/j.2153-3490.1964.tb00181.x

Darling W., Bath AH. 1988. A stable isotope study of recharge processes in the English chalk. *Journal of Hydrology* **101**: 31–46

David K, Timms W, Baker A. 2015. Direct stable isotope porewater equilibration and identification of groundwater processes in heterogeneous sedimentary rock. *Science of the Total Environment* **538**: 1010–1023 DOI: 10.1016/j.scitotenv.2015.08.075

Desaulniers DE, Cherry JA, Fritz P. 1981. Origin, age and movement of pore water in argillaceous Quaternary deposits at four sites in southwestern Ontario. *Journal of Hydrology* **50** (C): 231–257 DOI: 10.1016/0022-1694(81)90072-X

Devito KJ, Hill AR, Roulet N. 1996. Groundwater-surface water interactions in headwater forested wetlands of the Canadian Shield. *Journal of Hydrology* **181** (1–4): 127–147 DOI: 10.1016/0022-1694(95)02912-5

Dincer T, Hutton LG, Kupee BBJ. 1979. Stduy, using stable isotope , of flow distribution, surface -groundwater relations and evapotranspiration in the Okavango Swamp, Bostwana. In *Proceedings of an International Symposium on Isotope Hydrology Jointly Organized by the International Atomic Energy Agency and the United Nations Educational, Scientific and Cultural Organization and Held in Neuh Erberg, 19-23 June 1978*International Atomic Energy Agency: Vienna; 3–29.

Dogramaci S, Firmani G, Hedley P, Skrzypek G, Grierson PF. 2015. Evaluating recharge to an ephemeral dryland stream using a hydraulic model and water, chloride and isotope mass balance. *Journal of Hydrology* **521**: 520–532 DOI: 10.1016/j.jhydrol.2014.12.017

Euliss NH, Gleason RA, Olness A, McDougal RL, Murkin HR, Robarts RD, Bourbonniere RA, Warner BG. 2006. North American prairie wetlands are important nonforested land-based carbon storage sites. *Science of The Total Environment* **361** (1–3): 179–188 DOI: 10.1016/j.scitotenv.2005.06.007

Euliss NH, LaBaugh JW, Fredrickson LH, Mushet DM, Laubhan MK, Swanson G a., Winter TC, Rosenberry DO, Nelson RD. 2004. The wetland continuum: A conceptual framework for interpreting biological studies. *Wetlands* **24** (2): 448–458 DOI: 10.1672/0277-

5212(2004)024[0448:TWCACF]2.0.CO;2

Fang X, Minke A, Pomeroy J, Brown T, Westbrook C, Guo X, Guangul S. 2007. A Review of Canadian Prairie Hydrology : Principles , Modelling and Response to Land Use and Drainage Change. *October* (October): 32

Fernández AM, Sánchez-Ledesma DM, Tournassat C, Melón A, Gaucher EC, Astudillo J, Vinsot A. 2014. Applying the squeezing technique to highly consolidated clayrocks for pore water characterisation: Lessons learned from experiments at the Mont Terri Rock Laboratory. *Applied Geochemistry* **49**: 2–21 DOI: 10.1016/j.apgeochem.2014.07.003

Fortin G, van der Kamp G, Cherry JAA. 1991. Hydrogeology and hydrochemistry of an aquifer-aquitard system within glacial deposits, Saskatchewan, Canada. *Journal of Hydrology* **126** (3–4): 265–292 DOI: 10.1016/0022-1694(91)90160-J

Fritz P, Drimmie RJ, Frape SK, O'Shea K. 1987. The isotopic composition of precipitation and groundwater in Canada. *Isotopic Techniques in Water Resources Development* **143** (3–4): 539–549 DOI: 10.1016/0022-1694(93)90212-R

Fritz P, Drimmie RJ, Render F. 1974. Satble isotope contents of major Prairie aquifer in Central Manitoba, Canada. *Isotope Techniques in groundwater Hydrology* **1** (4): 379–398 DOI: 10.1017/CBO9781107415324.004

Gammons CH, Poulson SR, Pellicori DA, Reed PJ, Roesler AJ, Petrescu EM. 2006. The hydrogen and oxygen isotopic composition of precipitation, evaporated mine water, and river water in Montana, USA. *Journal of Hydrology* **328** (1–2): 319–330 DOI: 10.1016/j.jhydrol.2005.12.005

Garvelmann J, Külls C, Weiler M. 2011. A porewater – based stable isotope approach for the investigation of subsurface hydrological processes. *Hydrology and Earth System Sciences Discussions* **8** (5): 9089–9112 DOI: 10.5194/hessd-8-9089-2011

Gat JR. 1995a. *Stable Isotopes of Fresh and Saline Lakes*. DOI: 10.1016/0016-7037(96)83277-7

Gat JR. 1996. Oxygen and Hydrogen Isotopes in the Hydrologic Cycle. *Annual Review of Earth and Planetary Sciences* **24** (1): 225–262 DOI: 10.1146/annurev.earth.24.1.225

Gat JR. 2008. The isotopic composition of evaporating waters - Review of the historical evolution leading up to the Craig-Gordon model. *Isotopes in Environmental and Health Studies* **44** (1): 5–9 DOI: 10.1080/10256010801887067

Gat JR, Levy Y. 1978. Isotope hydrology of inland sabkhas in the Bardawil area, Sinai.

Limnology and Oceanography **23** (5): 841–850 DOI: 10.4319/lo.1978.23.5.0841

Gat YR. 1995b. The relationship between the isotopic composition o f precipitation , surface runoff and groundwater for semiarid and arid zones. *Vienna Symposium* (232): IAHS Publication No. 232

Gazis C, Feng X. 2004. A stable isotope study of soil water: Evidence for mixing and preferential flow paths. *Geoderma* **119** (1–2): 97–111 DOI: 10.1016/S0016-7061(03)00243-X

Gibson J. 2002a. A new conceptual model for predicting isotopic enrichment of lakes in seasonal climates. *Pages News* (July): 1–3 Available at: http://www.science.uwaterloo.ca/~jjgibson/mypdfs/ms_conceptmod.pdf

Gibson JJ. 2002b. Short-term evaporation and water budget comparisons in shallow Arctic lakes using non-steady isotope mass balance. *Journal of Hydrology* **264** (1–4): 242–261 DOI: 10.1016/S0022-1694(02)00091-4

Gibson JJ, Edwards TWD. 2002. Regional water balance trends and evaporation-transpiration partitioning from a stable isotope survey of lakes in northern Canada. *Global Biogeochemical Cycles* **16** (2): 10–11 DOI: 10.1029/2001GB001839

Gibson JJ, Reid R. 2014. Water balance along a chain of tundra lakes: A 20-year isotopic perspective. *Journal of Hydrology* **519** (PB): 2148–2164 DOI: 10.1016/j.jhydrol.2014.10.011

Gibson JJ, Birks SJ, Edwards TWD. 2008a. Global prediction of δA and δ2H- δ18O evaporation slopes for lakes and soil water accounting for seasonality. *Global Biogeochemical Cycles* **22** (2): 1–12 DOI: 10.1029/2007GB002997

Gibson JJ, Birks SJ, Yi Y. 2016. Stable isotope mass balance of lakes: A contemporary perspective. *Quaternary Science Reviews* **131**: 316–328 DOI: 10.1016/j.quascirev.2015.04.013

Gibson JJ, Edward TW., Bursey GG, Prowse T. 1993. Estimating evaporation using stable isotopes: Quantitative results and sensitivity analysis for two catchments in northern Canada. *Nordic Hidrology* **24**: 79–94

Gibson JJ, Edwards TWD, Birks SJ, St Amour NA, Buhay WM, McEachern P, Wolfe BB, Peters DL. 2005. Progress in isotope tracer hydrology in Canada. *Hydrological Processes* **19** (1): 303–327 DOI: 10.1002/hyp.5766

Gibson JJ, Edwards TWD, Prowse TD. 1996. Development and Validation of an Isotopic Method for Estimating Lake Evaporation. *Hydrological Processes* **10** (10): 1369–1382 DOI: 10.1002/(SICI)1099-1085(199610)10:10<1369::AID-HYP467>3.0.CO;2-J

Gibson JJ, Prepas EE, McEachern P. 2002. Quantitative comparison of lake throughflow, residency, and catchment runoff using stable isotopes: Modelling and results from a regional survey of Boreal lakes. *Journal of Hydrology* **262** (1–4): 128–144 DOI: 10.1016/S0022-1694(02)00022-7

Gibson JJ, Reid R, Spence C. 1998. A six-year isotopic record of lake evaporation at a mine site in the Canadian subarctic: results and validation. *Hydrological Processes* **12** (10–11): 1779–1792 DOI: 10.1002/(SICI)1099-1085(199808/09)12:10/11<1779::AID-HYP694>3.0.CO;2-7

Gibson JJ, Sadek MA, Stone DJ., Hughes CE, Hankin S, Cendon DI, Hollins SE. 2008b. Evaporative isotope enrichment as a constraint on reach water balance along a dryland river. *Isotopes in Environmental and Health Studies* **44** (1): 83–98 DOI: 10.1080/10256010801887489

Gilath C, Gonfiantini R. 1983. *Lake Dynamics* (IAEA, ed.). International Atomic Energy Agency: Vienna.

Gleeson T, Befus KM, Jasechko S, Luijendijk E, Cardenas MB. 2015. The global volume and distribution of modern groundwater. *Nature Geoscience* **Advance on** (November): 1–15 DOI: 10.1038/ngeo2590

Goldhaber MB, Mills CT, Morrison JM, Stricker CA, Mushet DM, LaBaugh JW. 2014. Hydrogeochemistry of prairie pothole region wetlands: Role of long-term critical zone processes. *Chemical Geology* **387**: 170–183 DOI: 10.1016/j.chemgeo.2014.08.023

Goldhaber MB, Mills CT, Mushet DM, McCleskey BB, Rover J. 2016. Controls on the Geochemical Evolution of Prairie Pothole Region Lakes and Wetlands Over Decadal Time Scales. *Wetlands* **36**: 255–272 DOI: 10.1007/s13157-016-0854-4

Goldsmith GR, Muñoz-Villers LE, Holwerda F, Mcdonnell JJ, Asbjornsen H, Dawson TE. 2012. Stable isotopes reveal linkages among ecohydrological processes in a seasonally dry tropical montane cloud forest. *Ecohydrology* **5** (6): 779–790 DOI: 10.1002/eco.268

Gonfiantini R. 1986. Environmental isotopes in lake studies. In *Handbook of Environmental Isotope Geochemistry, The Terrestrial Environment*, Fritz, P., Fontes J-C (ed.).Elsevier,

Amsterdam; 113–168.

Granger RJ, Gray DM, Dyck GE. 1984. Snowmelt infiltration to frozen Prairie soils. *Canadian Journal of Earth Sciences* **21** (6): 669–677 DOI: 10.1139/e84-073

Grasby S, Osadetz K, Betcher R, Render F. 2000. Reversal of the regional-scale flow system of the Williston basin in response to Pleistocene glaciation. *Geology* **28** (7): 635–638 DOI: 10.1130/0091-7613(2000)28<635:ROTRFS>2.0.CO;2

Grasby SE, Betcher RN. 2002. Regional hydrogeochemistry of the carbonate rock aquifer, southern Manitoba. *Canadian Journal of Earth Sciences* **39** (7): 1053–1063 DOI: 10.1139/e02-021

Grasby SE, Osborn J, Chen Z, Wozniak PRJ. 2010. Influence of till provenance on regional groundwater geochemistry. *Chemical Geology* **273** (3–4): 225–237 DOI: 10.1016/j.chemgeo.2010.02.024

Harrington GA, Hendry MJ. 2005. Chemical heterogeneity in diffusion-dominated aquitards. **41** (March): 1–13 DOI: 10.1029/2004WR003928

Harrington GA, Gardner WP, Smerdon BD, Hendry MJ. 2013. Palaeohydrogeological insights from natural tracer profiles in aquitard porewater, Great Artesian Basin, Australia. *Water Resources Research* **49** (7): 4054–4070 DOI: 10.1002/wrcr.20327

Harrington GA, Hendry MJ, Robinson NI. 2007. Impact of permeable conduits on solute transport in aquitards : Mathematical models and their application. *Water Resources Research* **43** (W05441): 1–16 DOI: 10.1029/2005WR004144

Hayashi M. 1996. Surface-subsurface Transport Cycle of Chloride Induced by Wetland-focused Groundwater Recharge.PhD Thesis. Department of Earth Science, University of Waterloo.

Hayashi M, Van Der Kamp G. 2000. Simple equations to represent the volume-area-depth relations of shallow wetlands in small topographic depressions. *Journal of Hydrology* **237** (1–2): 74–85 DOI: 10.1016/S0022-1694(00)00300-0

Hayashi M, van der Kamp G, Rosenberry DO. 2016. Hydrology of Prairie Wetlands: Understanding the Integrated Surface-Water and Groundwater Processes. *Wetlands* **36**: 237–254 DOI: 10.1007/s13157-016-0797-9

Hayashi M, van der Kamp G, Rudolph DLL. 1998. Water and solute transport between a prairie wetland and adjacent upland, 1. Water balance. *Journal of Hydrology* **207**: 42–55 DOI: 1016/S0022-1694(98)00098-5

Hayashi M, Van Der Kamp G, Rudolph DL. 1997. Use of tensiometer response time to determine the hydraulic conductivity of unsaturated soil. *Soil Science* **162** (8): 566–575 DOI: 10.1097/00010694-199708000-00005

Hayashi M, Van Der Kamp G, Schmidt R. 2003. Focused infiltration of snowmelt water in partially frozen soil under small depressions. *Journal of Hydrology* **270** (3–4): 214–229 DOI: 10.1016/S0022-1694(02)00287-1

Heagle D, Hayashi M, Kamp G Van Der. 2013. Surface–subsurface salinity distribution and exchange in a closed-basin prairie wetland. *Journal of Hydrology* **478**: 1–14 DOI: 10.1016/j.jhydrol.2012.05.054

Heagle DJ. 2008. Surface-subsurface solute cycling in wetlands receiving groundwater discharge.PhD Thesis. Department of Geoscience, University of Calgary.

Heagle DJ, Hayashi M, van der Kamp G. 2007. Use of solute mass balance to quantify geochemical processes in a prairie recharge wetland. *Wetlands* **27** (4): 806–818 DOI: 10.1672/0277-5212(2007)27[806:UOSMBT]2.0.CO;2

Healy R, Winter TC, LaBaugh JW, Franke OL. 2007. Water Budgets : Foundations for Effective Water-Resources and Environmental Management. *USGS Circular*: 90

Healy RW, Scanlon BR. 2010. *Estimating Groundwater Recharge*. Cambridge University Press: Cambridge, UK.

Henderson N, Sauchyn D. 2008. Climate change impacts on Canada's prairie provinces: a summary of our state of knowledge

Hendry JM, Barbour LS, Schmeling EE. 2015a. Defining near-surface groundwater flow regimes in the semi-arid glaciated plains of North America. *Isotopes in Environmental and Health Studies* **0** (0): 1–11 DOI: 10.1080/10256016.2016.1092966

Hendry MJ. J, Wassenaar LI. 2000. Controls on the distribution of major ions in pore waters of a thick surficial aquitard. *Water Resources Research* **36** (2): 503–513 DOI: 10.1029/1999WR900310

Hendry MJ. 1983. Groundwater recharge through a heavy textured soil. *Journal of Hydrology* **63** (1982): 201–209

Hendry MJ. 1988. Hydrogeology of Clay Till in a Prairie Region of Canada. *Ground water* **26** (5): 607–614

Hendry MJ, Harrington GA. 2014. Comparing vertical profiles of natural tracers in the Williston

Basin to estimate the onset of deep aquifer activation. *Water Resources Research* **50**: 6496–6506 DOI: 10.1002/2014WR015652

Hendry MJ, Wassenaar LI. 1999. Implications of the distribution of ??D in pore waters for groundwater flow and the timing of geologic events in a thick aquitard system. *Water Resources Research* **35** (6): 1751–1760 DOI: 10.1029/1999WR900046

Hendry MJ, Wassenaar LI. 2004. Transport and geochemical controls on the distribution of solutes and stable isotopes in a thick clay-rich till aquitard, Canada. *Isotopes in environmental and health studies* **40** (1): 3–19 DOI: 10.1080/10256010310001644942

Hendry MJ, Wassenaar LI. 2009. Inferring heterogeneity in aquitards using high-resolution δd and δ18 Profiles. *Ground Water* **47** (5): 639–645 DOI: 10.1111/j.1745-6584.2009.00564.x

Hendry MJ, Barbour SL, Novakowski K, Wassenaar LI. 2013. Paleohydrogeology of the Cretaceous sediments of the Williston Basin using stable isotopes of water. *Water Resources Research* **49** (8): 4580–4592 DOI: 10.1002/wrcr.20321

Hendry MJ, Barbour SL, Zettl J, Chostner V, Wassenaar LI. 2011. Controls on the long-term downward transport of δ^2H of water in a regionally extensive, two-layered aquitard system. *Water Resources Research* **47** (6): W06505 DOI: 10.1029/2010WR010044

Hendry MJ, Cherry J. A, Wallick EI. 1986. Origin and Distribution of Sulfate in a Fractured Till in Southern Alberta, Canada. *Water Resources Research* **22** (1): 45–61 DOI: 10.1029/WR022i001p00045

Hendry MJ, Kelln CJ, Wassenaar LI, Shaw J. 2004. Characterizing the hydrogeology of a complex clay-rich aquitard system using detailed vertical profiles of the stable isotopes of water. *Journal of Hydrology* **293** (1–4): 47–56 DOI: 10.1016/j.jhydrol.2004.01.010

Hendry MJ, Schmeling E, Wassenaar LI, Barbour SL, Pratt D. 2015b. Determining the stable isotope composition of pore water from saturated and unsaturated zone core: Improvements to the direct vapour equilibration laser spectrometry method. *Hydrology and Earth System Sciences* **19** (11): 4427–4440 DOI: 10.5194/hess-19-4427-2015

Hendry MJ, Wassenaar LI, Kotzer T. 2000. Cloride and chlorine of solute migration in a thick , clay-rich aquitard system. *Water Resources Research* **36** (1): 285–296

Herve-Fernandez P, Oyarzún C, Brumbt C, Huygens D, Bodé S, Verhoest NEC, Boeckx P. 2016. Assessing the " two water worlds hypothesis " and water sources for native and exotic evergreen species in south-central Chile. *Hydrological Processes* **4241** (April): 2–3 DOI:

10.13140/RG.2.1.4527.5121

Hogan JM, Conly FM. 2002. *St . Denis National Wildlife Area Land Cover Classification : 1997*.

Horita J. 2009. Isotopic evolution of saline lakes in the low-latitude and polar regions. *Aquatic Geochemistry* **15** (1–2): 43–69 DOI: 10.1007/s10498-008-9050-3

Horita J, Wesolowski DJ. 1994. Liquid-vapor fractionation of oxygen and hydrogen isotopes of water from the freezing to the critical temperature. *Geochimica et Cosmochimica Acta* **58** (16): 3425–3437 DOI: 10.1016/0016-7037(94)90096-5

Horita J, Rozanski K, Cohen S. 2008. Isotope effects in the evaporation of water: a status report of the Craig-Gordon model. *Isotopes in environmental and health studies* **44** (1): 23–49 DOI: 10.1080/10256010801887174

Hsieh J. C., Chadwick OA, Kelly EF, Savin S. . 1998. Oxygen isotopic composition of soil water: Quantifying evaporation and transpiration. *Geoderma* **82** (1–3): 269–293 DOI: 10.1016/s0016-7061(97)00105-5

Huang M, Hilderman JN, Barbour L. 2015. Transport of stable isotopes of water and sulphate within reclaimed oil sands saline–sodic mine overburden. *Journal of Hydrology* **529**, **Part**: 1550–1561 DOI: http://dx.doi.org/10.1016/j.jhydrol.2015.08.028

Huang T, Pang Z. 2012. The role of deuterium excess in determining the water salinisation mechanism: A case study of the arid Tarim River Basin, NW China. *Applied Geochemistry* **27** (12): 2382–2388 DOI: 10.1016/j.apgeochem.2012.08.015

Hunt RJ, Bullen TD, Krabbenhoft DP, Kendall C. 1998. Using stable isotopes of water and strontium to investigate the hydrology of a natural and a constructed wetland. *Ground Water* **36** (October 2015): 434–443 DOI: 10.1111/j.1745-6584.1998.tb02814.x

Hunt RJ, Coplen TB, Haas NL, Saad D a., Borchardt M a. 2005. Investigating surface water–well interaction using stable isotope ratios of water. *Journal of Hydrology* **302** (1–4): 154–172 DOI: 10.1016/j.jhydrol.2004.07.010

IAEA. 1992. Statistical treatment of data on environmental isotopes in precipitation. *Technical Report Series 331,*: 783

IAEA. 2009. Laser Spectroscopic Analysis of Liquid Water Samples for Stable Hydrogen and Oxygen Isotopes. *Isotope Hydrology Section International Atomic Energy Agency*: 49

Ireson AM, van der Kamp G, Nachshon U, Butler PA. 2013. Modeling Groundwater-Soil-Plant-Atmosphere Exchanges in Fractured Porous Media. *Procedia Environmental Sciences* **19**

(306): 321–330 DOI: 10.1016/j.proenv.2013.06.037

Jacob H, Sonntag C. 1991. An 8-year record of the seasonal variation of D and O-18 in atmospheric water vapour and precipitation at Heidelberg, Germany. *Tellus* **43b**: 291–300 DOI: 10.1034/j.1600-0889.1991.t01-2-00003.x

Jasechko S, Birks SJ, Gleeson T, Wada Y, Fawcett PJ, Sharp ZD, McDonnell JJ, Welker JM. 2014. The pronounced seasonlity of global groundwater recharge. *Water Resources Research* **50**: 8845–8867 DOI: 10.1002/2014WR015809.Received

Jasechko S, Sharp ZD, Gibson JJ, Birks SJ, Yi Y, Fawcett PJ. 2013. Terrestrial water fluxes dominated by transpiration. *Nature* **496** (7445): 347–350 DOI: 10.1038/nature11983

Jasechko S, Wassenaar LI, Mayer B. 2017. Isotopic evidence for widespread cold-season-biased groundwater recharge and young streamflow across central Canada. *Hydrological Processes* **31** (12): 2196–2209 DOI: 10.1002/hyp.11175

Johnsgard PA. 2010. "Waterfowl of North America: SURFACE-FEEDING DUCKS Tribe Anatini. *Waterfowl of North America,* **Revised Ed** (Paper II): 181–299

Johnson WC, Werner B, Guntenspergen GR, Voldseth R a., Millett B, Naugle DE, Tulbure M, Carroll RWH, Tracy J, Olawsky C. 2010. Prairie Wetland Complexes as Landscape Functional Units in a Changing Climate. *BioScience* **60** (2): 128–140 DOI: 10.1525/bio.2010.60.2.7

Jolly ID, McEwan KL, Holland KL. 2008. A review of groundwater–surface water interactions in arid/semi-arid wetlands and the consequences of salinity for wetland ecology. *Ecohydrology* **1** (November): 43–58 DOI: 10.1002/eco

Jones MD, Cuthbert MO, Leng MJ, McGowan S, Mariethoz G, Arrowsmith C, Sloane HJ, Humphrey KK, Cross I. 2016. Comparisons of observed and modelled lake δ18O variability. *Quaternary Science Reviews* **131**: 329–340 DOI: 10.1016/j.quascirev.2015.09.012

Joshi B, Maule C. 1999. Vadose Zone Flow and Transport in Cracked Heavy Textured Soil. *Journal of Irrigation and Drainage Engineering* **125** (JUNE): 122–130 DOI: 10.1061/(ASCE)0733-9437(1999)125:3(122)

Joshi B, Maulé C. 2000. Simple analytical models for interpretation of environmental tracer profiles in the vadose zone. *Hydrological Processes* **14** (8): 1503–1521 DOI: 10.1002/1099-1085(20000615)14:8<1503::AID-HYP990>3.0.CO;2-Z

Kalbus E, Reinstorf F, Schirmer M, Kalbus E, Reinstorf F, Measuring MS. 2006. Measuring methods for groundwater ? surface water interactions : a review To cite this version : Measuring methods for groundwater – surface water interactions : a review

van der Kamp G, Hayashi M. 1998. The groundwater recharge function of small wetlands in the semi-arid northern prairies. *Great Plains Research* **8** (1): 39–56

van der Kamp G, Hayashi MM. 2009. Groundwater-wetland ecosystem interaction in the semiarid glaciated plains of North America. *Hydrogeology Journal* **17** (1): 203–214 DOI: 10.1007/s10040-008-0367-1

van der Kamp G, Hayashi M, Bedard-Haughn A, Pennock D. 2016. Prairie Pothole Wetlands – Suggestions for Practical and Objective Definitions and Terminology. *Wetlands* **36**: 229–235 DOI: 10.1007/s13157-016-0809-9

van der Kamp G, Hayashi M, Gallén D. 2003. Comparing the hydrology of grassed and cultivated catchments in the semi-arid Canadian prairies. *Hydrological Processes* **17** (3): 559–575 DOI: 10.1002/hyp.1157

van der Kamp G, Keir D, Evans MS. 2008. Long-Term Water Level Changes in Closed-Basin Lakes of the Canadian Prairies. *Canadian Water Resources …* **33** (January 2008): 23–38 DOI: 10.4296/cwrj3301023

Karolytė R, Serno S, Johnson G, Gilfillan SMV. 2017. The influence of oxygen isotope exchange between CO 2 and H 2 O in natural CO 2 -rich spring waters: Implications for geothermometry. *Applied Geochemistry* **84**: 173–186 DOI: 10.1016/j.apgeochem.2017.06.012

Kebede S, Travi Y, Rozanski K. 2009. The δ18O and δ2H enrichment of Ethiopian lakes. *Journal of Hydrology* **365** (3–4): 173–182 DOI: 10.1016/j.jhydrol.2008.11.027

Keller CK, Kamp G van der, Cherry J. 1985. Fracture permeability and groundwater flow in clayey till near Saskatoon , Saskatchewan. *Canadian Geotechnical Journal* **23** (2): 229–240 DOI: 10.1139/t86-032

Keller CK, van der Kamp G, Cherry JA. 1991. Hydrogeochemistry of a clayey till 1. Spatial variability. *Water Resources Research* **27** (10): 2543–2554

Keller CK, Van Der Kamp G, Cherry JA, cherry J.A. 1988. Hydrogeology of two Saskatchewan tills, I. Fractures, bulk permeability, and spatial variability of downward flow. *Journal of Hydrology* **101** (1–4): 97–121 DOI: 10.1016/0022-1694(88)90030-3

Kelley LI, Holmden C. 2001. Reconnaissance hydrogeochemistry of economic deposits of sodium sulfate (mirabilite) in saline lakes , Saskatchewan , Canada. *Hydrbiologia* **466** (1–3): 279–289 DOI: 10.1023/A:1014565619506

Kelln C, Barbour L, Qualizza C. 2007. Preferential Flow in a Reclamation Cover: Hydrological and Geochemical Response. *Journal of Geotechnical and Geoenvironmental Engineering* **133** (10): 1277–1289 DOI: 10.1061/(ASCE)1090-0241(2007)133:10(1277)

Kumar B, Nachiappan RP. 1999. On the sensitivity of Craig and Gordon model for the estimation of the isotopic composition of lake evaporates. *Water Resources Research* **35** (5): 1689–1691 DOI: 10.1029/1999WR900011

Labaugh JW, Rosenberry DO, Schuster PF, Reddy MM, Aiken GR. 1997. Hydrological and chemical estimates of the water balance of a closed basin lake in north central Minnesota. *Water Resources Research* **33** (12): 2799–2812

Labaugh JW, Winter TC, Rosenberry DO. 1998. Hydrologic Functions of Prairie Wetlands. *Great Plains Research* **8** (1): 17–37

Labaugh JW, Winter TC, Swanson GA, Rosenberry DO, Nelson RD, Euliss NH. 1996. Changes in atmospheric circulation patterns affect midcontinent wetlands sensitive to climate. *Limnology and Oceanography* **41** (5): 864–870 DOI: 10.4319/lo.1996.41.5.0864

LaBaugh JW, Mushet DM, Rosenberry DO, Euliss NH, Goldhaber MB, Mills CT, Nelson RD. 2016. Changes in Pond Water Levels and Surface Extent Due to Climate Variability Alter Solute Sources to Closed-Basin Prairie-Pothole Wetland Ponds, 1979 to 2012. *Wetlands* **36**: 343–355 DOI: 10.1007/s13157-016-0808-x

Landwehr JM, Coplen TB. 2004. Stable, Line-Conditioned Excess: A New Method for Characterizing Systems, Hydrogen and Oxygen Isotope Ratios in Hydrologic systems. In *International Conference on Isotopes in Environmental Studies – Aquatic Forum 2004*303–304. DOI: 10.8/S

Landwehr JM, Coplen TB, Stewart DW. 2014. Spatial, seasonal, and source variability in the stable oxygen and hydrogen isotopic composition of tap waters throughout the USA. *Hydrological Processes* **28** (21): 5382–5422 DOI: 10.1002/hyp.10004

Leibowitz SG, Vining KC. 2003. Temporal connectivity in a prairie pothole complex. *Wetlands* **23** (1): 13–25 DOI: 10.1672/0277-5212(2003)023[0013:TCIAPP]2.0.CO;2

Leibowitz SG, Mushet DM, Newton WE. 2016. Intermittent Surface Water Connectivity: Fill

and Spill Vs. Fill and Merge Dynamics. *Wetlands* **36**: 323–342 DOI: 10.1007/s13157-016-0830-z

Levy ZF, Siegel DI, Dasgupta SS, Glaser PH, Welker JM. 2014. Stable isotopes of water show deep seasonal recharge in northern bogs and fens. *Hydrological Processes* **28** (18): 4938–4952 DOI: 10.1002/hyp.9983

Lis G, Wassenaar LI, Hendry MJ. 2008. High-precision laser spectroscopy D/H and 18O/16O measurements of microliter natural water samples. *Analytical chemistry* **80** (1): 287–93 DOI: 10.1021/ac701716q

Lissey A. 1971. Depression -focused transient groundwater flow patterns in Manitoba. *The Geological Assocation of Canada* **Special Pa** (9): 333–341

Liu W, Li P, Li H, Duan W. 2006. Estimation of evaporation rate from soil surface using stable isotopic composition of throughfall and stream water in a tropical seasonal rain forest of Xishuangbanna, Southwest China. *Acta Ecologica Sinica* **26** (5): 1303–1310 DOI: 10.1016/S1872-2032(06)60022-X

Manna F, Walton KM, Cherry JA, Parker BL. 2017. Mechanisms of recharge in a fractured porous rock aquifer in a semi-arid region. *Journal of Hydrology* **555**: 869–880 DOI: 10.1016/j.jhydrol.2017.10.060

Maule CPP, Chanasyk DSS, Muehlenbachs K. 1994. Isotopic determination of snow-water contribution to soil water and groundwater. *Journal of Hydrology* **155** (1–2): 73–91 DOI: 10.1016/0022-1694(94)90159-7

McGinn SM. 2010. Weather and Climate Patterns in Canada's Prairie Grasslands. In *Arthropods of Canadian Grasslands (Volume 1): Ecology and Interactions in Grassland Habitats*, Floate. JDS and KD (ed.).Biological Survey of Canada; 105–119. DOI: 10.3752/9780968932148.ch5

McKay L., Cherry J., Gillham R. 1993. Field experiments in a fractured clay till 1. Hydraulic conductivity and fracture aperture. *Water Resources Research* **29** (4): 1149–1162

Mcmonagle AL. 1987. Stable isotope and chemical compositions of surface and subsurface waters in Saskatchewan: 108

Mekonnen MA, Wheater HS, Ireson AM, Spence C, Davison B, Pietroniro A. 2014. Towards an improved land surface scheme for prairie landscapes. *Journal of Hydrology* **511**: 105–116 DOI: 10.1016/j.jhydrol.2014.01.020

Meyboom P. 1966. Unsteady groundwater flow near a willow ring in hummocky moraine. *Journal of Hydrology* **4**: 38–62

Meyboom P. 1967. Groundwater Studies in the Assiniboine River Drainage Basin: Hydroloic Characteristics of Phreatophytic vegetation in the south-central Saskatchewan. *Bulletin 139*: 65

Millar JB. 1971. Shoreline-area ratio as a factor in rate of water loss from small sloughs. *Journal of Hydrology* **14**: 259–284

Miller JJ, Acton DF, St. Arnaud RJ. 1985. The Effect of Groundwater on Soil Formation in a Morainal Landscape in Saskatchewan. *Canadian Journal of Soil Science* **65** (May 1984): 293–307 DOI: 10.4141/cjss85-033

Morgenstern U, Taylor CB. 2009. Ultra low-level tritium measurement using electrolytic enrichment and LSC. *Isotopes in Environmental and Health Studies* **45** (2): 96–117 DOI: 10.1080/10256010902931194

Morton FI. 1983. Operational estimates of lake evaporation. *Journal of Hydrology* **66** (1–4): 77–100 DOI: 10.1016/0022-1694(83)90178-6

Mould DJ, Frahm E, Th. Salzmann, Miegel K, Acreman1 MC. 2010. Evaluating the use of diurnal groundwater fluctuations for estimating evapotranspiration in wetland environments: case studies in southeast England and northeast Germany. *Ecohydrology* **3** (May): 294–305 DOI: 10.1002/eco

Mueller MH, Alaoui A, Kuells C, Leistert H, Meusburger K, Stumpp C, Weiler M, Alewell C. 2014. Tracking water pathways in steep hillslopes by δ18O depth profiles of soil water. *Journal of Hydrology* **519** (PA): 340–352 DOI: 10.1016/j.jhydrol.2014.07.031

Murkin HR. 1998. Freshwater functions and values of prairie wetlands. *Great Plains Research* **8** (1): 3–15

Nachshon U, Ireson A, van der Kamp G, Davies S., Wheater HS. 2014. Impacts of climate variability on wetland salinization in the North American prairies. *Hydrology and Earth System Sciences* **18** (4): 1251–1263 DOI: 10.5194/hess-18-1251-2014

Nachshon U, Ireson A, van der Kamp G, Wheater HS. 2013. Sulfate salt dynamics in the glaciated plains of North America. *Journal of Hydrology* **499**: 188–199 DOI: 10.1016/j.jhydrol.2013.07.001

Nilsson KA, Rains MC, Lewis DB, Trout KE. 2013. Hydrologic characterization of 56

geographically isolated wetlands in west-central Florida using a probabilistic method. *Wetlands Ecology and Management* **21** (1): 1–14 DOI: 10.1007/s11273-012-9275-1

Orlowski N, Pratt DL, McDonnell JJ. 2016. Intercomparison of soil pore water extraction methods for stable isotope analysis. *Hydrological Processes* **30** (19): 3434–3449 DOI: 10.1002/hyp.10870

Parkhurst RS, Winter TC, Rosenberry DO, Sturrock AM. 1998. Evaporation from a small Prairie wetland in the Cotton Wood Lake Area, North Dakota - An energy budget study. *Wetlands* **18** (June): 272–287

Parsons DF, Hayashi M, van der Kamp G. 2004. Infiltration and solute transfort under a seasonal wetland: Bromide tracer experiments in Saskatoon, Canada. *Hydrological Processes* **18** (11): 2011–2027 DOI: 10.1002/hyp.1345

Pavlovskii I, Hayashi M, Lennon MR. 2017. Transformation of snow isotopic signature along groundwater recharge pathways in the Canadian Prairies. *Journal of Hydrology* DOI: 10.1016/j.jhydrol.2017.09.053

Peng H, Mayer B, Harris S, Krouse HR. 2004a. A 10-year record of stable isotope ratios of hydrogen and oxygen in precipitation at Calgary, Alberta, Canada. *Tellus, Series B: Chemical and Physical Meteorology* **56** (2): 147–159 DOI: 10.1111/j.1600-0889.2004.00094.x

Peng H, Mayer B, Harris S, Krouse HR. 2004b. A 10-year record of stable isotope ratios of hydrogen and oxygen in precipitation at Calgary, Alberta, Canada. *Tellus, Series B: Chemical and Physical Meteorology* **56** (2): 147–159 DOI: 10.1111/j.1600-0889.2004.00094.x

Pennock D, Bedard-Haughn A, Kiss J, van der Kamp G. 2014. Application of hydropedology to predictive mapping of wetland soils in the Canadian Prairie Pothole Region. *Geoderma* **235**–**236**: 199–211 DOI: 10.1016/j.geoderma.2014.07.008

Pham S V, Leavitt PR, McGowan S, Wissel B, Wassenaar LI. 2009. Spatial and temporal variability of prairie lake hydrology as revealed using stable isotopes of hydrogen and oxygen. *Limonology And Oceanography* **54** (1): 101–118 DOI: 10.4319/lo.2009.54.1.0101

Phillips FM, Mills S, Hendrickx MH, Hogan J. 2003. Environmental Tracers applied to quantifying causes of salinity in arid-region rivers: results from the Rio Grande Basin, Southwestern USA. In *Water Resorces Perspectives:Evaluation, Management and Poilcy.*,

Aisharhan A., , Wood WW (eds).Armsterdam; 327–334.

Remenda VH, Van Der Kamp G, Cherry JA. 1996. Use of vertical profiles of ??18O to constrain estimates of hydraulic conductivity in a thick, unfractured aquitard. *Water Resources Research* **32** (10): 2979–2987 DOI: 10.1029/96WR01778

Renée Brooks J, Barnard HR, Coulombe R, McDonnell JJ. 2010. Ecohydrologic separation of water between trees and streams in a Mediterranean climate. *Nature Geoscience* **3** (2): 100–104 DOI: 10.1038/ngeo722

Reynolds S. 1970. The gravimetric method of soil moisture determination. *Journal of Hydrology* **11**: 258–273

Richardson JL, Amdt JL, Freeland J. 1994. WETLAND SOILS OF THE PRAIRIE POTHOLE. *Advances in Agronomy* **52**: 121–171

Rosenberry DO, Winter TC. 1997. Dynamics of water-table fluctuations in an upland between two prairie-pothole wetlands in North Dakota. *Journal of Hydrology* **191** (1–4): 266–289 DOI: 10.1016/S0022-1694(96)03050-8

Rothfuss Y, Biron P, Braud I, Canale L, Durand JL, Gaudet JP, Richard P, Vauclin M, Bariac T. 2010. Partitioning evapotranspiration fluxes into soil evaporation and plant transpiration using water stable isotopes under controlled conditions. *Hydrological Processes* **24** (22): 3177–3194 DOI: 10.1002/hyp.7743

Rozanski K, Chmura L. 2008. Isotope effects accompanying evaporation of water from leaky containers. *Isotopes in Environmental and Health Studies* **44** (1): 51–59 DOI: 10.1080/10256010801887141

Rozanski K, Araguás-Araguás L, Gonfiantini R. 1992. Relation between long-term trends of oxygen-18 isotope composition of precipitation and climate. *Science (New York, N.Y.)* **258** (5084): 981–5 DOI: 10.1126/science.258.5084.981

Saxena RK. 1984. Seasonal variation of oxygen-18 in soil moisture and estimation of groundwater recharge in esker and moraine formations. *Nordic Hydrology* **15**: 235–242

Scanlon BR. 1991. Evaluation of moisture flux from chloride data in desert soils. *Journal of Hydrology* **128** (1–4): 137–156 DOI: 10.1016/0022-1694(91)90135-5

Scanlon BR, Healy RW, Cook PG. 2001. Choosing appropriate technique for quantifying groundwater recharge. *Hydrogeology Journal* **10**: 18–39 DOI: 10.1007/s10040-0010176-2

Seelig B, DeKeyser S. 2006. Water Quality and Wetland Function in the Northern Prairie

Pothole Region. Fargo.

Seyfried MS, Schwinning S, Walvoord MA, Pockman WT, Newman BD, Jackson RB, Phillips FM. 2005. Ecohydrological control of deep drainage in arid and semiarid regions. *Ecology* **86** (2): 277–287 DOI: 10.1890/03-0568

Shaw DA, van der Kamp G, Conly FM, Pietroniro A, Martz L. 2012a. The Fill-Spill Hydrology of Prairie Wetland Complexes during Drought and Deluge. *Hydrological Processes* **26** (20): 3147–3156 DOI: 10.1002/hyp.8390

Shaw DA, Vanderkamp G, Conly FM, Pietroniro A, Martz L. 2012b. The Fill-Spill Hydrology of Prairie Wetland Complexes during Drought and Deluge. *Hydrological Processes* **26** (20): 3147–3156 DOI: 10.1002/hyp.8390

Shook K, Pomeroy JW, Spence C, Boychuk L. 2013. Storage dynamics simulations in prairie wetland hydrology models: evaluation and parameterization. *Hydrological Processes* **27** (13): 1875–1889 DOI: 10.1002/hyp.9867

Siegel D. 1988. The recharge -discharge function of wetlands near Juneau, Alaska: Part 1. Hydrogeological invetsiagtions. *Ground Water* **26** (4): 427–434

Simpkins WW, Bradbury KR. 1992. Groundwater flow , velocity , and age in a thick , fine-grained till unit in southeastern Wisconsin. *Journal of Hydrology* **132** (1–4): 283–319 DOI: 10.1016/0022-1694(92)90183-V

Skrzypek G, Dogramaci S, Grierson PF. 2013. Geochemical and hydrological processes controlling groundwater salinity of a large inland wetland of northwest Australia. *Chemical Geology* **357**: 164–177 DOI: 10.1016/j.chemgeo.2013.08.035

Skrzypek G, Mydłowski A, Dogramaci S, Hedley P, Gibson JJ, Grierson PF. 2015. Estimation of evaporative loss based on the stable isotope composition of water using Hydrocalculator. *Journal of Hydrology* **523**: 781–789 DOI: 10.1016/j.jhydrol.2015.02.010

Sloan C. 1972. Ground-water hydrology of prairie potholes in North Dakota: 1–29 Available at: http://library.ndsu.edu/exhibits/text/potholes/585c.html

Sophocleous M. 2005. Groundwater recharge and sustainability in the High Plains aquifer in Kansas, USA. *Hydrogeology Journal* **13** (2): 351–365 DOI: 10.1007/s10040-004-0385-6

Spence C, Woo M. 2003. Hydrology of subarctic Canadian shield: soil-filled valleys. *Journal of Hydrology* **279** (1–4): 151–166 DOI: 10.1016/S0022-1694(03)00175-6

Sprenger M, Erhardt M, Riedel M, Weiler M. 2016a. Historical tracking of nitrate in contrasting

vineyards using water isotopes and nitrate depth profiles. *Agriculture, Ecosystems and Environment* **222**: 185–192 DOI: 10.1016/j.agee.2016.02.014

Sprenger M, Leistert H, Gimbel K, Weiler M. 2016b. Illuminating hydrological processes at the soil-vegetation- atmosphere interface with water stable isotopes. *Reviews of Geophysics REVIEW* **54** (section 6): 119–161 DOI: 10.1002/2015RG000504.Received

Sprenger M, Volkmann THM, Blume T, Weiler M. 2015. Estimating flow and transport parameters in the unsaturated zone with pore water stable isotopes. *Hydrology and Earth System Sciences* **19** (6): 2617–2635 DOI: 10.5194/hess-19-2617-2015

Steinman BA, Rosenmeier MF, Abbott MB, Bain DJ. 2010. The isotopic and hydrologic response of small, closed-basin lakes to climate forcing from predictive models: Application to paleoclimate studies in the upper Columbia River basin. *Limnology and Oceanography* **55** (6): 2231–2245 DOI: 10.4319/lo.2010.55.6.2231

Van Stempvoort DR, Hendry MJ, Schoenau JJ, Krouse HR. 1994. Sources and dynamics of sulfur in weathered till, Western Glaciated Plains of North America. *Chemical Geology* **111** (1–4): 35–56 DOI: 10.1016/0009-2541(94)90081-7

Stewart BRE, Kantrud HA. 1972. Vegetation of prairie potholes, North Dakota, in relation to quality of water and other environmental factors. *Fisheries Bethesda* **U.S. Geolo** (1931): 41 Available at: http://library.ndsu.edu/exhibits/text/potholes/585d.html

Stewart RE, Kantrud HA. 1971. Classification of Natural Ponds and Lakes in the Glaciated Prairie Region.: 57

Stumpp C, Hendry MJ. 2012. Spatial and temporal dynamics of water flow and solute transport in a heterogeneous glacial till: The application of high-resolution profiles of ?? 18O and ?? 2H in pore waters. *Journal of Hydrology* **438**–**439**: 203–214 DOI: 10.1016/j.jhydrol.2012.03.024

Su M, Stolte WJ, Van Der Kamp G. 2000. Modelling Canadian prairie wetland hydrology using a semi-distributed streamflow model. *Hydrological Processes* **14** (14): 2405–2422 DOI: 10.1002/1099-1085(20001015)14:14<2405::AID-HYP92>3.0.CO;2-B

Sutanto SJ, Wenninger J, Coenders-Gerrits AMJ, Uhlenbrook S. 2012. Partitioning of evaporation into transpiration, soil evaporation and interception: A comparison between isotope measurements and a HYDRUS-1D model. *Hydrology and Earth System Sciences* **16** (8): 2605–2616 DOI: 10.5194/hess-16-2605-2012

Van Der Valk AG. 2005. Water-level fluctuations in North American prairie wetlands. *Hydrobiologia* **539** (1): 171–188 DOI: 10.1007/s10750-004-4866-3

Waiser MJ. 2006. Relationship between hydrological characteristics and dissolved organic carbon concentration and mass in northern prairie wetlands using a conservative tracer approach. *Journal of Geophysical Research: Biogeosciences* **111** (2): 1–15 DOI: 10.1029/2005JG000088

Wallick EI. 1981. Chemical evolution of groundwater in a drainage basin of Holoscene age, east - central Alberta, Canada. *Journal of Hydrology* **54**: 245–285

Walvoord MA, Plummer MA, Phillips FM, Wolfsberg A V. 2002. Deep arid system hydrodynamics 1. Equilibrium states and response times in thick desert vadose zones. *Water Resources Research* **38** (12): 1–15 DOI: 10.1029/2001WR000824

Wang S, Yang Y, Luo Y, Rivera A. 2013. Spatial and seasonal variations in evapotranspiration over Canada's landmass. *Hydrology and Earth System Sciences* **17** (9): 3561–3575 DOI: 10.5194/hess-17-3561-2013

Wang XF, Yakir D. 2000. Using stable isotopes of water in evapotranspiration studies. *Hydrological Processes* **14** (8): 1407–1421 DOI: 10.1002/1099-1085(20000615)14:8<1407::AID-HYP992>3.0.CO;2-K

Warner KL, Ayotte JD. 2014. *Water quality in the glacial aquifer system, northern United States, 1993-2009*. DOI: 10.3133/cir1352

Wassenaar LI. 1995. Evaluation of the origin and fate of nitrate in the Abbotsford Aquifer using the isotopes of15N and18O in NO3 -. *Applied Geochemistry* **10** (4): 391–405 DOI: 10.1016/0883-2927(95)00013-A

Wassenaar LI, Athanasopoulos P, Hendry MJ. 2011. Isotope hydrology of precipitation, surface and ground waters in the Okanagan Valley, British Columbia, Canada. *Journal of Hydrology* **411** (1–2): 37–48 DOI: 10.1016/j.jhydrol.2011.09.032

Wassenaar LI, Hendry MJ, Chostner VL, Lis GP. 2008. High resolution pore water δ2H and δ18O measurements by H2O(liquid)-H2O (vapor) equilibration laser spectroscopy. *Environmental Science and Technology* **42** (24): 9262–9267 DOI: 10.1021/es802065s

Wassenaar LI, Van Wilgenburg SL, Larson K, Hobson KA. 2009. A groundwater isoscape (??D, ??18O) for Mexico. *Journal of Geochemical Exploration* **102** (3): 123–136 DOI: 10.1016/j.gexplo.2009.01.001

Welsh B, Kerkhoven E. 2012. A winter water balance approach to quantifying lake-groundwater interactions in the Beaver River Basin , Alberta. *IAH 2012 Congress, Nagara Falls*: 6pp.

Wenninger J, Beza DT, Uhlenbrook S. 2010. Experimental investigations of water fluxes within the soil–vegetation–atmosphere system: Stable isotope mass-balance approach to partition evaporation and transpiration. *Physics and Chemistry of the Earth, Parts A/B/C* **35** (13–14): 565–570 DOI: 10.1016/j.pce.2010.07.016

Winter TC. 1999. Relation of streams, lakes, and wetlands to groundwater flow systems. *Hydrogeology Journal* **7** (1): 28–45 DOI: 10.1007/s100400050178

Winter TC. 2000. The Vulnerability of Wetlands To Climate Change: a Hydrologic Landscape Perspective. *Journal of the American Water Resources Association* **36** (2): 305–311 DOI: 10.1111/j.1752-1688.2000.tb04269.x

Winter TC, LaBaugh JW. 2003. Hydrologic considerations in defining isolated wetlands. *Wetlands* **23** (3): 532–540 DOI: 10.1672/0277-5212(2003)023[0532:HCIDIW]2.0.CO;2

Winter TC, Rosenberry DO. 1995. The interaction of groundwater with Prairie Pothole wetlands in the Cottonwood lake area, East-central North Dakota, 1979-1990. *Wetlands* **15** (3): 193–211

Winter TC, Rosenberry DO. 1998. Hydrology of Prairie pothole wetlands during drought and deluge: A 17 year study of the Cottonwood lake wetland complex in North dakota in the perspective of longer term measured and proxy hydrological records. *Climatic Change* (40): 189–209

Winter TC, Harvey JW, Franke OL, Alley WM. 1998. Ground Water U . S . Geological Survey Circular 1139. *USGS Publications* **Circular 1**: 79 Available at: http://pubs.usgs.gov/circ/circ1139/%5Cnhttp://books.google.com/books?hl=en&lr=&id=visG1yDeSooC&oi=fnd&pg=PR6&dq=Ground+Water+and+Surface+Water+A+Single+Resource&ots=-IZRIMY1y6&sig=RiCIBwUcoaIulLBwlTm4yHrRuA%5Cnhttp://water.usg

Winter TC, Rosenberry DO, LaBaugh JW. 2003. Where Does the Ground Water in Small Watersheds Come From? *Ground Water* **41** (7): 989–1000 DOI: 10.1111/j.1745-6584.2003.tb02440.x

Wittrock V, Beaulieu C. 2015. Climate Reference Station Saskatoon Annual Summary 2014. Saskatoon, Saskatchewan.

Woo MK, Rowsell RD. 1993. Hydrology of a prairie slough. *Journal of Hydrology* **146**: 175–207 DOI: 10.1016/0022-1694(93)90275-E

Wright CK, Wimberly MC. 2013. Recent land use change in the Western Corn Belt threatens grasslands and wetlands. *Proceedings of the National Academy of Sciences* **110** (10): 4134–4139 DOI: 10.1073/pnas.1215404110

Yakir D, Wang XF. 1996. fluxes of CO2 and water between terrestrial vegetation and the atmosphere estimated from isotope measurements. *Nature* **380** (11 April): 515–517

Yang W, Wang X, Gabor S, Boychuk L, Badiou P. 2008. Water Quantity and Quality Benefits from Wetland Conservation and Restoration in the Broughton's Creek Watershed. Stonewall, Manitoba.

Yepez EA, Williams DG, Scott RL, Lin G. 2003. Partitioning overstory and understory evapotranspiration in a semiarid savanna woodland from the isotopic composition of water vapor. *Agricultural and Forest Meteorology* **119** (1–2): 53–68 DOI: 10.1016/S0168-1923(03)00116-3

Zebarth B. J, De Jong E. 1989. Water flow in a hummocky landscape in central Saskatchewan, Canada, I. Distribution of water and soils. *Journal of Hydrology* **107** (1989): 309–327

Zebarth BJ, De Jong E, Henry JL. 1989. Water flow in a hummocky landscape in central Saskatchewan, Canada, II. Saturated flow and groundwater recharge. *Journal of Hydrology* **110** (1–2): 181–198 DOI: 10.1016/0022-1694(89)90243-6

Zimmermann U, Münnich KO, Roether W. 2013. Downward Movement of Soil Moisture Traced by Means of Hydrogen Isotopes. *Geophysical Monograph Series* **11**: 28–36 DOI: 10.1029/GM011p0028

Zuber A. 1983. On the environmental isotope method for determining the water balance components of some lakes. *Journal of Hydrology* **61** (4): 409–427 DOI: 10.1016/0022-1694(83)90004-5

APPENDICES AND SUPPORTING DOCUMENTATION

APPENDIX A

The script below is the implementation of the pond model described in Section 3. 1. in Python version 2.7. The model requires the open source python libraries numpy, matplotlib, pandas and scipy. The model reads data from two Excel files “Input_Template.xlsx” and “PondObservations.xlsx” (attached as supplementary materials) and it creates an output file called “output.xlsx”.Contents of file RunPondModel.py:

```
# <><><><><><><><><><><><><><><><><><><><><><><><><><><><><><>
<><><><>
# Import libraries
# <><><><><><><><><><><><><><><><><><><><><><><><><><><><><><>
<><><><>
from matplotlib import pyplot as plt
import numpy as np
import pandas
from scipy import optimize

# <><><><><><><><><><><><><><><><><><><><><><><><><><><><><><>
<><><><>
# Core model functions
# <><><><><><><><><><><><><><><><><><><><><><><><><><><><><><>
<><><><>
def PondDAV(pars,k=0.,V=0.,A=0.):
    p=pars['p']
    s=pars['s']
    ki=pars['ki']
    if k!=0:
        A=s*(k/ki)**(2/p)
        V=A*k/(1+2/p)
    elif A!=0:
        k=ki*(A/s)**(p/2)
```

```
        V=A*k/(1+2/p)
    elif V!=0:
        k=(V*(1+2/p)/s*ki**(-p/2))**(1/(1+2/p))
        A=s*(k/ki)**(2/p)
    return k,A,V
PondDAV=np.vectorize(PondDAV)

# Fractionation factor functions
def Alpha_O18(T):
    T=T+273
    Alp = -7.685+6.7123e3/T-1.6664e6/T**2+0.35041e9/T**3
    Al = np.exp(Alp/1000)
    return Al
    return Al

def Alpha_H2(T):
    T=T+273
    Al = 1158.8e-9*T**3 - 1620.1e-6*T**2 + 794.84e-3*T - 161.04 + 2.9992e9/T**3
    Al = np.exp(Al/1000)
    return Al



# Isotope balance model:
# t = time (d)
# dt = current time step length (d)
# df['P'] = Precip during timestep (mm/d)
# df['E'] = Evap during timestep(mm/d)
# df['I'] = Pond infiltration during timestep (mm/d)
# df['T'] = Temperature during time step (deg C)
# df['del_i'] = Initial isotope conc. of pond
# df['del_a'] = atmospheric isotopic conc. during timestep
```

```
# df['rh'] = Relative humidity during timestep (-)
# df['k'] = Initial water level.
# pars = library of parameters, including:
    # s = Pond geom. par
    # p = Pond geom. par
    # ki = Pond geom. par
    # thetanC = coefficient for kinetic isotopic separation

def ModelFun(E,I,k_i,del_i,dt,df,df_iso,pars,p_iso,alphafun):

    # Water balance
    h_t=np.max((0,h_i+(df['P']-E-I)/1000.*dt))
    dum,A,V=PondDAV(pars,h_i)

    # Isotope balance
    Al=alphafun(df['T'])
    Ep=1000*(Al-1)
    DelEp=p_iso['thetanC']*(1-df['rh'])

    B=(df['rh']*df_iso['Atm']+DelEp/1.+Ep/Al)/(1-df['rh']+DelEp/1000.)
    C=(df['rh']-DelEp/1000.-Ep/1000./Al)/(1-df['rh']+DelEp/1000.)

    X1=np.exp(-(A*df['P']/1000.+A*E/1000.*C)*dt/V)
    X2=(E/1000.*B+df['P']/1000.*df_iso['Prec'])/(df['P']/1000.+E/1000.*C)
    X3=(1-np.exp(-(A*df['P']/1000.+A*E/1000.*C)*dt/V))
    del_t=del_i*X1+X2*X3

    return k_t,del_t

def RunModel(E,I,k_ini,H2_ini,O18_ini,StartDate,df,df_O18,df_H2,pars,p_O18,p_H2):
```

```
    # Solve model
    df.ix[0,'k']=k_ini
    df_O18.ix[0,'Pond']=O18_ini
    df_H2.ix[0,'Pond']=H2_ini
    for i in range(1,len(df.index)):
        dt=(df.index[i]-df.index[i-1]).days
        k_t,del_O18_t = ModelFun(E,I,df.ix[i-1,'k'],df_O18.ix[i-1,'Pond'],df.ix[i,'dt'],df.iloc[i],df_O
18.iloc[i],pars,p_O18,Alpha_O18)
        df.ix[i,'k']=k_t
        df_O18.ix[i,'Pond']=del_O18_t
        k_t,del_H2_t = ModelFun(E,I,df.ix[i-1,'k'],df_H2.ix[i-1,'Pond'],df.ix[i,'dt'],df.iloc[i],df_H2.i
loc[i],pars,p_H2,Alpha_H2)
        df_H2.ix[i,'Pond']=del_H2_t

    dum,df['A'],df['V']=PondDAV(pars,k=df['k'])

    output=df['k'].to_frame()
    output['O18']=df_O18['Pond']
    output['H2']=df_H2['Pond']

    return output, df, df_O18, df_H2


# <><><><><><><><><><><><><><><><><><><><><><><><><><><><><><><>
<><><><>
# Functions used for optimization
# <><><><><><><><><><><><><><><><><><><><><><><><><><><><><><><>
<><><><>
# STAGE ONE - optimize the total water loss to the water levels
def OptFun1(E,I,k_ini,H2_ini,O18_ini,StartDate,df,df_O18,df_H2,pars,p_O18,p_H2):
    output, df, df_O18, df_H2 = RunModel(E,I,k_ini,H2_ini,O18_ini,StartDate,df,df_O18,df_H2,
```

```
pars,p_O18,p_H2)
    RMSE=ObFun_Level(depth,output)
    return RMSE

def ObFun_Level(depth,output):
    t_o=depth.index
    k_o=depth.values.squeeze()
    t_s=output.index
    k_s=output['k'].values.squeeze()

    if len(t_o) > len(t_s):
        t=t_s.to_julian_date()
        tx=t_o.to_julian_date()
        tx=tx-t[0]
        t=t-t[0]
        k_o=np.interp(t,tx,k_o)
    else:
        t=t_o.to_julian_date()
        tx=t_s.to_julian_date()
        tx=tx-t[0]
        t=t-t[0]
        k_s=np.interp(t,tx,k_s)

    RMSE = np.sqrt(np.mean((k_o-k_s)**2.))
    return RMSE

# STAGE TWO - optimize the evaporation to isotope values
def OptFun2(E,EI,k_ini,H2_ini,O18_ini,StartDate,df,df_O18,df_H2,pars,p_O18,p_H2):
    I = EI - E

    output, df, df_O18, df_H2 = RunModel(E,I,k_ini,H2_ini,O18_ini,StartDate,df,df_O18,df_H2,
```

```
pars,p_O18,p_H2)
    RMSE_O18=ObFun_Iso(pond,output,'O18')/np.abs(pond['O18'].mean())
    RMSE_H2=ObFun_Iso(pond,output,'H2')/np.abs(pond['H2'].mean())
    RMSE=RMSE_O18+RMSE_H2
    return RMSE

# RMSE for the pond depth function:
def ObFun_Iso(pond,output,isostr):
    t_o=pond.index
    iso_o=pond[isostr].values.squeeze()
    t_s=output.index
    iso_s=output[isostr].values.squeeze()

    if len(t_o) > len(t_s):
        t=t_s.to_julian_date()
        tx=t_o.to_julian_date()
        tx=tx-t[0]
        t=t-t[0]
        iso_o=np.interp(t,tx,iso_o)
    else:
        t=t_o.to_julian_date()
        tx=t_s.to_julian_date()
        tx=tx-t[0]
        t=t-t[0]
        iso_s=np.interp(t,tx,iso_s)

    RMSE = np.sqrt(np.mean((iso_o-iso_s)**2.))
    return RMSE


# <><><><><><><><><><><><><><><><><><><><><><><><><><><><><><>
```

```
<><><><>
# Load data in 3 categories: output observations, parameters, driving data
# <><><><><><><><><><><><><><><><><><><><><><><><><><><><><>
<><><><>

# ------------------------
# OUTPUT DATA
# ------------------------
# Load observations (heavy)
print "Loading observed data\n"
pond=pandas.read_excel('PondObservations.xlsx',index_col=0,sheetname='Isotopes')
depth=pandas.read_excel('PondObservations.xlsx',index_col=0,sheetname='Depth')



# ------------------------
# PARAMETERS
# ------------------------
# Read parameters
pardata = pandas.read_excel('Input_Template.xlsx',sheetname='Pars',index_col='Parameter')

StartDate=pardata['Value'].loc['StartDate']
EndDate=pardata['Value'].loc['EndDate']
E=pardata['Value'].loc['E']
I=pardata['Value'].loc['I']

# Pond geometry parameters:
pars={}
pars['s']=pardata['Value'].loc['s']
pars['p']=pardata['Value'].loc['p']
pars['hi']=pardata['Value'].loc['hi']
```

```
ShallIOptimize=pardata['Value'].loc['Optimize']
if ShallIOptimize!=0:
   print "Optimizing to level and then %s\n" % ShallIOptimize
else:
   print "Running the model without optimization\n"


# Isotopic parameters:
p_O18={}
p_H2={}
p_O18['thetanC']=pardata['Value'].loc['O18_thetanC']
p_H2['thetanC']=pardata['Value'].loc['H2_thetanC']

rh=pardata['Value'].loc['rh']
T=pardata['Value'].loc['T']

A_H2=pardata['Value'].loc['A_H2']
A_O18=pardata['Value'].loc['A_O18']


# ------------------------
# DRIVING DATA
# ------------------------
df=pandas.read_excel('Input_Template.xlsx',index_col=0,sheetname='Input')
# Get time step in days
df['dt']=0.
for i in range(1,len(df.index)):
   df.ix[i,'dt']=(df.index[i]-df.index[i-1]).days

# Convert precipitation into mm/d
df['P'] = df['P']/df['dt']
```

```
# Convert relative humidity into a fraction
df['rh']=rh/100.
df['T']=T

# Initialize columns to be populated:
df['k']=0.

# Create dataframes for the isotopes
df_O18=pandas.DataFrame()
df_O18['Prec']=df['P_O18']
df_O18['Atm']=A_O18
df_O18['Pond']=0.

df_H2=pandas.DataFrame()
df_H2['Prec']=df['P_H2']
df_H2['Atm']=A_H2
df_H2['Pond']=0.

# Truncate data to StartDate
if len(np.where(df.index==StartDate)[0])!=0:
    print "Start date coincides with driving data"
    df=df[StartDate:]
    df_O18=df_O18[StartDate:]
    df_H2=df_H2[StartDate:]
else:
    print "Start date does not coincide with driving data"
    # Find the row to replace with the start date:
    i=np.where(df.index>StartDate)[0]
    i=i[0]-1
    if i < 0:
```

```
        print "ERROR: Start date is too early. Please adjust and rerun"
        import sys
        sys.exit(0)
    df=df[i:]
    df_O18=df_O18[i:]
    df_H2=df_H2[i:]

    # Edit index:
    t=df.index.values
    t[0]=StartDate
    df.index=t
    df['dt'][1]=(df.index[1]-df.index[0]).days
    #df['P'][0]=df['P'][1]

# Truncate data to EndDate
if EndDate<df.index[-1]:
    print "End of model run was truncated"
    i=np.where(df.index<EndDate)[0]
    i=i[-1]+1
    df=df[0:i]
    df_O18=df_O18[0:i]
    df_H2=df_H2[0:i]
    t=df.index.values
    t[-1]=EndDate
    df.index=t
    df['dt'][-1]=(df.index[-1]-df.index[-2]).days

else:
    print "End of model run was not truncated"
#
```

```
# INTIAL CONDITIONS
k_ini=np.interp(StartDate.to_julian_date(),depth.index.to_julian_date(),depth['Depth'].values)
O18_ini=np.interp(StartDate.to_julian_date(),pond.index.to_julian_date(),pond['O18'].values)
H2_ini=np.interp(StartDate.to_julian_date(),pond.index.to_julian_date(),pond['H2'].values)


# <><><><><><><><><><><><><><><><><><><><><><><><><><><><><>
<><><><>
# Run the model
# <><><><><><><><><><><><><><><><><><><><><><><><><><><><><>
<><><><>
if ShallIOptimize!=0:
    print "Stage one optimization: get total water loss from the pond"
    EI = E + I
    I = 0.
    EI=optimize.fmin(func=OptFun1, x0=E,args=(I,k_ini,H2_ini,O18_ini,StartDate,df,df_O18,df
_H2,pars,p_O18,p_H2,))

    output, df, df_O18, df_H2 = RunModel(EI,I,k_ini,H2_ini,O18_ini,StartDate,df,df_O18,df_H2
,pars,p_O18,p_H2)
    RMSE1=ObFun_Level(depth,output)

    print "Stage two optimization: get evaporative loss from the pond"
    E=optimize.fmin(func=OptFun2, x0=E,args=(EI,k_ini,H2_ini,O18_ini,StartDate,df,df_O18,df
_H2,pars,p_O18,p_H2,))
    I = EI - E
    output, df, df_O18, df_H2 = RunModel(E,I,k_ini,H2_ini,O18_ini,StartDate,df,df_O18,df_H2,
pars,p_O18,p_H2)
    RMSE_O18=ObFun_Iso(pond,output,'O18')/np.abs(pond['O18'].mean())
    RMSE_H2=ObFun_Iso(pond,output,'H2')/np.abs(pond['H2'].mean())
    RMSE2=RMSE_O18+RMSE_H2
```

```
else:
    output, df, df_O18, df_H2 = RunModel(E,I,k_ini,H2_ini,O18_ini,StartDate,df,df_O18,df_H2,
pars,p_O18,p_H2)
    RMSE1=ObFun_Level(depth,output)
    RMSE_O18=ObFun_Iso(pond,output,'O18')/np.abs(pond['O18'].mean())
    RMSE_H2=ObFun_Iso(pond,output,'H2')/np.abs(pond['H2'].mean())
    RMSE2=RMSE_O18+RMSE_H2


# <><><><><><><><><><><><><><><><><><><><><><><><><><><><><><><><><><><><><><><><><><><><><><>
<><><><><><><>
# Save model output
# <><><><><><><><><><><><><><><><><><><><><><><><><><><><><><><><><><><><><><><><><><><><><><>
<><><><><><><>
numday=df.index[-1].to_julian_date()-df.index[0].to_julian_date()
k_fin=df['k'][-1]
outEI={}
outEI['RMSE_level']=RMSE1
outEI['RMSE_iso']=RMSE2
outEI['E (mm/d)']=E
outEI['I (mm/d)']=I
outEI['E (mm)']=E*numday
outEI['I (mm)']=I*numday
outEI['Number of days']=numday
P=(df['P'][1:]*df['dt'][1:]).sum()/numday
outEI['P (mm/d)']=P
outEI['P (mm)']=P*numday
outEI['Sim_deltaStorage (mm)']=(E+I-P)*numday
outEI['Obs_deltaStorage (mm)']=1000*(k_ini-k_fin)
outEI['k ini (mm)']=k_ini*1000
```

```
outEI['k fin (mm)']=k_fin*1000
outEI['Pond area ini (m2)']=PondDAV(pars,k=k_ini)[1]
outEI['Pond area fin (m2)']=PondDAV(pars,k=k_fin)[1]
outEI=pandas.DataFrame(data=outEI,index=np.array(['Simulation:']))

# print outcome to screen
print "RMSE (level) = %0.2f" % RMSE1
print "RMSE (%s) = %0.2f" % (ShallIOptimize,RMSE2)
print "E = %0.2f" % E
print "I = %0.2f" % I

# Save result
writer=pandas.ExcelWriter('output.xlsx')
outEI.transpose().to_excel(writer,'Outputs')
output.to_excel(writer,'Timeseries')
writer.save()
```

APPENDIX B

The pond model described in Section 3. 1. Excel implementation files “Input_Template.xlsx” and “PondObservations.xlsx” (attached)

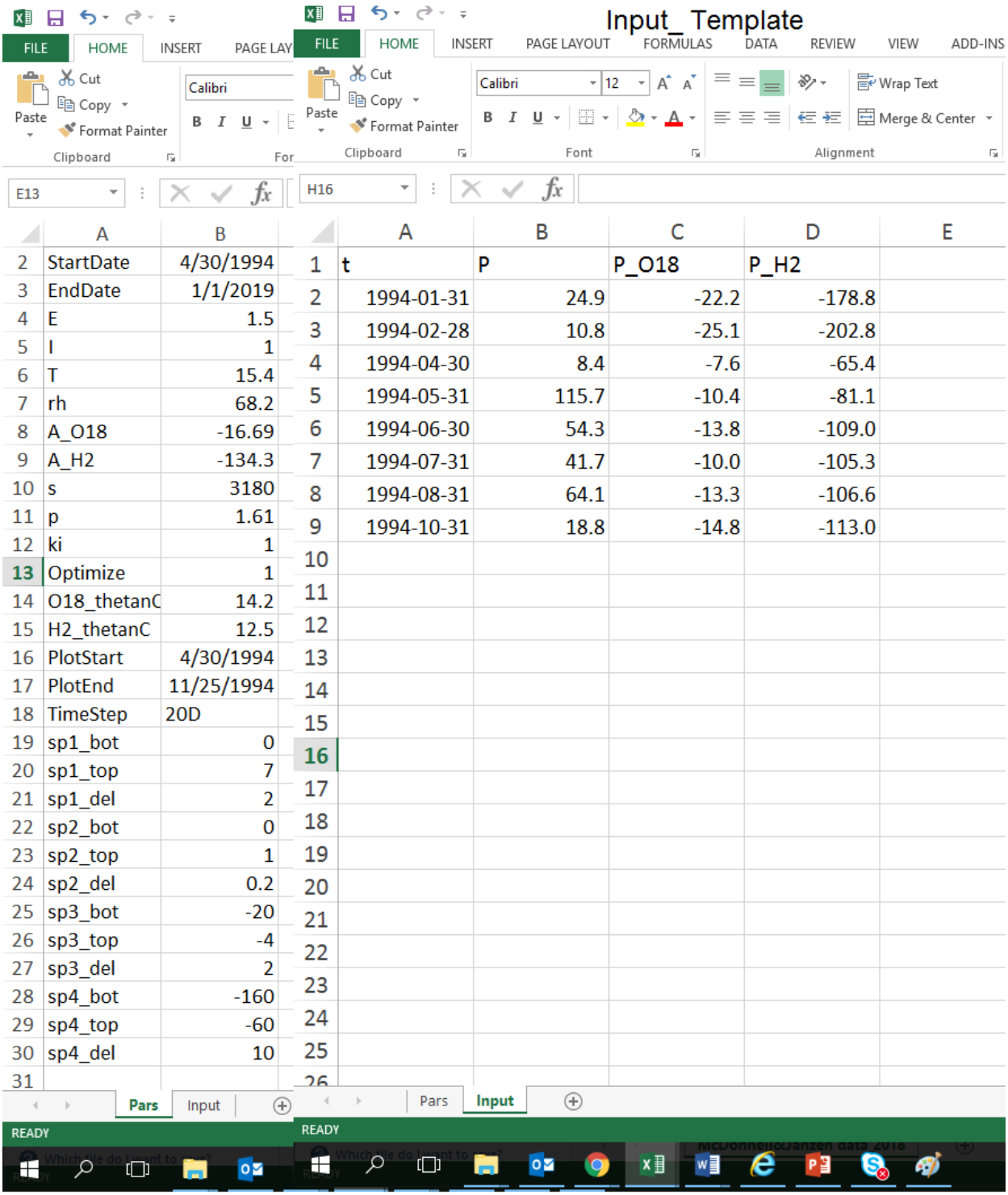

	A	B
2	StartDate	4/30/1994
3	EndDate	1/1/2019
4	E	1.5
5	I	1
6	T	15.4
7	rh	68.2
8	A_O18	-16.69
9	A_H2	-134.3
10	s	3180
11	p	1.61
12	ki	1
13	Optimize	1
14	O18_thetanC	14.2
15	H2_thetanC	12.5
16	PlotStart	4/30/1994
17	PlotEnd	11/25/1994
18	TimeStep	20D
19	sp1_bot	0
20	sp1_top	7
21	sp1_del	2
22	sp2_bot	0
23	sp2_top	1
24	sp2_del	0.2
25	sp3_bot	-20
26	sp3_top	-4
27	sp3_del	2
28	sp4_bot	-160
29	sp4_top	-60
30	sp4_del	10
31		

	A	B	C	D	E
1	t	P	P_O18	P_H2	
2	1994-01-31	24.9	-22.2	-178.8	
3	1994-02-28	10.8	-25.1	-202.8	
4	1994-04-30	8.4	-7.6	-65.4	
5	1994-05-31	115.7	-10.4	-81.1	
6	1994-06-30	54.3	-13.8	-109.0	
7	1994-07-31	41.7	-10.0	-105.3	
8	1994-08-31	64.1	-13.3	-106.6	
9	1994-10-31	18.8	-14.8	-113.0	
10					
11					
12					
13					
14					
15					
16					
17					
18					
19					
20					
21					
22					
23					
24					
25					

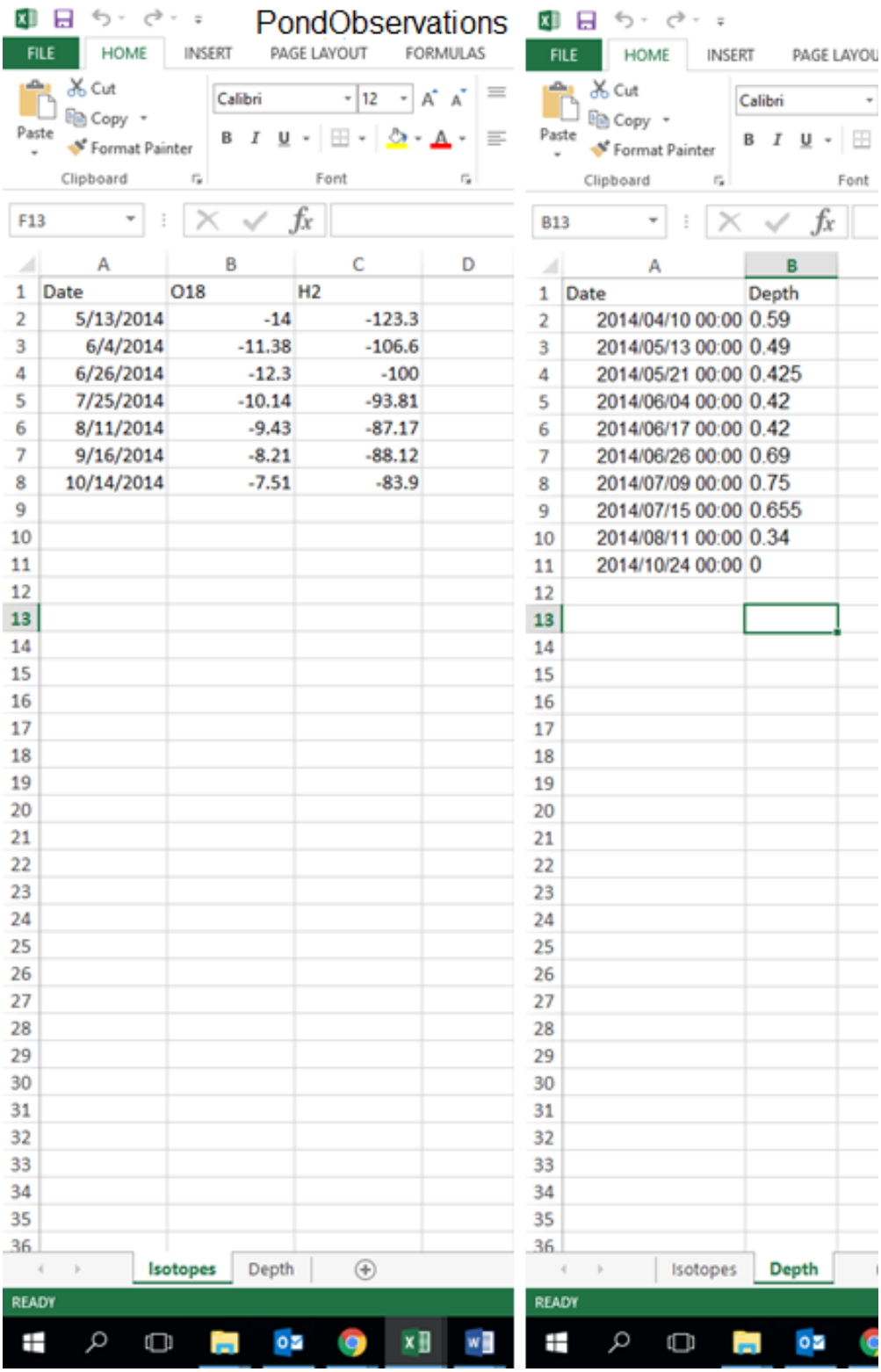
PondObservations
FILE
HOME
INSERT
PAGE LAYOUT
FORMULAS
Cut
Copy
Format Painter
Paste
Clipboard
Calibri
12
Font
F13
A
B
C
D
1 Date O18 H2
2 5/13/2014 -14 -123.3
3 6/4/2014 -11.38 -106.6
4 6/26/2014 -12.3 -100
5 7/25/2014 -10.14 -93.81
6 8/11/2014 -9.43 -87.17
7 9/16/2014 -8.21 -88.12
8 10/14/2014 -7.51 -83.9
Isotopes
Depth
READY
B13
1 Date Depth
2 2014/04/10 00:00 0.59
3 2014/05/13 00:00 0.49
4 2014/05/21 00:00 0.425
5 2014/06/04 00:00 0.42
6 2014/06/17 00:00 0.42
7 2014/06/26 00:00 0.69
8 2014/07/09 00:00 0.75
9 2014/07/15 00:00 0.655
10 2014/08/11 00:00 0.34
11 2014/10/24 00:00 0

APPENDIX C

Model performances compared to field observations for the years 1997, 1998 and 1999 for which all required field observations were available for pond 109 and 50.